Spring 2022

Cryopreservation Studies Of An Antifreeze Protein From The Desert Beetle Anatolica Polita

Jonathan Sreter
University of New Hampshire, Durham

CRYOPRESERVATION STUDIES OF AN ANTIFREEZE PROTEIN FROM THE DESERT BEETLE ANATOLICA POLITA

BY

JONATHAN ALBERT SRETER

Bachelor of Science in Biomedical Sciences: Medical Microbiology, University of New Hampshire, 2013

DISSERTATION

Submitted to the University of New Hampshire

in Partial Fulfillment of

the Requirements for the Degree of

Doctor of Philosophy

in

Microbiology

May 2022

This thesis was examined and approved in partial fulfillment of the requirements for the degree of Doctor of Philosophy in Microbiology by:

Thesis Director, Dr. Krisztina Varga, Associate Professor of Microbiology

Dr. Feixia Chu, Associate Professor of Biochemistry

Dr. Sherine Elsawa, Associate Professor of Microbiology

Dr. Thomas L. Foxall, Professor of Biology

Dr. W. Kelley Thomas, Professor of Microbiology

On April 25, 2022

Original approval signatures are on file with the University of New Hampshire Graduate School.

DEDICATION

I would like to dedicate this thesis to my father, Albert, and thank him for all he has done and still does to show me what it means to be a good man. None of this would be possible without him. I would also like to thank my sisters, Allison and Andrea, for their continued love and support. This is also dedicated to my late mother, Lorinda Sreter, late Nagypapa, Dr. Frank Sreter, and late Babu, Julia Sreter. I hope I've made them proud. To my wonderful girlfriend Mona, thank you for being there for me. I would like to thank Dr. Aaron Margolin for his continued mentorship and friendship and for getting me interested in research many years ago. To my friends Wade, Chris, Matt, Keir, Seth, Zach, and Kevin, thank you for your support and friendship.

ACKNOWLEDGEMENTS

I would thank my advisor, Dr. Krisztina Varga, first and foremost for her mentorship and guidance throughout this project and my time as a graduate student. It has been a privilege to have a kind and patient advisor to direct my research and studies. A special thank you to my close collaborator and committee member Dr. Thomas Foxall for his mentorship and generosity. Thank you to my committee members Dr. Feixia Chu, Dr. Sherine Elsawa, and Dr. W. Kelley Thomas for their guidance and time throughout my graduate studies.

I would like to acknowledge former Varga group members, Dr. K. Wade Elliott and Dr. Christopher Nordyke for their advice and project input. Thank you to Ms. Katarina Jovic for her assistance in the initial stages of the antifreeze characterization.

This research was supported by an Institutional Development Award (IDeA) [CIBBR, P20GM113131] and by the award [GM135903] from the National Institute of General Medical Sciences of the National Institutes of Health. This work was also partially supported by the National Aeronautics and Space Administration Established Program to Stimulate Competitive Research program [80NSSC18M0034], and the by the National Science Foundation (awards CHE-1740399).

Table of Contents

LIST OF FIGURES

LIST OF TABLES

ABSTRACT

CRYOPRESERVATION STUDIES OF AN ANTIFREEZE PROTEIN FROM THE DESERT BEETLE ANATOLICA POLITA

by

Jonathan Albert Sreter

University of New Hampshire, May 2022

Antifreeze proteins (AFPs) are specialized evolutionary adaptations by certain cold climate organisms, including fish, plants, fungi, bacteria, and insects, to prevent cryo-injury. AFPs contribute to freeze resistance or tolerance by binding to the surface of ice crystals and preventing their growth, as well as inhibiting ice recrystallization (i.e., small crystals restructuring into large crystals) during large temperature fluctuations and constant sub-zero temperatures. AFPs have potential applications in cryopreservation and in the development of cryo-functional materials for medicine, the food industry, and agriculture. We investigated the ability of an antifreeze protein from the desert beetle *Anatolica polita*, ApAFP752, to confer cryoprotection in human embryonic kidney (HEK) 293T cells. HEK 293T cells were transfected with ApAFP752, and/or ApAFP752 was added to extracellular media prior to freezing at cryogenic temperature. AFP was assessed for its cryoprotective effects both intra- and extracellulary and both simultaneously at different concentrations with and without DMSO at different concentrations. After freezing and thawing, comparisons were made to DMSO or medium alone. ApAFP752 significantly improved cryopreserved cell survival when used with DMSO intracellularly. Extracellular ApAFP752 also significantly

improved cryopreserved cell survival when included in the DMSO freezing medium. Intra- and extracellular ApAFP752 used together demonstrated the most significantly increased cryoprotection compared to DMSO alone at all DMSO concentrations. Together, these findings present potential methods for using an insect antifreeze protein to confer cryoprotection and improve the viability of cryopreserved mammalian cells.

PROJECT AIMS AND HYPOTHESIS

Project: Cryopreservation studies of the antifreeze protein ApAFP752

Low temperature conditions, such as freezing, can be lethal to cellular organisms. There are various causes of low temperature damage: (i) direct effects of low temperature, such as cold induced protein denaturation (unfolding), (ii) direct effects of freezing, *e.g.* formation of ice crystals which physically rupture cell membranes and tissues, and (iii) indirect effects of freezing, *i.e.,* elevated concentration of solutes (parts per trillion (ppt) of buffer salts) or pH changes due to exclusion by ice, as ice is a poor solvent. Nature employs a variety of compounds and strategies for freeze avoidance and freeze tolerance that enhance survival of certain organisms in extreme cold environments. In the 1960's antifreeze proteins were first discovered in the blood plasma of Antarctic fish[1] and have since been identified in diverse organisms that thrive in cold environments, including bacteria, insects, and plants. Antifreeze proteins have the ability to bind to ice crystals and inhibit crystal growth that would otherwise occur at the bound surfaces by a mechanism that is not fully understood.[2,3] Potential applications of antifreeze proteins include their application in cryopreservation protocols.

Effective cryopreservation and long-term storage are essential requirements to the commercial, research, and clinical applications of cell-based therapies. Although successful cell preservation protocols have been developed over the past decades, they have significant limitations. Long-term storage is

accomplished by freezing and storing the cells at -196 °C in liquid nitrogen. However, effective cryoprotection during storage is essential to maintain the viability of cells after thawing to avoid irreparable damage due to ice crystals and solution effects. Most cryopreservation procedures utilize 5-10% dimethyl sulfoxide (DMSO) as the cryoprotectant, but DMSO can have harmful effects by causing adverse reactions in patients and exhibiting cellular toxicity. Alternative cryoprotectant formulations are needed to avoid the undesirable effects of high concentrations of DMSO. The goals of the project were accomplished in the following specific aims:

Aim 1: Characterize the antifreeze activity of the antifreeze protein ApAFP752. *We hypothesized that ApAFP752 not only exhibits thermal hysteresis activity, but also potent ice recrystallization inhibition.* Ice recrystallization is a phenomenon that occurs when small ice crystals fuse together to form large ice crystals. AFPs can bind directly with the ice surface to inhibit ice recrystallization. To that end we developed methods of measuring both the ice recrystallization inhibition (IRI) and thermal hysteresis activity (THA) of ApAFP752. IRI was measured using a flash freezing microcapillary tube assay developed in collaboration with Paul Baures of Florida State University (previously at Keene State College, NH). THA was measured using a differential scanning calorimetry assay developed in collaboration with John Tsavalas of the University of New Hampshire.

Aim 2: Examine the extracellular cryoprotective activity of ApAFP752 for mammalian cell cryopreservation. *We hypothesized that purified ApAFP752 added to the freezing solution would offer cryoprotection to mammalian cells during freeze/thaw.* We supplemented the freezing medium of human embryonic kidney cells (HEK 293T) with recombinantly expressed and purified ApAFP752 protein. We tested the cryoprotective effect of the AFP in combination with 0, 5, and 10% v/v DMSO concentrations in the freezing medium, and cell viability and cellular damage was determined using three assays (trypan blue, LDH, and MTS).

Aim 3: Examine the intracellular cryoprotective activity of ApAFP752 in mammalian cells. *We hypothesized that intracellular ApAFP752 would offer better cryoprotection during freeze/thaw than extracellular AFP.* First, we transfected HEK 293T cells with a plasmid containing a gene for EGFP-ApAFP752 expression, where EGFP is the enhanced green fluorescence protein that was used as a reporter for transfection efficiency. We determined the cryoprotective effect of intracellular AFP compared to the control groups of untransfected cells and EGFP transfected cells with 0, 5, 15, 15, and 20% v/v DMSO concentrations using three different cell viability and cellular damage measurements (trypan blue, LDH, and MTS). We have also tested the cryoprotective effect of a combined intracellular and extracellular AFP.

CHAPTER 1

INTRODUCTION TO ANTIFREEZE PROTEINS

Almost all cells and cellular organisms are destroyed or damaged by freezing, and much is still not understood about how to counteract its adverse effects. Researchers look to nature for answers, because many organisms have natural compounds and strategies to avoid or tolerate freezing in order to survive in extreme cold. These organisms produce what are known as ice binding proteins (IBPs). Ice binding proteins are aptly named, as all of these proteins bind to ice. There are large differences in both structure and function of ice binding proteins. Antifreeze proteins (AFPs) and antifreeze glycoproteins (AFGPs) are types of ice binding proteins that inhibit ice growth. Ice nucleating proteins, on the other hand, are a type of ice binding protein that reduce supercooling and promote the nucleation of ice crystals and freezing.[1,2] Here we focused on AFPs. Antifreeze proteins were first discovered in the plasma of Antarctic fish, and AFPs are adaptations that allow the fish to survive the sub-zero conditions (-1 to -2 °C) in the Antarctic Ocean.[3] The first AFP discovered was an antifreeze glycoprotein (AFGP) from Antarctic notothenioids (winter flounder).[3] Over the past few decades it has been discovered that a wide range of organisms (e.g. bacteria, fish, fungi, insects, plants) produce AFPs for protection against freezing.[4-6] Mammals, however, are homeotherms and have not been found to produce AFPs.

AFPs inhibit ice growth, reduce the freezing point, and prevent ice recrystallization in cold adapted organisms as a result of becoming adsorbed to the nascent ice surface by an unusual mechanism.[7-9] By preventing ice crystals from expanding past the size of

small microcrystals, AFPs are able to reduce the damaging effects of ice.[10] Though they all share the same ligand, ice, AFPs have vastly diverse structures and sequences. The reason for this remarkable diversity is the independent evolutionary development of these proteins.[11] AFP production as an evolutionary adaptation has been crucial for the survival of species experiencing climates of extreme temperature fluctuations within a day and near or sub-zero temperatures. These AFP producing organisms are further classified based on their survival strategies, freeze-avoidant or freeze-tolerant.[12-14] Freeze-avoidant organisms are able to survive freezing conditions to a few degrees below freezing, however, if conditions surpass thresholds and ice forms in their cells, they are unable to survive. On the other hand, freeze-tolerant organisms are able to survive ice forming in their extracellular fluids. These differing survival strategies are part of what has led to different structures and degrees of functionality, which correspond to sequence homology.[5,15] AFPs have long been of interest in the scientific community and have numerous, far-reaching potential applications across fields such as agriculture, biotechnology, and medicine.[16-20]

AFPs have been classified into 7 categories based on their highly variable structures: antifreeze glycoproteins (AFGPs), type I-IV antifreeze proteins, plant antifreeze proteins, and hyperactive antifreeze proteins.

I. Antifreeze Glycoproteins

Fish, such as ocean pout, northern cods, and Antarctic notothenioids express both AFGPs and AFPs, and these are among the most well-studied antifreeze proteins.[21-23] AFGPs differ from AFPs because they contain 4 to 50 tripeptide repeats of (Ala or Pro)–

Ala–Thr with an O-linked disaccharide chain attached to each Thr hydroxyl group (Figure 1).[5,23,24] There are 8 classes of AFGPs based upon their size. The largest, AFGP1 has a molecular weight of 33.7 kDa, while the smallest, AFGP8, has a molecular weight of 2.6 kDa.[25-27] The larger AFGPs typically have more antifreeze activity than the smaller ones. This is thought to be due to higher molecular weight AFGPs having a larger size, thus covering a larger surface of ice than lower molecular weight (smaller) AFGPs, and therefore inhibiting ice crystal growth more effectively.[6]

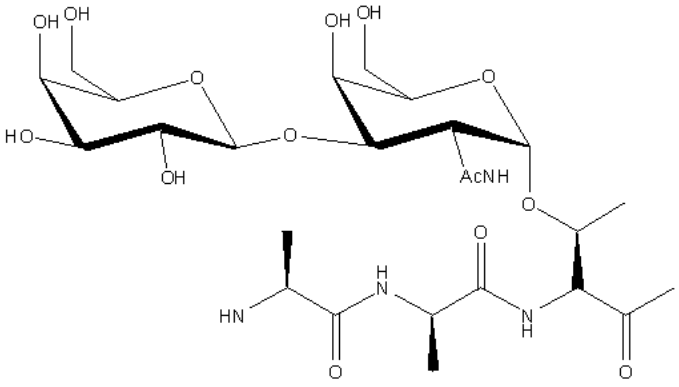

Figure 1: Typical antifreeze glycoprotein chemical structure depicting the AAT repeats joined with a dissacharide.[28]

II. Type I-IV Antifreeze Proteins

Fish AFPs are numbered I-IV based on their structure and the order of their discovery.[11] The structures of type I-IV AFPs are highly variable with each type containing unique features. Type I AFPs are commonly found in many Antarctic and Arctic fishes such as plaice, sculpin, and winter flounder.[6,11] Type I AFPs are alanine-rich, amphipathic, α-helical proteins. [28-30] Type I AFPs have a molecular weight of 3-33 kDa. The most well-studied type I AFP, HPLC6, from the winter flounder, had its molecular structure

determined using X-ray crystallography.[31] The HPLC6 structure showed an amphipathic, α-helical protein with 37 amino acids and 11 repeating units. These alanine-rich repeating units play a significant role in the ice binding mechanism of type 1 AFPs.[32] Much larger type I AFPs have also been discovered, such as the 195 residue AFP Maxi in winter flounder.[33] This protein has higher antifreeze activity than smaller type I AFPs, and this is again thought to be due to its larger size and modified ice binding mechanism.

Type II AFPs are cysteine-rich, globular, disulfide-bonded proteins that are commonly found in fish such as herring, poacher, and sea raven.[34-37] Type II AFPs have a molecular weight of 18-24 kDa and are composed of nine β-sheets and two α-helices stabilized by disulfide-bonded cysteines. There are 2 sub-groups within type II AFPs, Ca^{2+}-dependent and Ca^{2+}-independent. Ca^{2+}-dependent type II AFPs typically require Ca^{2+} binding in order to bind ice and exhibit antifreeze activity.[35] The only exception to this is the type II AFP is found in Japanese smelt, HniAFP, and can bind Ca^{2+}, but still exhibits antifreeze activity when Ca^{2+} is removed.[38] Ca^{2+}-dependent type II AFPs display structural similarity to C-type lectin domains (CTLDs), which use Ca^{2+} to bind sugars, and therefore are thought to have evolved from CTLDs.[39]

Type III AFPs are globular proteins without cysteines that form twisted loops folded into β-sheets and α-helices.[22,40] These AFPs have a molecular weight around 6.5 kDa and are commonly found in eelpout and wolffish.[41,42] Type III AFPs are also divided into two sub-groups based on sequence similarities and binding affinity for quaternary-amino-ethyl (QAE) and sulfopropyl (SP) sephadex, respectively. Type III AFPs have notable stability through both hydrogen bonds and hydrophobic interactions and have been shown to retain antifreeze activity from pH 2 to pH 11, and in other experiments at 80 °C

and 400 MPa of pressure for one-minute durations.[43,44] The current accepted hypothesis is type III AFPs have a flat surface containing a threonine 18 residue thought to be involved with ice binding.[45]

Type IV AFPs are a glutamine- and glutamate-rich, four-helix bundle of α-helices.[46,47] These AFPs have a molecular weight around 12 kDa and are found in longhorn sculpin, shorthorn sculpin, and flounder.[48,49] Type IV AFPs have a high sequence identity and similar four-helix bundle structure to apolipoproteins found in hemolymph and serum.[47] Type IV AFPs are found in low physiological concentrations (0.05 to 0.1 mg/mL) in nature and even exhibit significantly lower antifreeze activity compared to type I-III AFPs when tested at the same concentration.[49,50]

III. Plant Antifreeze Proteins

Plant AFPs are AFPs of varying structures found in the apoplast of cold-acclimated plants.[7] Plant AFPs have varying structures and some contain multiple β-sheets in their conformation. Plant AFPs are not very well studied among AFPs, but the two most studied plant AFPs are DcAFP, from the carrot *Dacus carrotova*, and LpAFP, from the perennial ryegrass *Lolium perenne*.[28,51] The original theoretical model for LpAFP was proposed to have a left-handed β-helix with two flat ice binding surfaces facing opposite to each other.[52,53] LpAFP has 7 loops with 14-15 residues per turn and a repeating Asn-X-Val-X-Gly/Asn-X-Val-X-X-Gly motif thought to be involved with ice binding.[54] These X residues are typically serine, threonine, and valine, and are responsible for binding ice.[55] Asparagine is also present in the ice binding motifs of DcAFP. The plant AFP DcAFP is leucine-rich and composed of two β-sheets and nine 3_{10} helices.[28,56,57] DcAFP contains a

24-residue repeat thought to be involved with ice binding with a Pro-X-X-X-X-X-Leu-X-X-Leu-X-X-Leu-X-Leu-Ser-X-Asn-X-Leu-X-Gly-X-Ile motif. [30] Interestingly, the Asparagine residues are highly conserved and are critical for optimal levels of antifreeze activity.[58]

IV. Hyperactive Antifreeze Proteins

Antifreeze proteins are further classified into moderately active or hyperactive based on their antifreeze activity. The aforementioned type I-IV and plant AFPs are moderately active, meaning they lower the freezing point of water by about 0.2-2 °C.[59] Hyperactive AFPs are typically found in bacteria, diatoms, fungi, and insects, and lower the freezing point of water by about 2 to 13 °C.[60-65]. Hyperactive AFPs have more potent antifreeze activity than that of moderately active AFPs because they bind to the primary and secondary prism planes as well as the basal plane of ice, and their antifreeze activity at the same concentration has been shown to lower the freezing point of water about 10 times more than moderately active AFPs, such as Type I, II, and III, which only bind to the prism planes and/or the pyramidal plane of ice.[5,66,67] This increased antifreeze activity is proportional to the extreme cold temperatures to which these terrestrial organisms are exposed. A notable exception to this is a hyperactive type I (hyp-type I) AFP that has been discovered.[68] This hyp-type I AFP shares some structural similarities with moderately active type I AFPs, but has a much larger surface area of ice binding sites which allow binding to both prism and basal planes and THA measurements similar to hyperactive insect AFPs.[69] Typically, hyperactive AFPs are rich in cysteine, serine, and threonine, and range in molecular weight from around 8-34 kDa. The insect AFP from the mealworm beetle *Tenebrio molitor* (TmAFP) has been the most well-studied hyperactive

AFP to date.[70-72] TmAFP is one of the smallest hyperactive AFPs with a molecular weight of 8-9 kDa. MpAFP, from the Antarctic bacterium *Marinomonas primoryensis*, is one of the largest hyperactive AFPs with a molecular weight of 34 kDa.[73] Most hyperactive AFPs have a large, flat ice binding surface with multiple Thr-X-Thr motifs involved with binding to multiple planes of ice, giving them more potent antifreeze activity (Figure 2).[74] However, MpAFP mostly uses a long flat surface of outward projecting Thr-Gly-Asn motifs as its ice binding surface.[73]

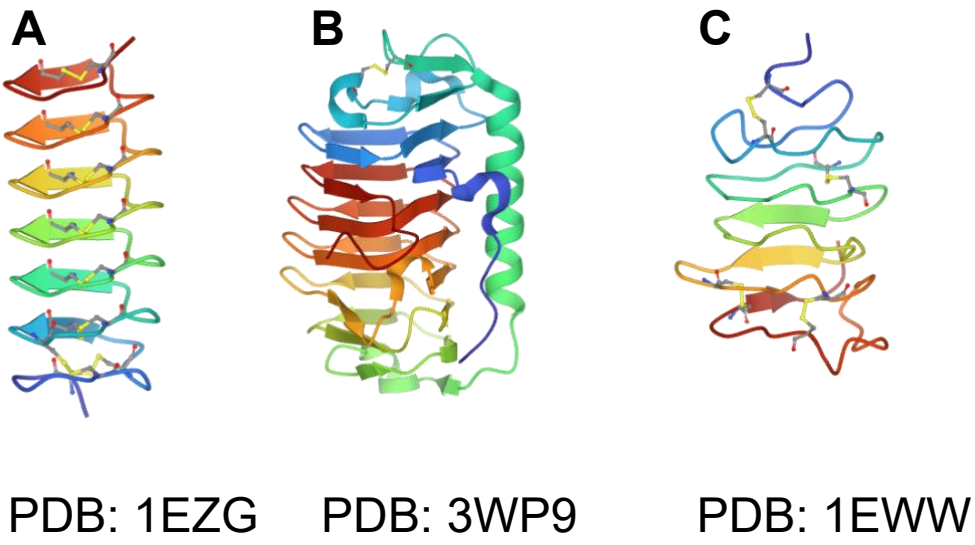

Figure 2: Examples of hyperactive AFP structures. (**A)** Crystal structure of an AFP from the mealworm beetle *Tenebrio molitor* (TmAFP).[75] **(B)** Crystal structure of an AFP from the Antarctic sea ice bacterium *Colwellia sp.* (ColAFP).[76] **(C)** Solution structure of an AFP from the spruce budworm beetle (sbwAFP).[77]

V. Insect Antifreeze Proteins

Insect antifreeze proteins have been found to have potent thermal hysteresis activity and are hyperactive in most cases.[4] As with most hyperactive AFPs, insect AFPs

have a large ice binding surface consisting of a series of Thr-X-Thr repeats. These outward-facing Thr residues are on a flat ice binding surface of the β-helical protein which is stabilized by disulfide-bonded cysteines.[78] Apart from the aforementioned TmAFP, the antifreeze protein from the longhorn beetle *Rhagium inquisitor* (RiAFP) has also been well-studied.[79]

VI. Antifreeze Protein Properties

The main functions of AFPs are ice crystal shaping, ice recrystallization inhibition, and thermal hysteresis.[5] A typical ice cube is made up of many individual ice crystals of non-uniform size and shape. Hexagonal ice crystals have three basic planes: basal, prism, and pyramidal (Figure 3). The ice crystals form about the basal plane (c-axis), prism plane (a-axis), and pyramidal plane (between the c- and a-axes).[5] This planar binding allows AFPs to have the ability to dynamically shape these ice crystals (Figure 4). This function gives another distinction between moderately active and hyperactive AFPs. Moderately active AFPs bind only to the prism and/or pyramidal planes of ice, and in doing so mainly prevent crystal growth about the a-axis. Thus, ice crystal expansion is limited to the c-axis, resulting in a needle-like, hexagonal bipyramidal shape.[6,30,80] Alternatively, hyperactive AFPs bind to ice on both the prism and basal planes, restricting ice growth along all axes, ultimately resulting in an ellipsoid or 'lemon shaped' ice crystal.[6,81] Fluorescence-based ice plane affinity (FIPA) analysis is a technique used to observe the ice crystal planes to which AFPs bind.[82] AFPs are labeled with a fluorescent tag or dye and then slowly incorporated into a static ice crystal. This static ice crystal must be pre-

formed, hemispherical, and oriented such that the a- and c-axes are determined. Images are then taken under filtered UV light to visualize the AFP-bound ice crystal planes.

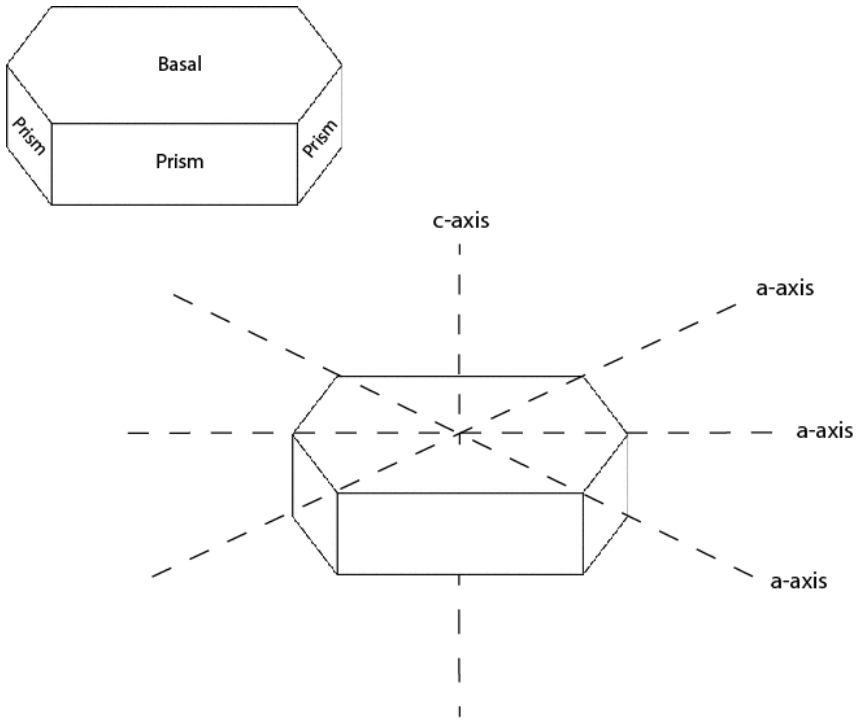

Figure 3*:* A model of the planes associated with a hexagonal ice crystal. The basal plane corresponds with the c-axis, and the prism plane corresponds with the a-axis.[83]

The second function of AFPs is ice recrystallization inhibition (IRI). Ice recrystallization is the phenomenon that occurs when many small ice crystals fuse together to form larger crystals.[84] The smaller ice crystals have high internal energy, and the resulting fusion and formation of larger ice crystals is thermodynamically favorable.[85,86] IRI is especially important for cells that experience multiple freeze/thaw cycles.[87] Expanding ice crystals, both endogenous and exogenous, mechanically destroy

cells, tissues, and the textures of frozen materials, especially during near zero freeze-thaw cycles.[66,88,89] AFPs have been shown to inhibit ice recrystallization by binding to ice, even at low concentrations.[90] IRI activity is measured by using a 'splat assay' with polarized optical microscopy (POM) and or digital imaging.[91,92] In a splat assay, a solution of a known concentration of AFP is dropped onto a frozen glass slide or coverslip, and the resulting instantly frozen wafer of ice is immediately transferred to a cooling stage and observed using POM and/or digital imaging. IRI activity is quantified by taking measurements of the ice crystals and calculating the mean ice crystal grain size.[92,93] IRI is thought to be an important characteristic for membrane protection, as it is likely the most crucial AFP function for freeze-tolerant organisms.[85,94,95]

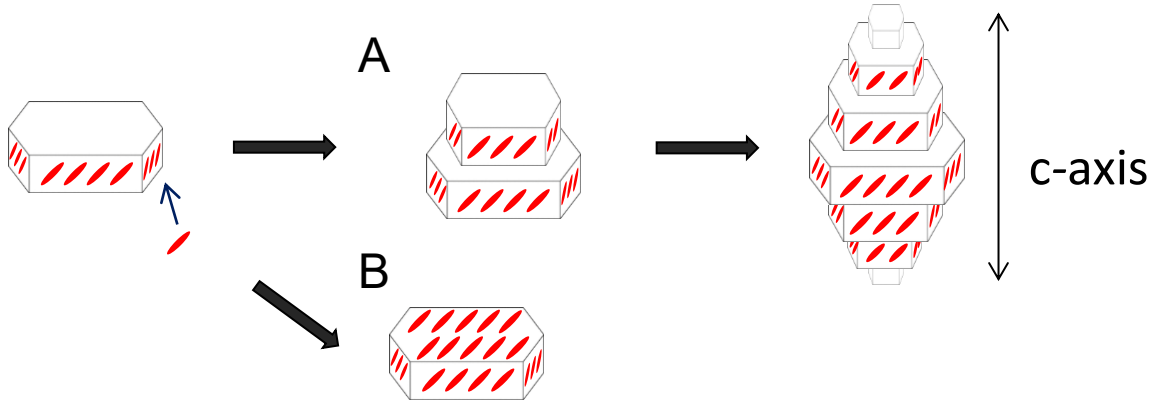

Figure 4: The ice crystal shaping function of antifreeze proteins (red). (A) Moderate active antifreeze proteins bind along the prism plane (a-axis) of ice, resulting in growth about the c-axis and a 'needle-like' hexagonal bipyramidal crystal shape. (B) Hyperactive antifreeze proteins bind along both the a- and c-axes of ice, resulting in an ellipsoid hexagonal disk crystal shape.

The third function of AFPs is thermal hysteresis activity (THA). By binding to ice crystals, AFPs lower the hysteresis freezing point and create what is known as a 'thermal hysteresis gap' (Figure 5).[96] Within this thermal hysteresis gap, the growth of ice crystals

is prevented, until the temperature is decreased to the non-equilibrium freezing point.[97,98] This means AFPs lower the freezing point (T_f) below the melting point (T_m) to achieve a temperature difference known as thermal hysteresis activity (THA) $T_m - T_f = THA$.[67,97] This freezing point depression occurs without affecting the melting point. THA is achieved when binding of the AFP to an ice plane induces curvatures in the ice between binding sites.[99] These curved ice surfaces induced by AFP binding are energetically unfavorable for continued ice crystal growth.[66,67] If an AFP binds both the basal and prism plane of ice, it has higher THA than an AFP that only binds to the prism and/or pyramidal ice planes and is typically considered to be hyperactive (Figure 1).[24,100] THA is typically measured by nanoliter osmometry with a cooling stage and visualized with a light microscope and/or digital camera.[5,81] This is also a means of observing dynamic ice crystal shaping. With nanoliter osmometry, solutions containing known concentrations of AFPs are completely frozen (-40 °C), then the system temperature is increased until a single ice crystal is observed. The single ice crystal is then very slowly cooled under visual observation and precise temperature measurements until a sudden burst of ice crystal growth. The temperature when a single ice crystal remains is the melting point and the temperature of the ice crystal burst is the freezing point. The difference between these temperatures is the THA of the AFP solution.[81] THA is most beneficial for the survival of freeze-avoidant organisms such as shallow water dwelling polar notothenoids.[5] In these fish, AF(G)Ps prevent the growth of accumulated internalized ice crystals in organs, such as the spleen, and allows the organism to survive despite these ice crystals being present for the entire life of the fish.[98]

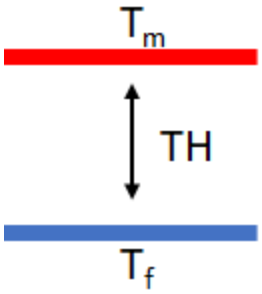

$$TH = T_m - T_f$$

Figure 5: Thermal hysteresis (TH) activity is the difference between the melting point (T_m) and the freezing point (T_f) of water.

VII. Ice Binding Mechanisms

AFPs are capable of binding to a single ice crystal and preventing ice crystal growth that would otherwise occur on an unbound surface. In Figure 3, the various crystal planes of ice to which AFPs bind can be seen.[66,78] The exact mechanism of ice binding has been debated for over 40 years.[101] The first theory proposed in 1977 was the adsorption-inhibition mechanism.[99] This theory describes a step-pinning model in which AFPs irreversibly bind to growing nascent ice crystals. The bound AFPs physically take up space on the ice crystal, preventing growth about the bound portion, and forcing ice crystals to grow between the areas bound by AFPs. The crystal growth occurring between these bound AFPs produces an ever-increasing curvature in the ice surface, once a certain critical surface density is reached. This curvature is thermodynamically unsuitable for continued ice growth and therefore decreases the freezing point via the Gibbs-Thompson (Kelvin) effect.[97,102,103] THA is observed when the aforementioned AFP binding-induced ice curvature causes any further ice growth to be stopped.[99]

One of the more recently proposed theories for the ice binding mechanism of AFPs is known as the anchored clathrate model. This theory describes ice-like water forming a

clathrate, or water cage, about the hydrophobic methyl group of the previously described Thr residues in the AFP involved with ice binding. Hydrogen bonding anchors this clathrate to the hydroxyl groups of the Thr residues as well as the main chain nitrogen atoms of the AFP. The AFP now has a quasi-liquid membrane around it, formed by the clathrate, and binds to the ice surface while preventing further ice crystal growth.[33,73,104] It should be noted that the spacing of these Thr residues on the ice binding surface of AFPs are proposed to be complimentary to the spacing of water molecules in the ice lattice along both the a- and c-axes.[105]

Interestingly, the ice-binding domains of fish and insect AFPs are flat and relatively hydrophobic. In order to gain more understanding of the importance of specific amino acids for both ice-binding and antifreeze activity, the ice-binding sites of type I and III AFPs have been altered.[45,90] While there is no universally accepted ice binding mechanism, ice binding likely involves a complex combination of van der Waals interactions, hydrogen bonding, hydrophobic forces, and water structuring. [5,22,30,33,73,106-108] The duration of ice binding is also debated. AFPs were originally thought to bind irreversibly to ice, however, studies have shown this is not always the case and binding can be reversed.[101,109,110] More recently, a GFP-tagged type III and GFP-tagged insect AFP observed under fluorescence microscopy show a “quasi-permanent” ice binding.[111,112]

VIII. ApAFP752

The insect antifreeze protein ApAFP752 is a 9.4 kDa AFP from the central Asian desert beetle *Anatolica polita*. *A. polita* is commonly found in the Gurbantunggut desert area of the Xinjiang province of China. These deserts can experience extreme temperature

fluctuations up to 40 °C in a single day, and lows down to -40 °C.[105,113,114] These extreme temperatures necessitate ApAFP752 having high THA, similar to other insect AFPs. Homology models predicted this protein to be a right-handed parallel β-helix consisting of six repetitive 12-amino acid loops.[105] It is important to note all published studies have been done using a thioredoxin fusion protein TrxA-ApAFP752, as the Varga group has been the first to successfully stabilize and study the pure, non-fusion ApAFP752.[105,113-116] The structure of ApAFP752 has been determined by nuclear magnetic resonance (NMR) spectroscopy and resolved using CS-Rosetta (Figure 6) (unpublished data).[117,118] ApAFP752 is a right-handed β-helix stabilized by disulfide bonded cysteine residues with a flat ice binding surface consisting of multiple Thr-Cys-Thr repeats. This structure is similar to a previously reported homology model from Mao *et al*.[105] The structure is also similar to other insect AFPs, such as those from the beetles *Tenebrio molitor* (TmAFP) and *Rhagium inquisitor* (RiAFP).[79,119] TmAFP and RiAFP both have a Thr-X-Thr ice-binding motif, however X is always a cysteine residue in *Ap*AFP752. TmAFP, RiAFP, and ApAFP752 are all β-helical proteins.[71] These cysteine residues are disulfide bonded to other cysteine residues on the opposing side of the helix, increasing structural rigidity and creating the flat ice binding surface necessary for the ApAFP752's thermal hysteresis activity.[120] The β-helix of RiAFP is only stabilized by a single disulfide bond. Both TmAFP and ApAFP752 have their β-helical secondary structure stabilized by multiple intraloop disulfide bonds, where a single helical turn consists of 12 amino acid residues. Additionally, each ice-binding surface is dominated by five parallel β-sheets. The activity of ApAFP752 as a TrxA-ApAFP752 fusion protein has been previously demonstrated with the use of differential scanning calorimetry (DSC) and has been shown to confer partial

cryoprotection to human skin fibroblast cells and *Xenopus laevis* eggs.[115,121-124] It should be noted that the THA of TrxA-ApAFP752 measured via DSC was 0.65 °C.[124] This measured THA is not as high as other β-helical AFPs, however, these other AFPs were measured by a different means, nanoliter osmometry with a cooling stage.[77,125,126] Also of note, is the fact that TrxA-ApAFP752 has been observed to cause the formation of rounded ellipsoid ice crystals. This indicates binding of both the prism and basal planes of ice, and by some definitions would make TrxA-ApAFP752 a hyperactive AFP. These reasons, as well as the structural similarities between ApAFP752 and other hyperactive β-helical AFPs, particularly in the Thr-X-Thr ice binding motif, warrant future studies to measure the THA of ApAFP752 via nanoliter osmometry with a cooling stage, as a more direct comparison.

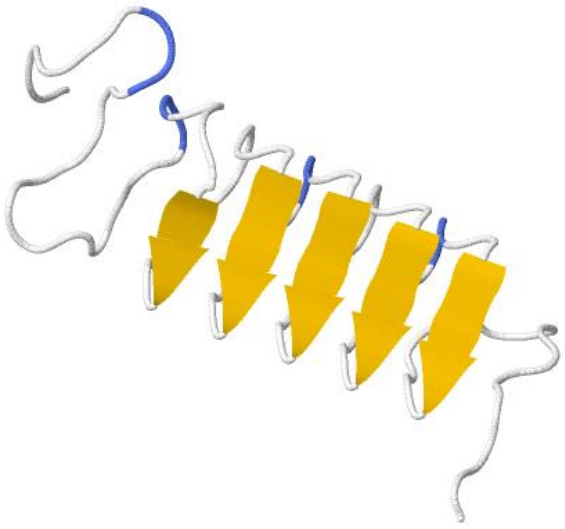

Figure 6: The structure of ApAFP752 determined by NMR and resolved using CS-ROSETTA. Yellow arrows correspond to the flat ice-binding surface.

CHAPTER 2

INTRODUCTION TO CRYOPRESERVATION

The field of cryobiology studies sub-physiological temperature effects on biological systems. Within this field, cryopreservation involves protecting these biological systems from the destructive effects of freezing. Cryopreservation is a powerful tool for advancing development in the fields of agriculture, food science, and medicine.[127-131] For example, in the animal agricultural industry, cryopreservation of sperm amounts to billions of dollars for international trade.[132] Apart from the large strides in reproductive technologies, new cryopreservation methods are being developed to reduce freezing damage in plants.[133] In medicine, cells, tissues, embryos for in-vitro fertilization, and organs must be cryopreserved for research, development of therapeutics, and transplantation.[134-136] The aforementioned research also calls for a need to further improve existing cryopreservation methods, as well as develop novel means of cryopreservation. Improving current methods and developing new methods of cryopreservation can be daunting due to the multiple factors that must be taken into account. In the first place, the exact mechanisms of freezing damage are not completely understood, which can be further complicated by the need to optimize cryopreservation methods based on the types of cells and/or tissues present as well as the selected method of cryopreservation.[5] Here we will focus on cryopreservation as it pertains to cell-based research.

A specific example of cell-based research is found in the cutting-edge area of cellular therapy. Cellular therapies such as those using stem cells and CAR-T cells offer

precise, potent, and cutting-edge treatment options for complex diseases, such as cancer, neurodegeneration, hematologic diseases, inflammatory bowel disease, cardiovascular disease, and diabetes.[137-142] Immune cells, adult, embryonic, hematopoietic, induced pluripotent, and mesenchymal stem cells, as well as hepatocytes are commonly used in cellular therapies.[143-145] These cells cannot be stored at 4 °C for more than 2-4 days due to decreased viability from metabolic decline.[143] In order to address this issue, manufacturers often turn to lower temperatures (below -80 °C or below -140 °C) using cryopreservation for a more practical, longer-term storage solution.[131,146] Likewise, eggs and embryos are also frozen to temperatures below -140 °C for long-term storage.

I. Freezing

Water in frozen biological solutions is separated into three categories: free water, weakly bound water, and tightly bound water (Figure 7).[147] Of these three categories, the first to freeze is free water. Free water is defined as water which is unbound to non-water constituent molecules of the biological solution and freezes from about 0 to -4 °C.[148] Weakly bound water requires a lower temperature to freeze than free water (about -4 to -20 °C), and tightly bound water will freeze at temperatures far below -20 °C or does not freeze.[149] This is determined mainly by the increased solute concentration in weakly bound or tightly bound water. The increase in solute concentration, among other changes, lowers the freezing point of the water in the biological solution.[150] As each biological solution may have differing cells, concentration, and media/serum conditions, the amounts of weakly bound or tightly bound water differ. This in turn changes the freezing

curve for each unique biological solution. This freezing point depression is due to the colligative properties of solutions.

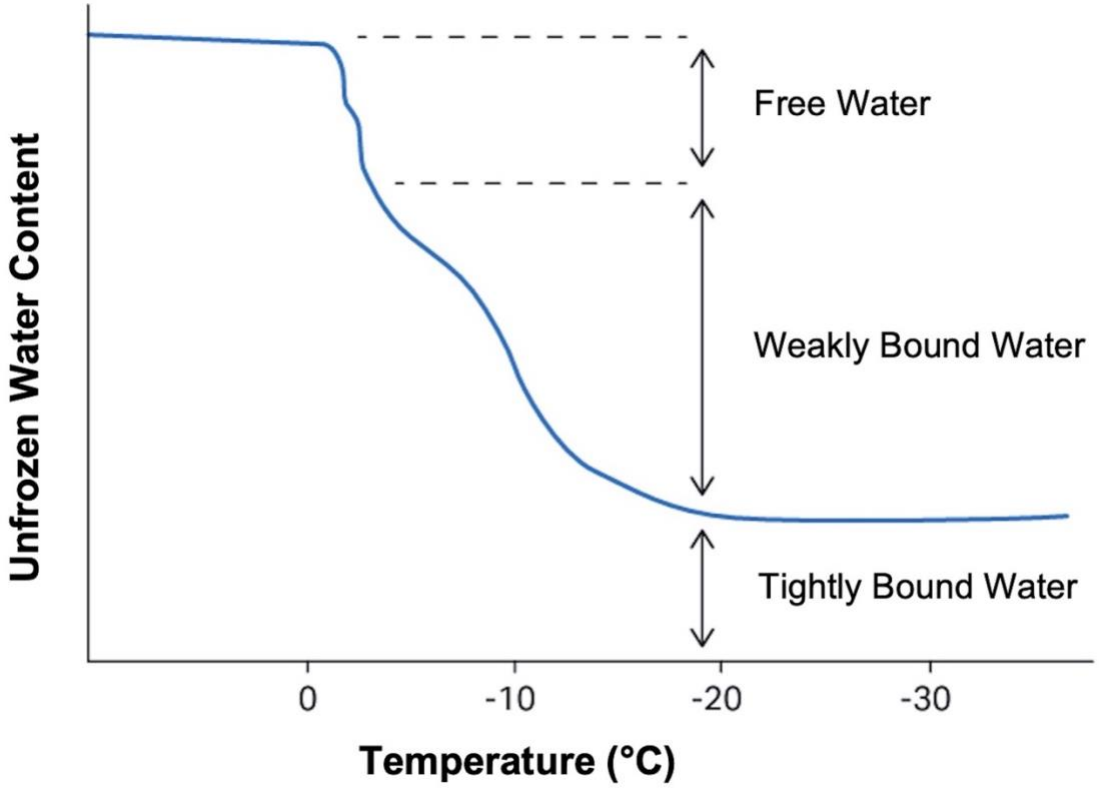

Figure 7. A freezing curve demonstrating the tentative definition of “weakly bound water” and “tightly bound water”. Modified from Poulsen and Lindelov.[147,150]

Biological solutions are able to be stored frozen for extended periods of time. However, there are 3 different reactions that occur in frozen biological solutions and each reaction has a different temperature optima.[147] The reactions occurring in frozen biological solutions are enzymatic (enzyme activity), the browning (Maillard) reaction, and auto-oxidation (Figure 8).[147] Briefly, sub-freezing auto-oxidation occurs when oxygen is available to perform oxidative processes. The browning reaction is mainly studied in food science, where this reaction changes the color, taste, and smell of foods. Without getting

overly technical, the browning (Maillard) reaction is a series of ring opening reactions in sugars. Typically, enzymatic activity decreases as temperature decreases due to slower moving molecules and therefore reduced frequency of enzyme-substrate collisions. However, after the freezing temperature lowers below 0 °C, solute concentration increases, bringing reactive molecules in nearer proximity, and enzymatic activity actually increases until a certain temperature is reached. As demonstrated by the theoretical freezing curves in Figure 8, about -80 °C is a point at which auto-oxidation, the browning (Maillard) reaction, and enzyme activity are at near theoretical minima. This is a reason for freezers being set to such a temperature for relatively long-term storage of many biological samples. For storage at -80 °C there are also a larger selection of freezing containers, more available space, etc., over storage at lower temperatures requiring liquid nitrogen. However, all three reactions will continue to take place to some extent at -80 °C. Liquid nitrogen vapor phase (-196°C) is below the theoretical maxima for all three reactions and is therefore the most suitable for long-term freezing of biological solutions and cells.

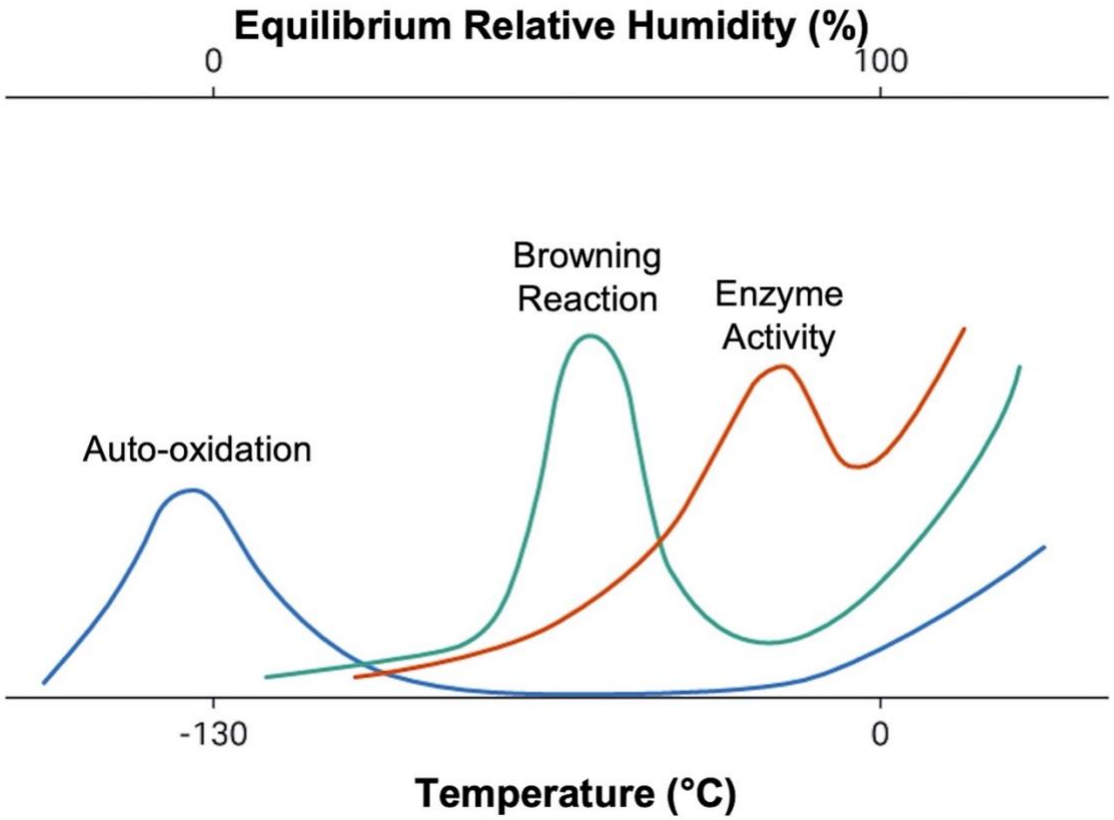

Figure 8. Curves demonstrating the varying optima and influence of temperature and water activity on the three main reactions occurring in frozen biological solutions: auto-oxidation, browning, and enzyme activity (partly theoretical). Modified from Poulsen and Lindelov. [147,150]

II. Cellular Freezing Damage and Mechanisms

Freezing living cells in suspension diminishes the viability of the cells in a multi-event process.[151] As the solution is cooled, water surrounding the cells is the first component in the cell suspension to freeze and change to ice. This freezing process begins at temperatures below 0 °C, and the actual temperature of freezing depends on the varying supercooling properties of the suspension. The liquid water begins to solidify and form ice crystals as the suspension of cells is cooled. When these ice crystals begin to form, an exothermic reaction occurs where heat energy, known as the latent heat of fusion, is

released. This exothermic reaction can be observed with a calorimeter by a measurable rise in the temperature of the cell suspension. Ice crystal formation is stochastic in the sense that the probability of ice formation is proportional to the amount of water in the suspension.[152] This stochastic nature of ice formation means a larger volume has a higher probability of ice formation than does a smaller volume.[153] The extracellular space surrounding the cells is the first area of ice crystal formation because it is much larger than the volume of any individual cell within the solution.[152,154] During cooling, any dissolved components are not incorporated into the developing ice crystals. When water solidifies as ice, it expands and becomes less dense. This decrease in density causes the forming ice to float and pushes the excluded components, such as salts, downward in the solution. These excluded components in time become supersaturated and viscous and can possibly precipitate out and crystallize.[150]

The molecules of water must align with each other in a strict lattice to form ice. When solutes such as salts are present, the structure of ice is disrupted, and ice forms with mostly pure water with few other molecules present.[152,155] As mentioned before, the solutes are excluded into an unfrozen fraction containing very high concentrations of the various solutes (proteins, sugars, etc.).[156] This concentration of solutes potentially damages cells in various ways and further depresses the freezing point. The high solute concentration can change protein conformation, phospholipid bilayer structure, and salt out proteins in the cells within the freezing solution. High solute concentrations can also cause tremendous osmotic stress on the cells, as water moves across the plasma membrane and out of the cells and into the extracellular space in an attempt to re-

equilibrate the solute gradient.[151] This further increases the salt concentration and depresses the freezing point.

Apart from this solute damage from changes in electrolyte concentration, dehydration, and physical damage to cells due to the ice crystal formation, there are yet more mechanisms to consider when cryopreserving cells.[157] In fact, many mechanisms are responsible for the damage caused during freezing. In addition to the dehydration, solute effects, and intracellular ice formation, other damaging effects include molecular effects such as biochemical pathway uncoupling, decreased available energy and metabolic activity, and stress response pathway activation.[151,158,159] These all need to be considered when cryopreserving cells, as many of these effects are both temperature and time sensitive. For example, even at -80 °C metabolism is not stopped, but slowed, and metabolic waste products cannot be cleared due to the low temperature. This can eventually cause an accumulation of these toxic metabolic waste products that can damage cells or activate stress responses upon thawing.[151]

III. Cooling Rate

The rate at which the cell solution is cooled affects the cells in different ways. For example, if the cell solution is cooled too rapidly, that leaves less time for water to escape the cells. The larger volume of water within the cells will become supercooled and can eventually nucleate to form intracellular ice.[151,152] Intracellular ice can cause irreparable damage and is almost always lethal for cells. On the other hand, if the cell solution is cooled too slowly, the cells will be exposed to the high solute concentration for a longer period of time. More osmotic pressure will be applied to the cells and they will undergo

dehydration, both of which can be lethal.[143] This is why the cooling rate is so crucial for cryopreserving cells. There must be a cooling rate that does not cause intracellular ice formation nor cellular dehydration and would therefore be optimal to maximize cell viability.[160-162] The optimal cooling rate varies depending on the type of cell being cryopreserved. For example, a cooling rate of -1 °C/min is optimal for most mammalian cells to retain maximum viability (Figure 9).[151] However, for red blood cells, the optimal cooling rate is ten to one hundred times as fast depending on the makeup of the cryopreservation medium. On the other hand, hepatocytes have an optimal cooling rate closer to 0.5 °C/min.

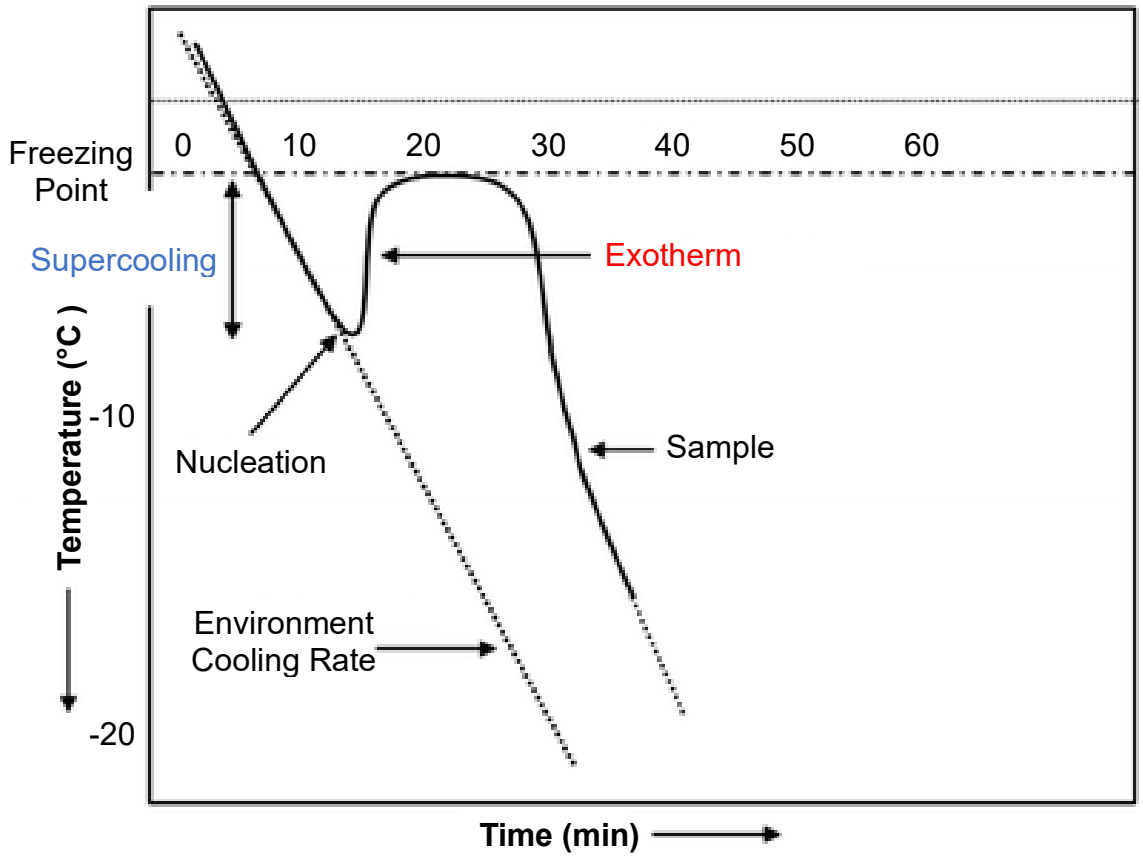

Figure 9. Typical cooling rate profile of cell solution frozen at a controlled, slow rate. The schematic shows both supercooling and the exothermic reaction of nucleation. Modified from Baust 2017.[151]

To achieve a more consistent and controlled rate of cooling, cryovials containing cells can be placed in various freezing containers. The first option for cooling cells is the least expensive, but also the least consistent means of controlled and consistent cooling, and that is a simple insulated container such as a styrofoam box. However, the inconsistency of these simple insulated containers is not suitable for many cell types or applications. For increased consistency a common, cost-effective means of achieving a cooling rate of approximately -1 °C/min is by using a specialized freezing container such as a Mr. Frosty™ or a CoolCell™.[131] A Mr. Frosty™ freezing container is filled with an appropriate volume of isopropanol, then samples prepared in cryotubes are placed in a cryotube holder inside the freezing container. The container is insulated and designed such that it can approximate a cooling rate of -1 °C/min when placed in a -80 °C freezer. After 2 hours, samples reach -80 °C and can remain at this temperature or be moved to liquid nitrogen vapor phase (-196 °C). A CoolCell™ freezing container offers an alcohol-free alternative to the Mr. Frosty™ with a similar protocol. For the most accurate cooling rate and to adjust the cooling rate for other cell types, a programmable controlled-rate freezer is the best option.[151] Cells should be stored at -196 °C (liquid nitrogen), as having them remain at -80 °C can allow for the aforementioned reactions to occur. Over time, these changes can reduce cell function and viability.[163]

IV. Cryoprotective Agents

In an effort to protect cells from the previously mentioned damaging effects of freezing, cryoprotective agents are used. Cryoprotective agents (CPAs) have various mechanisms of action for cryopreserving cells. The exact mechanisms of various CPAs are still unknown and debated, even for some well-studied CPAs. In terms of differentiation, there are two major categories of CPAs: penetrating and non-penetrating (Figure 10).[154,164] As their name implies, non-penetrating CPAs cannot penetrate cell membranes and are typically polymers, such as polyvinyl alcohol (PVA), or small molecules, such as the sugar trehalose.[165-167] Penetrating CPAs, like dimethyl sulfoxide (DMSO) or glycerol are the most commonly used of all CPAs.[152,168]

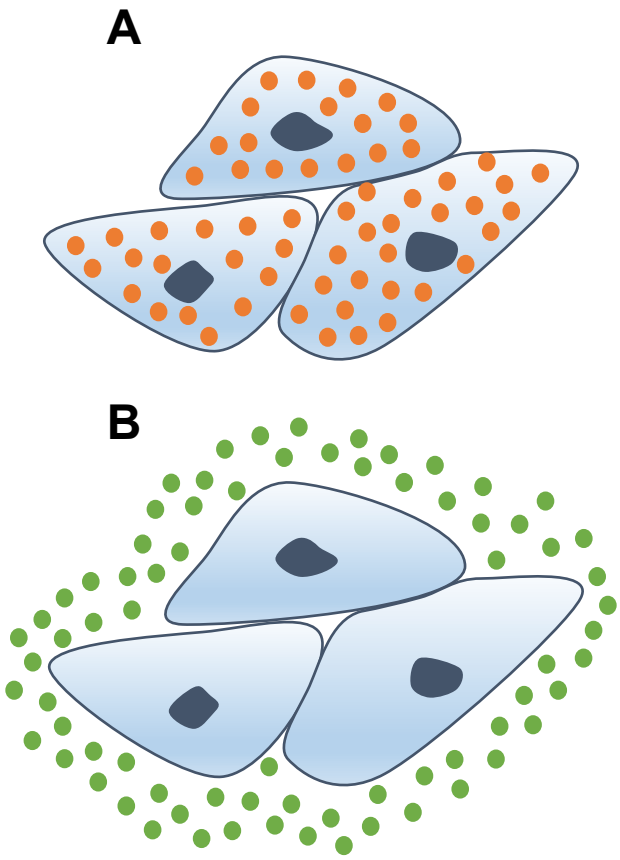

Figure 10. Illustration demonstrating the two major classes of cryoprotectant agents (CPAs) (A) penetrating and (B) non-penetrating. Penetrating cryoprotectants enter cells while non-penetrating cryoprotectants remain in the extracellular space.

Non-penetrating CPAs, like long chain polymers or sugars, are formulated into various cryoprotective solutions. Though they do not enter cells, non-penetrating CPAs prevent ice crystal growth. Non-penetrating CPAs are a less toxic alternative to penetrating CPAs, and can be used to reduce the amount of penetrating CPAs included in a cryoprotective solution.[152] In most cases, non-penetrating CPAs dehydrate the cells by increasing the extracellular osmolarity, or number of solutes, of the extracellular solution. This increased extracellular osmolarity in turn dehydrates the cells via the solute

gradient and increases the concentration of solutes within the cells. The increased concentration of solutes within the dehydrated cells prevents intracellular ice formation.[169] This is the rationale for including non-penetrating CPAs in media used for thawing cells, as they can reduce the rate at which the cells are rehydrated to prevent lysis or traumatic effects of osmotic shock.[152,164] In addition to increasing extracellular osmolarity, there is some evidence that non-penetrating CPAs also have the ability to interact with cell membranes and provide them with a means of stabilization during phase transition, but this is debated.[170]

Penetrating cryoprotectants have a more complex method of protecting cells from freezing damage, as they interact with more than just the extracellular environment. Penetrating cryoprotectants pass through the cell membrane and prevent intracellular ice formation. The penetrating CPAs typically consist of molecules such as alcohols, amides, and sulfoxides.[171] Penetrating CPAs interact with various cellular components and have many different methods of action which are not completely understood. Due to this interaction with cellular components, penetrating CPAs are more toxic than non-penetrating CPAs.

The basic function of penetrating CPAs is lowering the freezing point of the cellular solvent. Penetrating CPAs reduce the propensity of intracellular ice formation and can also reduce the magnitude of dehydration for both the cells themselves and the organelles within them.[143] It should be noted that penetrating cryoprotectants require a certain amount of incubation time to allow them to permeate cells membranes, as they permeate membranes at a rate as much as 100 to 1000 times less than water.[172] This incubation period varies depending on the type of penetrating cryoprotectant being used as well as

the cell and media conditions. The incubation period is essential to functioning as a CPA, because there must be equilibration and distribution of the penetrating cryoprotects in both the intracellular and extracellular compartments.[143] A balance must be found in optimizing the incubation period for the penetrating CPA and mitigating any cellular toxicity by keeping the incubation period to a minimum.[173]

Some penetrating CPAs act by increasing the permeability of cell membranes and thereby enable more water to exit the cell. This decreases the likelihood of intracellular ice formation.[174] The most widely studied penetrating CPAs are DMSO and glycerol, and these CPAs may bind cell membranes and also provide some protection during phase transition. For example, DMSO is able to cause pore formations in membranes at high concentrations, while increasing membrane fluidity and also reducing membrane thickness at low concentrations.[175,176]

In mammalian cell culture, most cryopreservation procedures utilize 5-10% DMSO as the cryoprotectant, but as previously mentioned, DMSO can have harmful effects by exhibiting cellular toxicity, especially when exposed to cells, such as stem cells, at room temperature or warmer.[177] There is a need for less toxic or non-toxic alternatives to DMSO.[173] In some applications, mixtures of non-penetrating and penetrating CPAs, such as ethylene glycol and DMSO, have been shown to have a synergistic effect and provide significant improvement in cryopreservation over each individual CPA.[173] However, the issue of cellular toxicity still remains and the reduction in osmotic stress could be overshadowed by toxicity of the non-penetrating/penetrating CPA mixture, especially those containing DMSO, to the cells being cryopreserved.[143,173] In an effort to reduce the toxicity of CPAs, they can be added gradually in a stepwise manner to achieve the desired

final concentration.[178] This adds time and requires optimization for various cell systems and applications. In addition, the toxicity of CPAs can be reduced by lowering the temperature at which they are added by using an ice bath or refrigerator to keep the system near 4 °C. This would also require optimization to ensure enough time is provided for the penetrating CPAs to be able to permeate the cells at this lower temperature, while ensuring the cells are not exposed to the CPAs for an amount of time that is toxic.[179]

V. Thawing

In order to recover the frozen cells, thawing must occur. In many ways, thawing can have just as critical an impact as freezing on cell survival and recovery.[131,180] Potential issues may arise when considering air exposure, dilution, mixing, and both the rate and temperature of thawing.[151] Typically, thawing should be performed as rapidly as possible (~50 to 100 °C/min). This will help reduce potential ice recrystallization damage, as well as limit exposure time to damaging concentrations of solutes as the ice is melting.[131] Frozen mammalian cell samples must be removed from a -80 °C freezer or liquid nitrogen (-196 °C) storage and actively warmed as quickly as possible to the point of a small ice fraction remaining in the otherwise liquid sample. Air exposure from passive rewarming during the period of time between transferring cells from frozen storage to active thawing can induce damaging intracellular ice formation and, given enough time, could even lead to complete sample loss.[181] Another reason for rapid thawing is to reduce the exposure time of the mammalian cells to toxic CPAs and thereby reduce the cytotoxic damage. The samples must also be mixed continuously and diluted as soon as possible after rapid thawing.[151]

The simplest and most widely accepted method of rapid thawing is with the use of a 37 °C water bath. The cell solution is gently agitated while maintaining contact with the water for about 3-5 minutes depending on the sample conditions. Care must be taken to avoid over-warming of the cell solution to temperatures above refrigerated temperature (approximately 4 °C) , as well as to avoid water bath-related contamination, especially if samples are not capped properly.[182] The cell solution should be warmed to near-refrigerated temperatures close to 4 °C (small ice fraction remaining). Warming the cell suspension to room temperature or warmer adds additional stress to the cells. For example, after thawing, warmed exposure to the cytotoxic CPA could prove lethal to the cells. Another method of rapid thawing is known as dry thawing. This less-common method uses specialized devices which deliver a more sterile and reproducible thawing rate, with some offering a live temperature readout. These dry thawing systems offer automatic agitation to reduce thermal gradients and help ensure sample homogeneity.[151] As with controlled rate freezers, these dry thawing systems have more clinical or industrial applications due to their automation and scaling potential. After visual confirmation that the last remnants of ice are being melted, the sample is then ready for dilution and CPA removal.

After thawing, the CPA must be removed from the cell solution regardless if it is penetrating or non-penetrating. This is achieved with dilution followed by centrifugation and resuspension. There are multiple methods to dilute and reduce/remove the CPA, and different cells and amounts of CPA require different handling techniques.[131] All methods aim to reduce/remove the CPA while mitigating the amount of osmotic shock experienced by the cells. The first method is a single step dilution of the cell solution via immediate

resuspension in ≥ 10 times the volume of fresh, CPA-free complete culture medium.[151] This is typical for cells stored in 5% CPA. Another method is a stepwise dilution to gradually expose cells in solution to fresh, CPA-free complete culture medium. This is to reduce the osmotic shock experienced by cells stored in 10% CPA.[151] The last method of CPA reduction/removal is with density gradient centrifugation using Percoll or Ficoll, and/or using osmotic buffers (ex: mannitol or sucrose) to help prevent cell swelling. These methods are less common and are mainly used for cells that are highly susceptible to freeze/thaw damage, such as hepatocytes.

VI. Viability Assessment

Post-thaw viability assessments are essential to optimizing cryopreservation protocols and determining the best choice for CPA by determining the state of the cells. There are a number of different assays from that can be used, and they can measure a variety of markers for viability and functional activity depending on the cells that were cryopreserved.[183,184] The importance of timing and reliability of post-thaw viability assessments has more recently become of concern in the field of cryobiology.[131,143,151]

In terms of assay selection, there are four tiers based upon the type of viability assessment.[151] Tier 1 assays test for membrane integrity. Tier 2 assays include assessments of enzymatic and molecular mechanisms. Tier 3 assays are cell-specific functional assays that can be performed on certain cells.[145] Finally, tier 4 assays test for proteomic and/or genomic changes, and are still under development. Best practices dictate that 2-3 assays, one from each applicable tier, should be performed to ensure the most accurate viability assessment.[151]

Tier 1 assays are necessary for rapid determination of post-thaw viability. These tests determine cellular membrane integrity, and are also known as live/dead tests.[151] The most common Tier one tests are those that rely on vital dye exclusion, where a vital dye such as trypan blue or erythrosin B is taken up by dead or dying cells with cell membranes that are no longer completely intact. Cells with intact membranes do not take up the vital dye, are left unstained, and are considered living. Tier 1 assays provide important initial viability determinations, but can sometimes overestimate cell viability by not accounting for cryopreservation-induced cell death in the form of apoptosis or necrosis occurring 24-48 hours post-thaw.[185]

Molecular cell death indicators and metabolic activity are the categories of assays which comprise tier 2 assessments. These assays are best performed between 4-48 hours post-thaw to detect longer term cryopreservation-induced cell death.[151] An example of a molecular cell death indicator is the detection of cytosolic enzymes released during necrosis or apoptosis, such as lactate dehydrogenase (LDH).[186,187] The LDH release assay can be detected and quantified by a colorimetric spectrophotometric plate reader. Another example of a common molecular cell death indicator is the Annexin V/PI assay. Apoptotic cells express phosphatidyl serine (PS) and are stained by Annexin V conjugated to a fluorescent dye such as Alexa Fluor 488. Propidium Iodide (PI) enters the membrane of dead or necrotic cells and stains them fluorescent red. Viable cells are left unstained. Annexin V/PI is multiparametric as it detects the PS on the surface of cells undergoing apoptosis, while PI determines membrane integrity. Annexin PI requires the use of a flow cytometer for detection and quantification.

Metabolic activity assays are good determinants of cell viability, proliferation, and cytotoxicity. Common examples include the MTT/MTS/XTT assays as well as the Alamar blue assay. The MTT/MTS/XTT assays involve cellular uptake of a yellow tetrazolium salt, which is then reduced by metabolically active cells to form an orange formazan dye.[188] For the Alamar Blue assay, resazurin permeates cells and is reduced by metabolically active cells to form the colored product resorufin.[189] The amount of colored product produced by the MTT/MTS/XTT and Alamar Blue assays can then be detected and quantified by a colorimetric spectrophotometric plate reader.

Tier 3 assays are functional assays to determine if viable cells have retained their specific functions. These assays are not appropriate for cells that do not have specific and detectable functions. Some cells, such as hepatocytes, can test as viable in tier 1 and/or tier 2 assay but no longer function as they did prior to cryopreservation.[151,190,191] Albumin secretion, cytochrome p450, and urea production can be negatively affected by cryopreservation, and functionality should be tested post-thaw. Cell specific functional assays are also necessary for immune cells to determine any changes to cell surface markers or protein receptors.

Tier 4 assays are a new set of assays to be considered. These assays are still under development and can be the most complicated of all four tiers.[151] The aim of tier 4 assays is to not only determine structural damage, but also to determine potential functional alterations, molecular changes, and/or selection or enrichment of subpopulations for cells following cryopreservation. These types of advanced and specific analyses are modeled after molecular diagnostics for diseases and could potentially provide comparisons between sample sets. Once developed, a tier 4 assay would have

the potential to replace some assays from other tiers and provide valuable genetic and functional information to assess cells used in cellular therapies and drug development.

VII. Additional Considerations

Both the age and quality of a cells can affect their ability to survive freezing. Cells subjected to stresses from manipulation or poor culture conditions prior to cryopreservation have significantly decreased function and viability post-thaw.[151] Multi-tiered viability testing is not only recommended for post-thaw assessments, but is also ideal to ensure the cells are damaged as little as possible prior to cryopreservation. Non-transformed cells, such as normal diploid somatic cells, should be cryopreserved at low passage numbers. Some types of cells require use at fewer than 6-12 passages to avoid senescence related functionality/viability issues.[192,193] For example, if some cells are too old (passage numbers above 12) they are less resistant to stresses associated with freezing. In general, cells harvested from late log or early stationary populations can have the greatest chance for recovery. However, the window of optimal growth can be quite narrow, and this is another reason for testing from more than one of the aforementioned tiers.

CHAPTER 3

EXPRESSION, PURIFICATION, AND CHARACTERIZATION OF ApAFP752

Cryoprotection is of interest in many fields of research, necessitating a greater understanding of different cryoprotective agents. In recent years, antifreeze proteins have been identified that have the ability to confer cryoprotection in certain organisms. Antifreeze proteins are an evolutionary adaptation that contributes to the freeze resistance of certain fish, insects, bacteria, and plants. These proteins adsorb to an ice crystal's surface and restrict its growth within a certain temperature range. In this chapter, we will examine **Aim 1: Characterize the antifreeze activity of the antifreeze protein ApAFP752** (see "Project Aims and Hypothesis").

I. INTRODUCTION

Effective cryoprotection is an important, unsolved, practical problem in medicine, pharmaceutical and food industries, and agriculture. Near-freezing and freezing temperatures are not ideal for the survival of eukaryotic organisms, but in nature there are a variety of compounds and strategies for freeze avoidance and freeze tolerance to enhance the survival of certain organisms that experience extremely low temperatures. Antifreeze proteins (AFPs) were originally discovered in the blood of Antarctic notothenіid fish[3] and have since been identified in other fish,[34,194] insects,[13] plants,[7,58] and bacteria[195] which live in extreme cold temperature environments. AFPs are structurally diverse; however, all AFPs have thermal hysteresis properties and inhibit ice recrystallization (the growth of small ice crystals into large ones) via the direct binding of AFPs to the surface of ice crystals.[90,196] Thermal hysteresis is the ability of AFPs to depress the freezing point of the solution without significantly affecting the melting point.[4,23] Insect AFPs are considered 'hyperactive' AFPs[24,100,197] relative to fish AFPs due to their higher TH activity, a property which helps insects survive much colder temperatures on land (e.g., -40 °C) than the temperatures fish encounter in the arctic ocean (e.g., -1 to -2 °C).[198] Although the exact mechanism of ice-growth inhibition at the molecular level has been much debated, it is likely that both the hydrophobic effect and hydrogen bonding contribute to AFP adsorption to ice.[73]

These studies deal with *Ap*AFP752, which originates from the desert beetle *Anatolica polita* found in the Gurbantunggut Desert within the Xinjiang province of China and parts of Central Asia.[116,199] *Ap*AFP752 is an ortholog of the antifreeze proteins DAFP from the beetle *Dendroides canadensis* [104,200] and *Tm*AFP from *Tenebrio molitor,*[60] both

of which are extensively disulfide bonded right-handed β-helical proteins,[120,201] and the ice-binding β-sheet contain Thr-Cys-Thr motifs in which the Thr residues line up with the oxygen atoms of the ice crystals. It is important to note that the most prior studies on AFP applications have utilized the better-characterized fish derived AFPs. AFPs from insects are thought to be more promising candidates for cryoprotection,[13] because they are hyperactive and the ice morphology they promote is different from fish AFPs (i.e., 'lemon-shaped' vs. 'needle-shaped' ice crystals respectively).[4,9] The protein is expressed in the laboratory as a thioredoxin-antifreeze fusion protein (TrxA-*Ap*AFP752) and has been shown to protect *E. coli* cells against cold damage in a concentration-dependent fashion[105] and to enhance the viability of human skin fibroblast cells after freeze-thaw.[115,121,122]

II. Expression and Purification of TrxA-*Ap*AFP752

Expression and purification of TrxA-*Ap*AFP752 has been reported previously.[115] The recombinant plasmid pET32b containing the TrxA-*Ap*AFP752 gene[105] (NCBI Accession code: MW187079) was transformed into *Escherichia coli* BL21 (DE3) pLysS (Promega). Luria-Bertani (LB) agar plates with 100 μg mL^{-1} ampicillin were inoculated with the transformed cells. Plates were then incubated at 37 °C for 12-14 hours. Single colonies were selected and used to inoculate 30 mL aliquots of Luria-Bertani (LB) medium with 100 μg mL^{-1} ampicillin. The inoculants were incubated in an orbital shaker at 37 °C and 225 rpm for 12-18 hours. These precultures were then used to inoculate LB medium with 100 μg mL^{-1} ampicillin at a rate of 4mL preculture/1L LB medium and incubated in an orbital shaker at 37 °C and 225 rpm until an optical density at 600 nm (OD_{600}) of 0.65 to 0.80 was achieved. Cells were then harvested by centrifugation at 9559 x *g*, 4 °C for 20

minutes, and resuspended in a minimal growth medium consisting of ^{15}N enriched (>99%) ammonium chloride (NH_4Cl) at a ratio of 1:4 minimal growth medium to LB broth. The cells were then incubated at 15 °C, 225 rpm for 45 minutes, and protein overexpression was induced by adding 1 mL of 400 mM (final concentration 0.4 mM) isopropyl β-D-1-thiogalactopyranoside (IPTG) and incubated at 15 °C, 225 rpm for 12 hours.[115] Finally, the cells were pelleted by centrifugation at 9559 x *g*, 4 °C for 25 minutes, and pellets were either used immediately or frozen at -80 °C for long term storage.

For purification, cell pellets were resuspended in a lysis buffer containing 3 mL 50 mM sodium phosphate, 150 mM NaCl, 30 µL Halt™ Protease Inhibitor Cocktail (Thermo Scientific), and 6 µL Benzonase Nuclease pH 8.0 per pellet. Resuspended cells were lysed by four rounds of pressing with a French Press at 1500 psi. Next, the cell lysate was centrifuged at 20,217 x *g*, 4 °C for 30 minutes, the supernatant was then collected and filtered through .45 and .22 µm filters. Fast protein liquid chromatography (FPLC; GE Healthcare ÄKTA purifier 900) was performed using Ni-affinity (first fast flow then high pressure) columns to take advantage of the 6xHis tag engineered into the protein sequence (Figures 11-14). The protein was eluted from the columns using a 500 mM imidazole gradient and dialyzed or buffer exchanged into a buffer containing 50 mM potassium phosphate, 20 mM NaCl, pH 8.0.

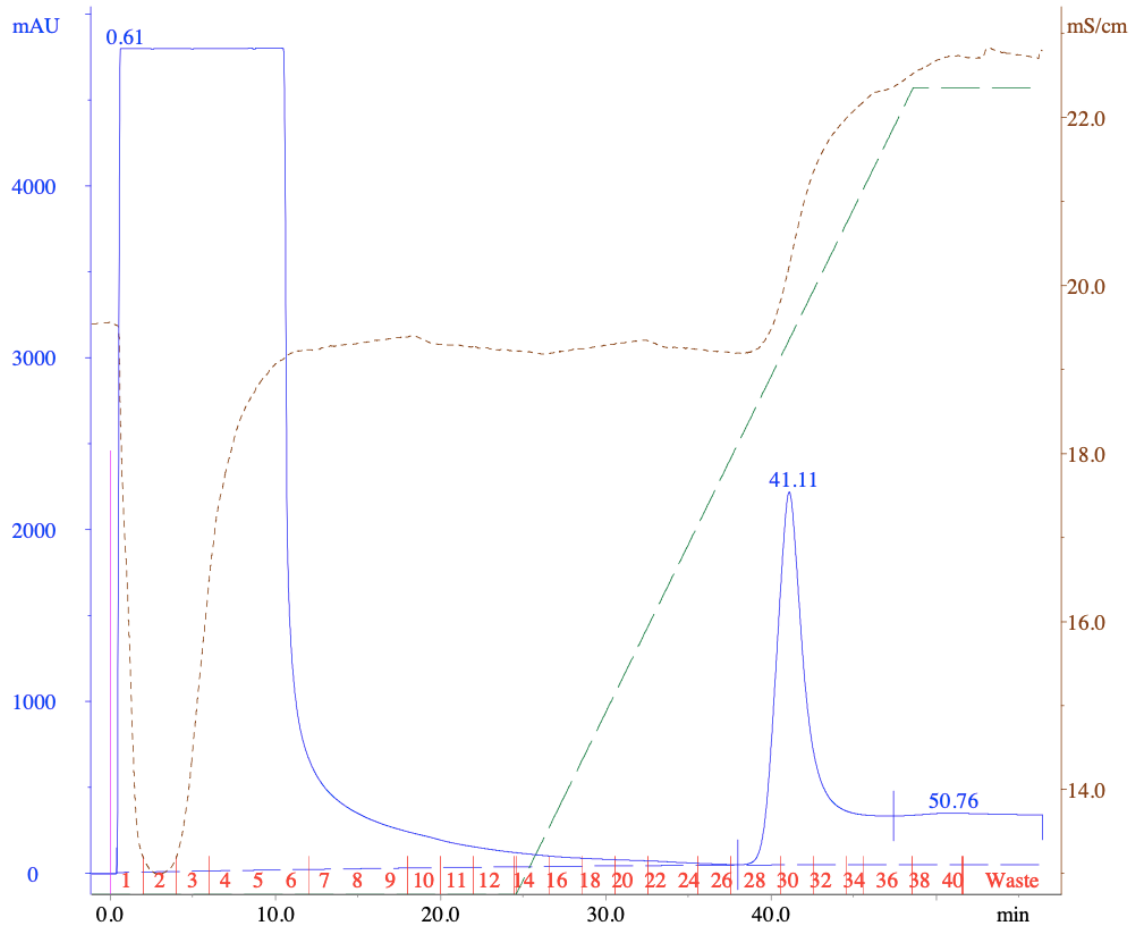

Figure 11. Chromatogram of the first of 2 HisFF Ni-affinity purifications for TrxA-ApAFP752 sample preparation. Colored lines represent following measurements: (Green) concentration of elution buffer relative to the starting imidazole concentration (%); (Blue) absorption at 280 nm; (Brown) conductivity of sample/solution in units of mS cm^{-1}. The peaks at fractions 28-32 correspond with the elution of TrxA-ApAFP752 fusion protein. Peaks prior to fraction 15 correspond with non-6xHis proteins, aggregated proteins, and debris.

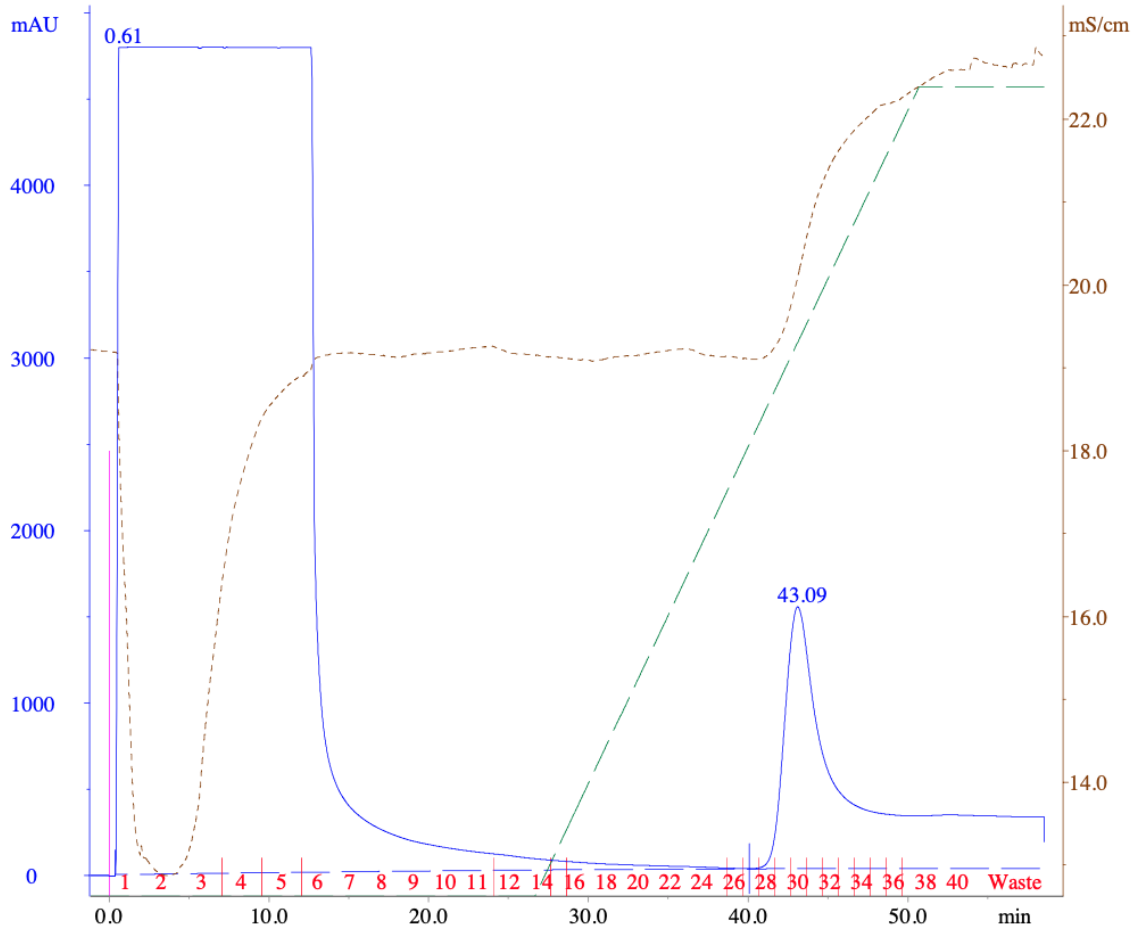

Figure 12. Chromatogram of the second of 2 HisFF Ni-affinity purifications for TrxA-ApAFP752 sample preparation. Colored lines represent following measurements: (Green) concentration of elution buffer relative to the starting imidazole concentration (%); (Blue) absorption at 280 nm; (Brown) conductivity of sample/solution in units of mS cm^{-1}. The peaks at fractions 28-32 correspond with the elution of TrxA-ApAFP752 fusion protein. Peaks prior to fraction 15 correspond with non-6xHis proteins, aggregated proteins, and debris.

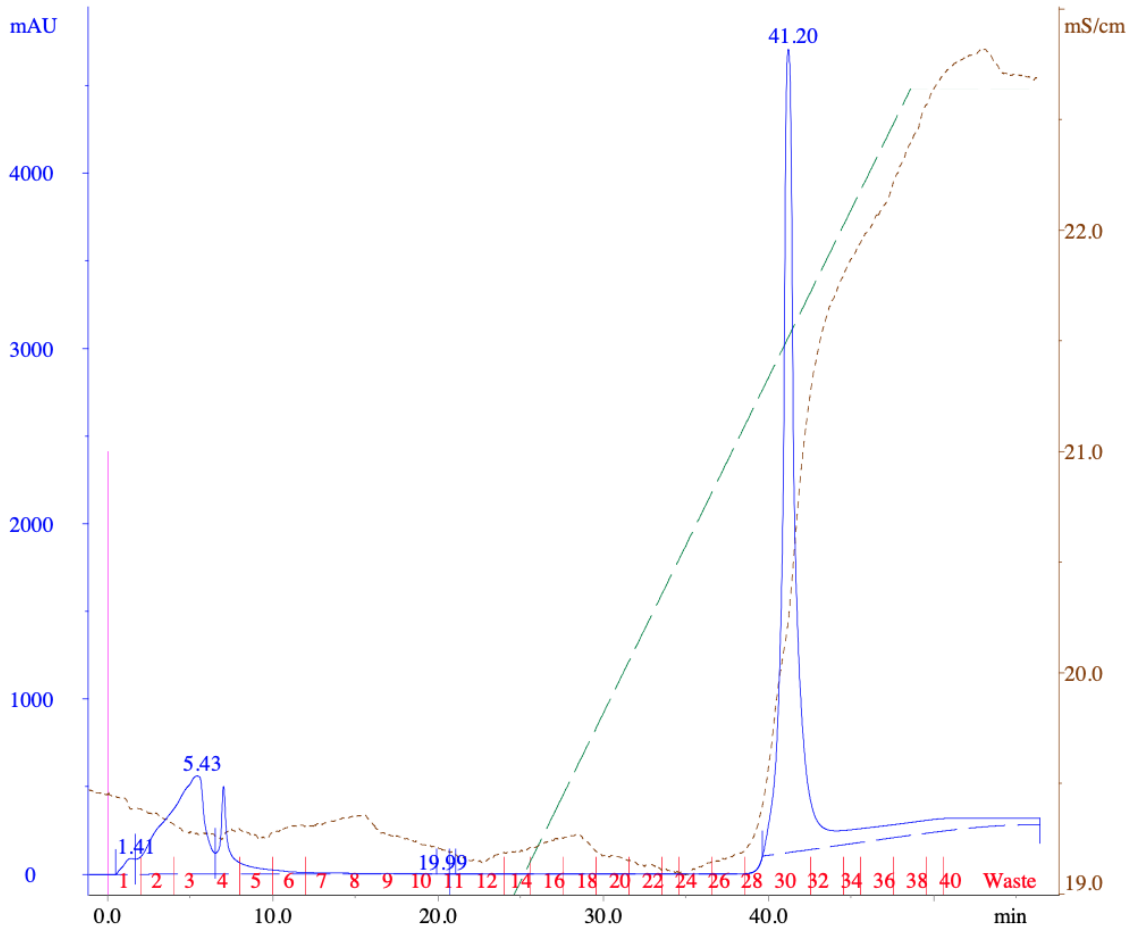

Figure 13. Chromatogram of the first of 2 HisHP Ni-affinity purifications for TrxA-ApAFP752 sample preparation. Colored lines represent following measurements: (Green) concentration of elution buffer relative to the starting imidazole concentration (%); (Blue) absorption at 280 nm; (Brown) conductivity of sample/solution in units of mS cm^{-1}. The peaks at fractions 28-32 correspond with the elution of TrxA-ApAFP752 fusion protein. Peaks prior to fraction 6 correspond with non-6xHis proteins, aggregated proteins, and debris.

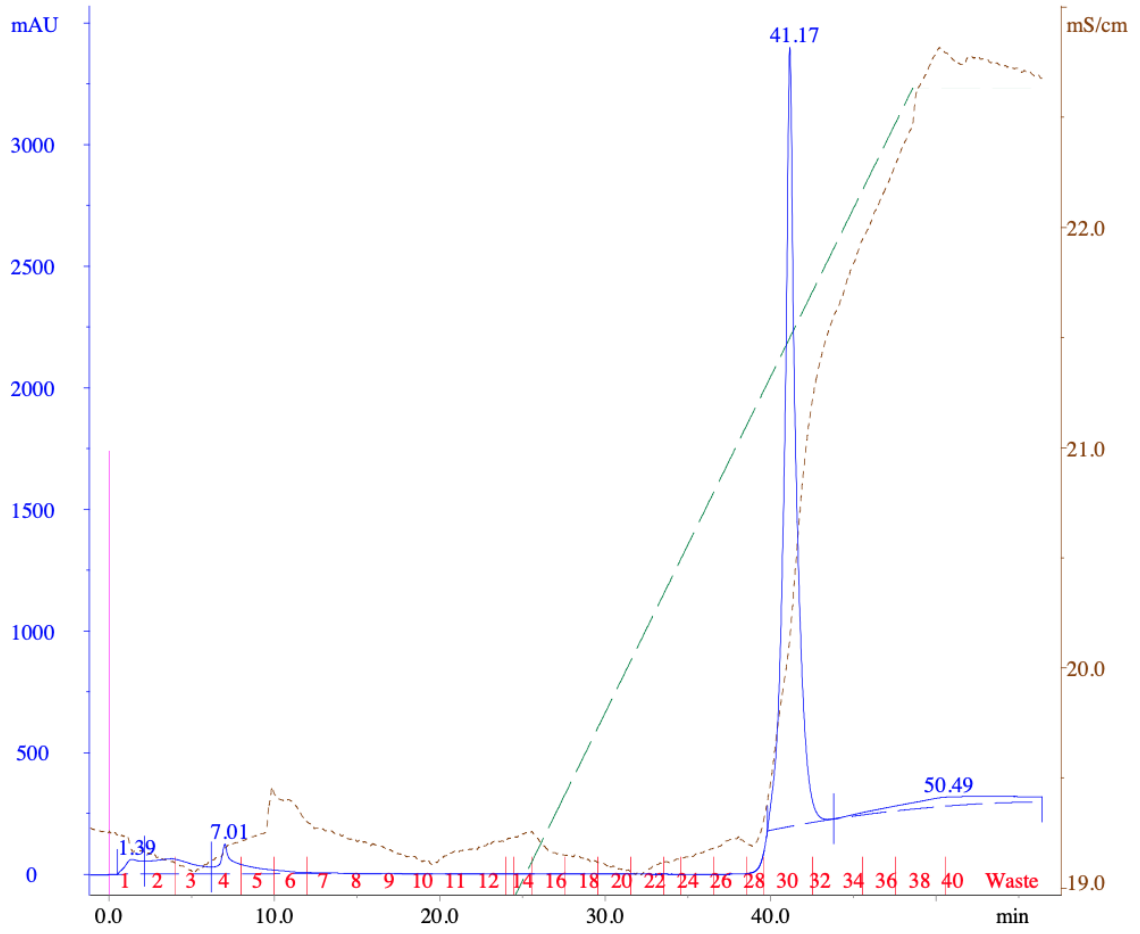

Figure 14. Chromatogram of the second of 2 HisHP Ni-affinity purifications for TrxA-ApAFP752 sample preparation. Colored lines represent following measurements: (Green) concentration of elution buffer relative to the starting imidazole concentration (%); (Blue) absorption at 280 nm; (Brown) conductivity of sample/solution in units of mS cm^{-1}. The peaks at fractions 28-32 correspond with the elution of TrxA-ApAFP752 fusion protein. Peaks prior to fraction 6 correspond with non-6xHis proteins, aggregated proteins, and debris.

Sodium dodecyl sulfate polyacrylamide gel electrophoresis (SDS-PAGE) stained with Coomasie brilliant blue was performed to determine protein purity (Figure 15). In some instances, anion exchange chromatography and/or size-exclusion chromatography were performed in order to improve protein purity. After concentrating to a desired concentration, some lyophilized protein samples were prepared for alternative long-term

storage studies in which the sample was lyophilized in buffer (50 mM potassium phosphate, 20 mM NaCl, and 1 mM NaN_3 at pH 8.0) overnight[115] and stored at room temperature (~21 °C) for 17 months. The sample was rehydrated with 18.2 MΩ Milli-Q® water (EMD Millipore) before cryopreservation studies and buffer exchanged into the Tris buffer. Heat inactivation of purified Trx-*Ap*AFP752 was achieved by incubating the protein at 60 °C for 15-20 minutes. TrxA-*Ap*AFP752 sample concentration was estimated using UV-Visible spectrophotometry (ε_{280} = 19,575 $M^{-1}cm^{-1}$) (Figure 16).

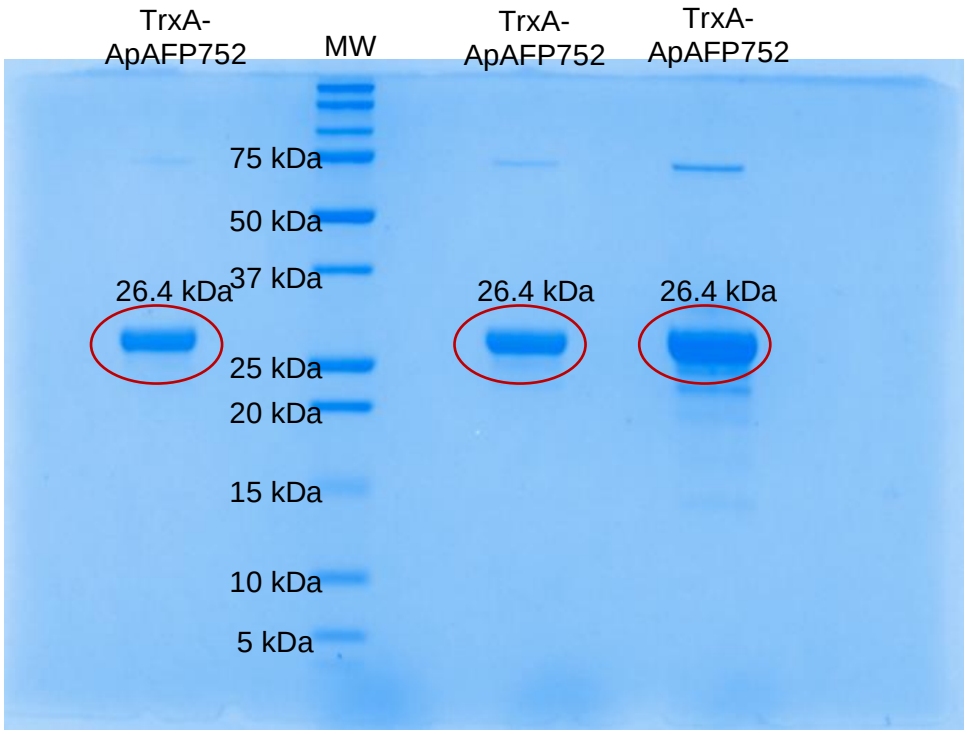

Figure 15. SDS-PAGE of 12% acrylamide gel stained with Coomasie brilliant blue. Various concentrations of TrxA-ApAFP752 were loaded into lanes surrounding the molecular weight (MW) marker, and bands appear around the 26.4 kDa consistent with the molecular weight of TrxA-ApAFP752.

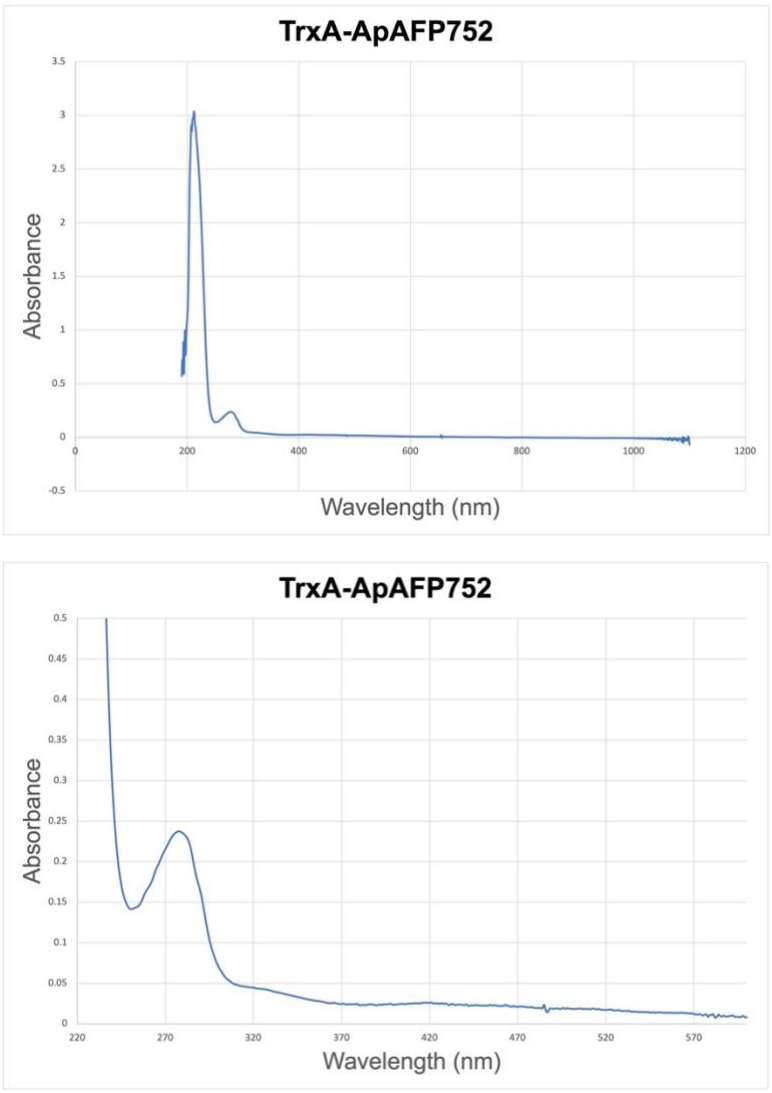

Figure 16. UV-Vis absorption spectra of TrxA-ApAFP752. The full spectrum is pictured above with a close-up of the 280 nm absorption pictured below.

III. Cleavage of TrxA-ApAFP752

*Ap*AFP752 was removed from the fusion protein via proteolytic cleavage using bovine His-enterokinase (Prospec-Tany). TrxA-*Ap*AFP752 cleavage was performed in Buffer B. A small-scale cleavage test was performed with a ratio of 1 IU bovine His-enterokinase to 400 µg TrxA-*Ap*AFP752 for six hours at 25 °C. Samples were taken every two hours to assess cleavage efficiency using SDS-PAGE and staining with Coomassie brilliant blue. Full cleavage was performed using 1 IU bovine His-enterokinase per 400 µg Trx-

*Ap*AFP752 for six hours at 25 °C. The *Ap*AFP752 sample was then purified using FPLC Ni-affinity and the flow through was collected (Figure 17). Purity was assessed using SDS-PAGE and visualized with silver staining (Figure 18). *Ap*AFP752 sample concentration was estimated using UV-Visible spectrophotometry (ε_{280} = 5,470 $M^{-1}cm^{-1}$) (Figure 19).

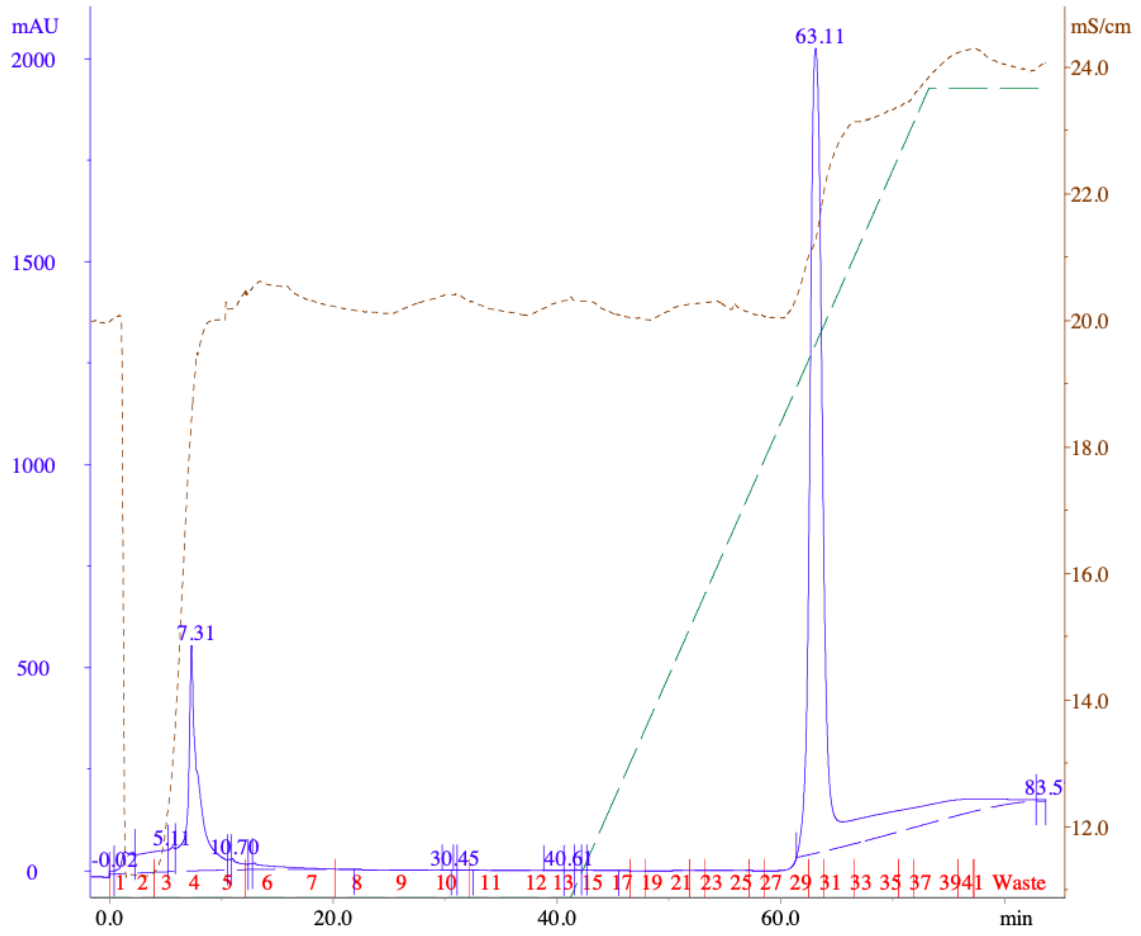

Figure 17. Chromatogram of TrxA-ApAFP752 after cleavage. Colored lines represent following measurements: (Green) concentration of elution buffer relative to the starting imidazole concentration (%); (Blue) absorption at 280 nm; (Brown) conductivity of sample/solution in units of mS cm^{-1}. The peak at fraction 4 corresponds with the elution of ApAFP752 protein in the column flow-through. Peaks at fractions 28-38 correspond with the elution of TrxA and bovine His-enterokinase.

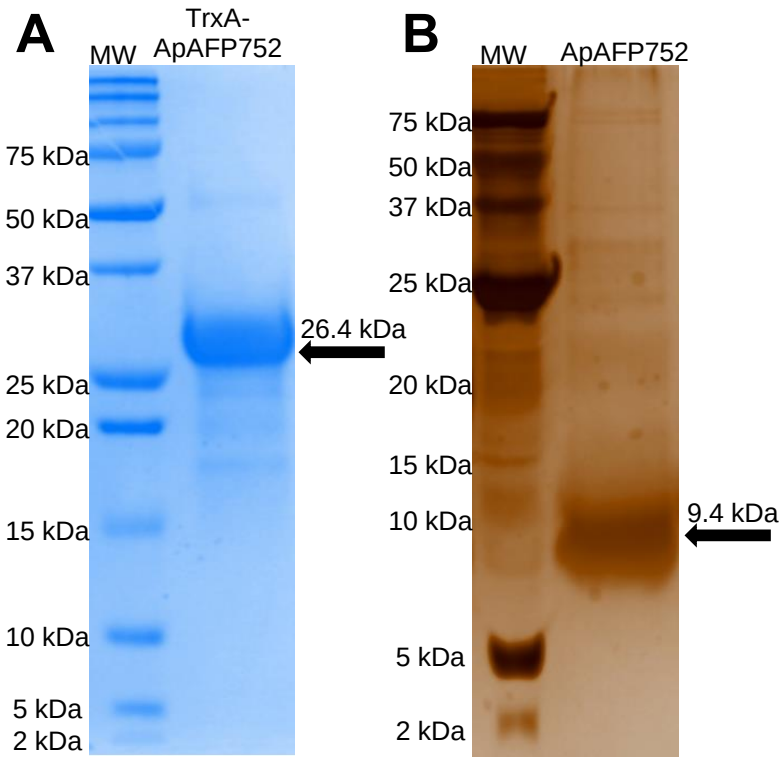

Figure 18. Comparison of fusion and cleaved protein. (A) Coomassie Blue staining of 26.4 kDa TrxA-AFP752 run through SDS-PAGE in a 12% acrylamide gel. (B) Silver staining of cleaved 9.4 kDa ApAFP752 run through SDS-PAGE in a 16% acrylamide gel.

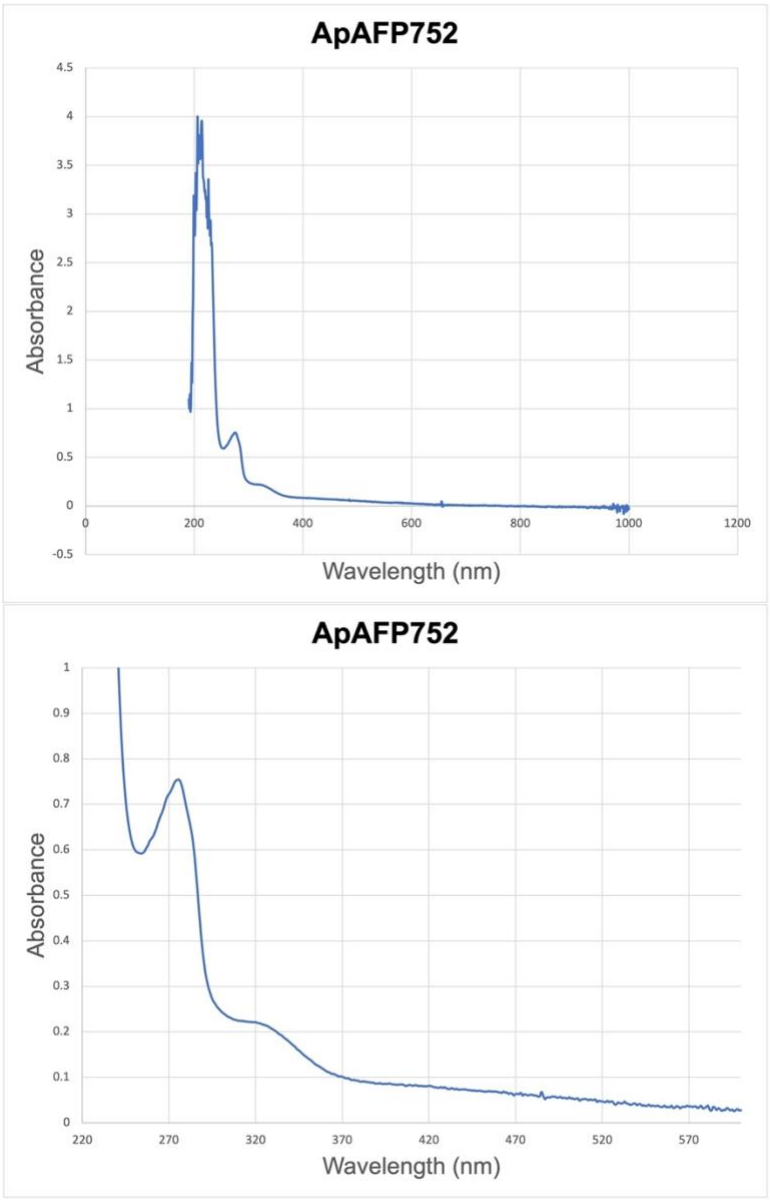

Figure 19. UV-Vis absorption spectra of ApAFP752. The full spectrum is pictured above with a close-up of the 280 nm absorption pictured below.

IV. Characterization of TrxA-ApAFP752

To characterize the antifreeze activity of the recombinantly expressed and purified TrxA-*Ap*AFP752, thermal hysteresis activity (THA) and the ice-recrystallization inhibition (IRI) activity assays were conducted.

Differential scanning calorimetry (DSC) was used to assay THA. Aqueous solutions of 180 µM TrxA-*Ap*AFP752 in buffer (50 mM K_2HPO_4, 20 mM NaCl, pH 8) were analyzed via differential scanning calorimetry (DSC, TA Instruments Q2000). Samples were first cooled to -40 °C and held for 10 minutes so as to completely freeze the solution. The next cycle involved heating from -40 to 10 °C at a rate of 1 °C/min to completely melt the solution and to capture the total enthalpy of melt for the sample. Subsequently, a sequence of cycles were run that consisted first of a 1 °C/min cooling back to -40 °C followed by 1 °C/min heating to a progressively higher hold temperature starting at -1 °C and increasing by 0.1 °C in the next heating cycle[199]. This cycling of heating and cooling profiles process continued through to a maximum of 0.5 °C for hold temperature. In the initial heating cycles, the goal was to only melt a small fraction of the ice, hold the system at that hold temperature for 5 minutes to come to steady state, and then on cooling to capture the exothermic profile of the refreezing of that water fraction. In early cycles, the melting and freezing endotherms and exotherms maintained symmetry, where for one (or two) cycles the freezing temperature is observed (Figure 20) at a temperature lower than the hold temperature (i.e., melting temperature for that cycle). This depression in freezing point is defined as the thermal hysteresis activity (THA). The derivative of that particular heat flow cycle also allows us to more easily observe the rapid change in slope at the onset of freezing near the first minimum just under 0 °C.

In Figure 20, a series of heating and cooling cycles are shown for the TrxA-*Ap*AFP752 in buffer (50 mM potassium phosphate, 20 mM sodium chloride, pH 8). The sample was first cooled to -40 °C so as to fully freeze the sample. Then, the sample was heated to a hold temperature subzero and held isothermal for 5 minutes, which induced

a partial melting of the sample. The melting endotherm associated with each heating cycle is shown as the dashed curves with negative heat flow. After the hold period, the respective cooling cycles follow with the exotherm on recrystallizing that fraction of water, seen as dashed profiles in the figure. The cycle where we can assess thermal hysteresis is emphasized with a solid profile in dark blue (where other cycles are shown in dashed gray) and the depression in the freezing point relative to the hold temperature is clearly observable. In this particular case, the hold temperature was -0.1 °C and the freezing point was observed as a rapid change in slope of the cooling exotherm at -0.75°C; thus, we observe a THA of 0.65 °C. Subsequent heating cycles (with higher hold temperatures) did not show an immediate freezing exotherm on cooling, but instead experienced supercooled freezing in the heterogeneous nucleation temperature range (observed at -22.9 °C, -22.6 °C, and -21.6 °C). We also wanted to assess whether lyophilized AFP retains cryoprotective activity, as lyophilization can be a very useful technique for protein storage. The AFP sample was lyophilized, reconstituted with water, and activity was

reassessed. Differential scanning calorimetry showed retention of thermal hysteresis activity after lyophilization.

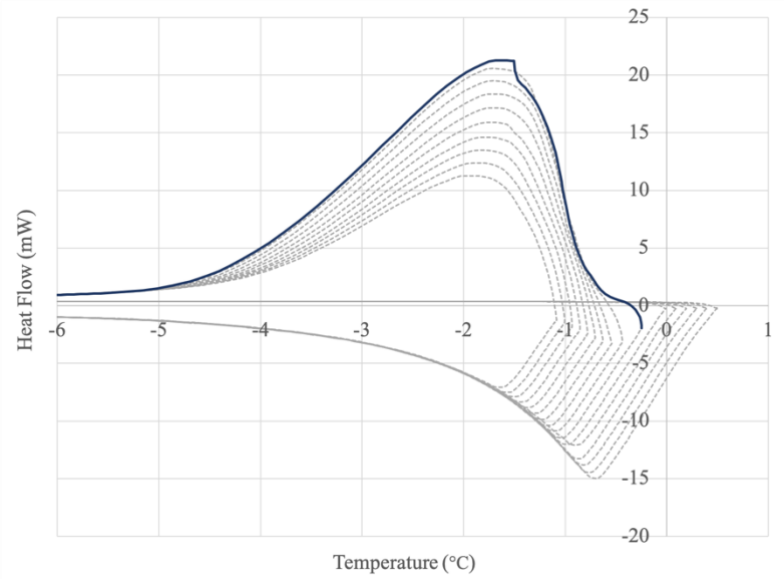

Figure 20. Differential scanning calorimetry measurement of thermal hysteresis activity of TrxA-*Ap*AFP752 (50 mM K_2HPO_4, 20 mM NaCl, pH 8). Negative heat flow endothermic profiles indicate partial melting of the ice, where positive exothermic profiles refer to the subsequent refreezing upon cooling. The solid exothermic profile refers to the particular cooling cycle used for thermal hysteresis activity analysis and shows the depression in the freezing point relative to the melting hold temperature for that cycle. THA data was collected in collaboration with John Tsavalas, University of New Hampshire.

For ice recrystallization inhibition assays, solutions of TrxA-*Ap*AFP752 were prepared at 20, 10, 5.0, 2.5, and 1.0 μM in 50 mM K_2HPO_4, 20 mM NaCl, pH = 8 buffer. Approximately 15 μL of sample was loaded by capillary action into a 25 μL microcapillary tube [Drummond] and the ends sealed in a flame.[202] The tubes were positioned next to one another and secured with a small amount of aluminum tape on each end. The solutions were flash frozen over 10-15 seconds in a stream of N_2 gas coming from a LN_2 tank, creating microcrystalline ice as seen in Figure 21A. The microcapillary tubes were positioned in a home-built apparatus to hold the samples at -6.0 °C while observing each

sample under magnification for 20 hours. An initial photograph at 0 h and end photograph at 20 hours are compared to the determine the extent of ice recrystallization across the different solutions.

Ice-recrystallization inhibition assays were performed before and after lyophilization. The IRI assays corroborate the THA performance and exhibit no change in ice-crystal granularity, indicating no change in the IRI activity at concentrations above 1 mM. The IRI assays with TrxA-*Ap*AFP752 demonstrate functional behavior at 5.0 µM (Figure 21), which is the concentration used for cryoprotection of the frog eggs. The concentration of TrxA-*Ap*AFP752 necessary for ice recrystallization inhibition was consistent across batches of the protein. Both of these assay methods indicated that lyophilization does not functionally alter the activity of the AFP.

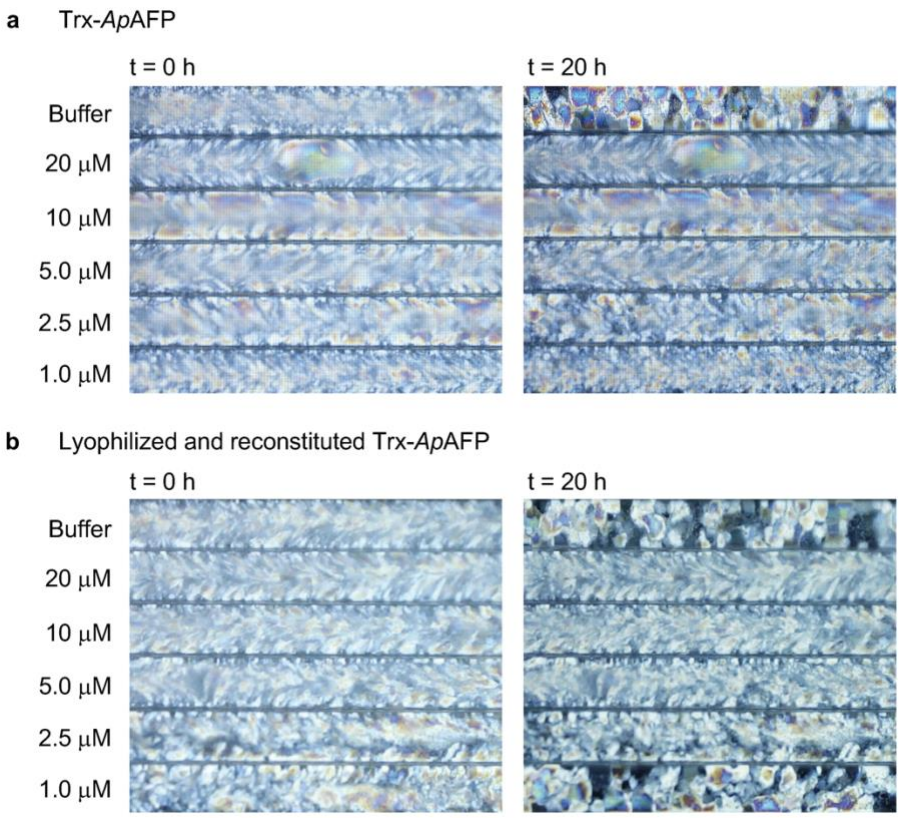

Figure 21. Ice recrystallization inhibition by TrxA-*Ap*AFP752 at different concentrations before and after lyophilization. A) Initial solutions, t = 0 h, of buffer alongside varying concentrations of TrxA-*Ap*AFP752 in microcapillary tubes after flash freezing to yield microcrystalline ice and the same solutions after holding for 20 h at -6.0 °C demonstrating significant ice recrystallization in the buffer but not the TrxA-*Ap*AFP752 solutions. B) A similar experiment using lyophilized and reconstituted TrxA-*Ap*AFP752 that demonstrates significant ice recrystallization inhibition for all concentrations higher than 1.0 μM. IRI data was collected by Paul Baures and Ian B. Lehner, Keene State College (P. B. is currently at Florida State University).

CHAPTER 4

MAMMALIAN CELL CRYOPRESERVATION WITH ApAFP752

The following chapter is taken from my publication in Biomolecules.[203]

Sreter, J. A., Foxall, T. L. & Varga, K. Intracellular and Extracellular Antifreeze Protein Significantly Improves Mammalian Cell Cryopreservation. *Biomolecules* **12**, doi:10.3390/biom12050669 (2022).

Intracellular and Extracellular Antifreeze Protein Significantly Improves Mammalian Cell Cryopreservation

Jonathan A. Sreter [1], Thomas L. Foxall [2], and Krisztina Varga [1,*]

[1] Department of Molecular, Cellular and Biomedical Sciences, University of New Hampshire, Durham, NH, 03824, USA; jonathan.sreter@unh.edu

[2] Department of Biological Sciences, University of New Hampshire, Durham, NH, 03824, USA; tom.foxall@unh.edu

***** Correspondence: krisztina.varga@unh.edu; Tel.: (603) 862-5375

Abstract: Cell cryopreservation is an essential part of the biotechnology, food, and healthcare industries. There is a need to develop more effective, less toxic cryoprotective agents (CPAs) and methods, especially for mammalian cells. In order to achieve **Aim 2: Examine the extracellular cryoprotective activity of ApAFP752 for mammalian cell cryopreservation** and **Aim 3: Examine the intracellular cryoprotective activity of ApAFP752 in mammalian cells**, we investigated the impact of an insect antifreeze protein from *Anatolica polita* (ApAFP752) on mammalian cell cryopreservation using the human embryonic kidney cell line HEK 293T. An enhanced green fluorescent protein (EGFP) tagged antifreeze protein, EGFP-ApAFP752 was transfected into the cells and the GFP was used to determine the efficiency of transfection. AFP was assessed for its cryoprotective effects intra- and extracellularly and both simultaneously at different concentrations with and without dimethyl sulfoxide (DMSO) at different concentrations. Comparisons were made to DMSO or medium alone. Cells were cryopreserved at -196 °C for ≥ 4 weeks. Upon thawing, cellular viability was determined using trypan blue, cellular damage was assessed by lactate dehydrogenase (LDH) assay, and cellular metabolism was measured using a metabolic activity assay (MTS). The use of this AFP significantly improved cryopreserved cell survival when used with DMSO intracellularly. Extracellular AFP also significantly improved cell survival when included in the DMSO freezing medium. Intra- and extracellular AFP used together demonstrated the most significantly increased cryoprotection compared to DMSO alone. These findings present a potential method to improve the viability of cryopreserved mammalian cells.

Keywords: Antifreeze protein; cryopreservation; cryoprotectants; freezing; mammalian cells

I. Introduction

Cryopreservation of cells has long been necessary in the use of cells in research, for in vitro fertilization, and the increased use of mammalian cells in the production of therapeutics, vaccines, and even food production [134,135,204,205]. Thus, there is a need for cryoprotectants and improved cryopreservation protocols that will enhance the viability of cells stored at low temperatures, and some of these can be found as naturally occurring proteins [152]. Cellular therapies offer precise, potent, and cutting-edge treatment options for complex diseases [137-142]. However, reliable and consistent long-term cryogenic storage of mammalian cells remains a challenge, and it has been recognized as a potential major obstacle in the development of complex cellular therapies [143,166]. Long-term storage and transport can also be further complicated, as some cells are especially sensitive to freezing damage [206]. For over 60 years, dimethyl sulfoxide (DMSO) has been added to cells to reduce ice formation when stored in liquid nitrogen (-196 °C), however DMSO can have harmful effects by causing adverse reactions in patients and exhibiting cellular toxicity [177,207].

Almost all cells and cellular organisms are damaged by freezing, and much is still not understood about how to counteract its adverse effects. Numerous organisms have natural compounds to avoid or tolerate freezing in order to survive in extreme cold. Antifreeze proteins (AFPs), a type of ice binding protein, were first discovered in Antarctic fish blood [3]. Over the past few decades, it has been discovered that a wide range of organisms produce AFPs for protection against freezing [4-6]. Mammals, however, have not been found to produce AFPs. AFPs inhibit ice growth, direct ice crystal shaping, and

prevent ice recrystallization in cold adapted organisms as a result of becoming adsorbed to the nascent ice surface by an unusual mechanism [7-9].

Previous work has investigated incorporating AFPs as cellular cryoprotectants [5,96,208-212]. However, these studies typically involved teleost or other moderately active AFPs that shape ice crystals into needle-like formations that can puncture cell membranes [209,213]. Insect AFPs induce formation of rounded ice crystals which may reduce cell membrane damage and provide better cryoprotective activity [214]. To date, these insect AFPs have been added to cryoprotective agents (CPAs) as a non-penetrating part of cryoprotectant solutions, and some have shown promising results in mammalian cells [215,216].

The insect antifreeze protein ApAFP752 was found in the central Asian desert beetle *Anatolica polita* [105]. These deserts can experience extreme temperature fluctuations up to +40 °C and down to -40 °C in a day [105,113,114]. ApAFP752 is a 9 kDa protein with a predicted highly disulfide bonded β-helical structure containing an array of Thr residues on the ice binding surface, similar to the homologous AFP from the beetle *Tenebrio molitor* (TmAFP) [120,201]. Current studies of ApAFP752 use the recombinant thioredoxin A (TrxA) fusion protein TrxA-ApAFP752 [105,115,121,208].

TrxA-ApAFP752 has previously been shown to provide cryoprotection to *E. coli* cells against cold damage [105], *Xenopus laevis* eggs [124] and human skin fibroblast cells [115,121,208]. In these studies, TrxA-ApAFP752 demonstrated cryoprotective activity when microinjected into the *Xenopus laevis* eggs [124], and when included in the freezing medium external to the *E. coli* [105] and human skin fibroblast cells [115]. In this study, the goal was to observe and determine both the extracellular and intracellular cryoprotective activity of

ApAFP752 in human cells. We designed plasmids for both an enhanced green fluorescent protein (EGFP-ApAFP752) fusion protein and EGFP alone. Cells were then left untransfected or transfected with either EGFP-ApAFP752 fusion protein or EGFP alone and the transfection efficiency and cryoprotective activity were assessed compared to varying concentrations of DMSO. Extracellular Trx-ApAFP752 will be denoted as EC AFP, and transfected EGFP-ApAFP752 will be referred to as intracellular or IC AFP. Extracellular TrxA-ApAFP752 (EC AFP) and intracellular EGFP-ApAFP752 (IC AFP) cryoprotection efficacy was then evaluated and compared using trypan blue for viability determination, lactate dehydrogenase (LDH) release for membrane damage, and metabolic activity from the cellular metabolism of (3-(4,5-dimethylthiazol-2-yl)-5-(3-carboxymethoxyphenyl)-2-(4-sulfophenyl)-2H-tetrazolium (MTS) assays.

II. Materials and Methods

Cells and Reagents

Human embryonic kidney (HEK) 293T cells were purchased from American Type Culture Collection (ATCC, Manassas, VA, USA), and cultured in Dulbecco's Modified Eagle Medium (DMEM) (Thermo Fisher Scientific, Waltham, MA, USA) supplemented with 10% v/v fetal bovine serum (Sigma-Aldrich, St. Louis, MO, USA). Cells were incubated in a humidified incubator at 37 °C and 5% CO_2. Cells were rinsed with Dulbecco's phosphate buffered saline (DPBS) (Thermo Fisher Scientific, Waltham, MA, USA) and dissociated from cultureware using 0.05% trypsin + 0.02% EDTA (Thermo Fisher Scientific, Waltham, MA, USA). Cell viability was determined using a hemocytometer and 0.4% trypan blue

solution (Thermo Fisher Scientific, Waltham, MA, USA) and an Invitrogen Countess™ II FL automated cell counter (Thermo Fisher Scientific, Waltham, MA, USA).

Transfection of HEK 293T Cells

Plasmids for EGFP and EGFP-ApAFP752 were designed and purchased from GeneArt (Thermo Fisher Scientific, Waltham, MA, USA). Transfection of EGFP-ApAFP752 plasmid (Figure S1) into HEK 293T cells was optimized according to manufacturer protocols. After optimization, 1×10^7 cells were seeded into T75 flasks with a final volume of 19.7 mL DMEM supplemented with 10% FBS and incubated overnight. The following day, cells were ~80% confluent. 20 µL of plasmid DNA (1 µg/µL) was combined with 2 mL of Gibco™ OptiMEM (Thermo Fisher Scientific, Waltham, MA, USA), then 60 µL of TransIT®-293 (Mirus Bio, Madison, WI, USA) was mixed in and left for 30 mins at room temperature to complex. The solution was then mixed, added to the ~80% confluent T75 flask of HEK 293T cells, and cells were incubated for 48 hours. Following incubation, cells were observed, and digital images were taken with epifluorescence microscopy to visualize EGFP and EGFP-ApAFP752 transfection.

Flow Cytometry

After visualization of optimal transfection conditions, transfection efficiency was quantified by measuring EGFP expression using flow cytometry. Transfected HEK 293T cells were released by trypsinization, centrifuged, and resuspended in DPBS. Flow cytometry was performed using a Sony SH-800Z sorting flow cytometer (Sony Biotechnology, San Jose, CA, USA) equipped with 405 nm, 488 nm, 561 nm, and 638 nm lasers capable of

detecting up to 8 parameters (6 fluorescent and 2 scatter channels). Sony cell sorter software was used to operate the instrument. Untransfected HEK 293T cells were used as a negative control. The 488 nm excitation laser was used with a 100 µM chip operating at 6 psi. EGFP (or EGFP-ApAFP752) fluorescence was detected using the fluorescence 2 (FL2) emission detector at 525 nm. The percentage of HEK 293T cells expressing EGFP (or EGFP-ApAFP752) was measured by gating for a region with <1% of untransfected HEK 293T cells in the EGFP gated region, as described previously [217]. The gating strategy can be found in Figure S2. All flow cytometry data was analyzed using FlowJo software (Becton Dickinson, Franklin Lakes, NJ, USA).

Expression and Purification of Recombinant TrxA-ApAFP752

TrxA-ApAFP752 was expressed and purified for testing it as an extracellular agent (EC AFP) and for comparison with intracellular EGFP-AFP (IC AFP) to determine which has more potent activity in HEK 293T cryopreservation. Expression and purification of TrxA-ApAFP752 was performed as described previously [115]. In short, the recombinant plasmid pET32b-TrxA-ApAFP752 was transformed into BL21 (DE3) pLysS competent *Escherichia coli* cells (Promega, Madison, WI, USA). Protein overexpression was induced with isopropanol-1-thio-β-D-galactopyranoside (IPTG) [105]. The cells were harvested via centrifugation and then lysed using a French press. TrxA-ApAFP752 was purified using an ÄKTA purifier 900 fast protein liquid chromatography (FPLC) system with nickel-affinity columns (Cytiva, Marlborough, MA, USA). Protein purity was assessed using SDS-PAGE and Coomassie blue staining. TrxA-ApAFP752 concentration was estimated using UV-Visible spectrophotometry (ε_{280} = 19,575 $M^{-1}cm^{-1}$). TrxA-ApAFP752 was used as

extracellular AFP (EC AFP) at final concentrations of 5 or 15 µM (0.13 or 0.40 mg/ml) in the cryoprotectant solutions.

Cryopreservation and Thawing

Prior to cryopreservation, all HEK 293T cell viability was > 90%. For studies comparing untransfected HEK 293T cells, those transfected with EGFP, or those transfected with EGFP-ApAFP752 (AFP), 1 mL of 5×10^6 cells were cryopreserved with 0, 5, 10, 15, and 20 % (v/v) concentrations of DMSO in Corning® cryogenic tubes (Corning, Corning, NY, USA). Cryotubes were placed in a Mr. Frosty™ freezing container (Thermo Fisher Scientific, Waltham, MA, USA) and cooled at -1 °C/min to -80 °C. After 24 hours, cryotubes were then stored in liquid nitrogen vapor phase (-196 °C) for ≥ 4 weeks. Cells were rapidly thawed using a 37 °C water bath, added to 5 mL of prewarmed DMEM supplemented with 10% FBS, and centrifuged for 5 mins at 200 × g. The resulting cell pellet was then resuspended in 5 mL of prewarmed DMEM supplemented with 10% FBS. The cryopreservation and thawing methods described previously were then used to compare the cryoprotective activity of extracellular AFP (EC AFP) and intracellular AFP (IC AFP) and both together. The following cryopreservation conditions were compared to untransfected HEK 293T cells frozen with the same DMSO concentrations (0, 5, and 10% v/v) and stored in liquid nitrogen vapor phase (-196 °C) for ≥ 4 weeks:

1) 5 µM EC AFP
2) 15 µM EC AFP
3) IC AFP

4) 5 µM EC AFP & IC AFP

5) 15 µM EC AFP & IC AFP

Viability Tests

Three different assays were utilized to assess cryopreservation efficacy of the HEK 293T cells after freeze/thaw: trypan blue, LDH release, and MTS assays. It is important to note that immediate post-thaw viability testing can fail to account for cellular apoptosis or necrosis in some cells, which may take 24-48 hours to occur [163,218]. To increase confidence in results from immediate post-thaw viability assays, such as trypan blue, additional viability assessments were conducted at multiple time points including both immediate (within 12 hours) and longer term (48 hours post-thaw) testing. The trypan blue viability assay is based on the principle that the vital dye, trypan blue, enters dead or dying cells with a damaged membrane while leaving viable cells with intact membranes unstained [219]. Any user error was mitigated by the use of an automated cell counter in conjunction with manual counting with a hemocytometer [220,221]. The LDH release assay is based on the fact that cells undergoing necrosis, apoptosis, or other cellular membrane damage will rapidly release LDH into the surrounding medium, and this is easily quantified by the LDH release assay [222]. Cellular metabolic activity was measured by the reduction of a tetrazolium compound, MTS (3-(4,5-dimethylthiazol-2-yl)-5-(3-carboxymethoxyphenyl)-2-(4-sulfophenyl)-2H-tetrazolium, and an electron coupling reagent (phenazine ethosulfate; PES) by metabolically active living cells to form a colored formazan product [223]. This assay is widely used to determine either cellular proliferation

or cytotoxicity by quantifying cellular metabolism. The same number of viable cells counted using trypan blue were plated for each treatment 48 hours prior to measurement.

Trypan Blue Assay

All HEK 293T cells were enumerated and viability was determined using a hemocytometer and 0.4% trypan blue vital dye solution (Thermo Fisher Scientific, Waltham, MA, USA) as well as an Invitrogen Countess™ II FL automated cell counter (Thermo Fisher Scientific, Waltham, MA, USA) [219]. Cell viability assessments using the trypan blue assay began within 1 hour after freeze/thaw and were completed within 12 hours.

LDH Assay

Within 1 hour post-thaw, the Cyquant™ LDH cytotoxicity assay (Thermo Fisher Scientific, Waltham, MA, USA) was performed to determine the amount of cell damage by following manufacturer protocols and absorbance values were read at 490 nm using a spectrophotometric plate reader (BioTek, Winooski, VT, USA) [222]. Total LDH released was determined by measuring Triton X-100 lysed HEK 293T cells as positive controls. All values were media subtracted and cell damage was expressed as % total LDH release.

MTS Assay

Viable cells for each condition were plated in a 96-well plate at a density of 1.5×10^4 cells/well. Cell media was changed after 24 hours and a CellTiter 96® Aqueous One Solution Cell Proliferation Assay kit (Promega, Madison, WI, USA) was used to perform

an MTS assay 48 hours post-thaw according to the manufacturer protocols. Absorbance values were read at 490 nm using a spectrophotometric plate reader (BioTek, Winooski, VT, USA). Percent (%) total metabolic activity was measured relative to fresh, non-cryopreserved HEK 293T cells.

Experimental Design and Statistical Analysis

First, the objective was to determine successful transfection of EGFP-ApAFP752 (IC AFP) and EGFP into HEK 293T cells. Next, we determined the cryoprotective effect of IC AFP compared to the control groups of untransfected cells and EGFP transfected cells at 0, 5, 15, 15, and 20% v/v DMSO concentrations using three different cell viability measurements (trypan blue, LDH, and MTS). After establishing AFP is responsible for the intracellular cryoprotective effect, comparisons were then made to determine the cryoprotective activity of extracellular AFP (EC AFP) and intracellular AFP (IC AFP) and both together at 0, 5, and 10% v/v DMSO concentrations again using three different cell viability measurements (trypan blue, LDH, and MTS). All experiments contained 3 biological repeats (n=3) with each containing 3 technical repeats. Statistical analyses were performed using GraphPad Prism 9 (GraphPad Software, San Diego, CA, USA).

III. Results

Transfection

To evaluate transfection efficiency, cells were observed and imaged using both light and epifluorescence microscopy at 24- and 48-hours post-transfection (Figure 22, Figure S3). Cells transfected with EGFP or EGFP-ApAFP752 produced green fluorescence when

excited by blue light (450-490 nm). No fluorescence was observed in untransfected cells. The amount of EGFP-ApAFP752 expression was higher after 48 hours vs. 24 hours, so 48 hours was selected for optimal protein expression and absence of cellular pathologies. It should be noted that cells were also examined 72-hours post-transfection, however, no increase in protein expression was observed. Flow cytometry was performed to quantify the percent of cells expressing EGFP (or EGFP-ApAFP752) fluorescence (transfection efficiency) and transfection efficiency was determined to be an average of 80%.

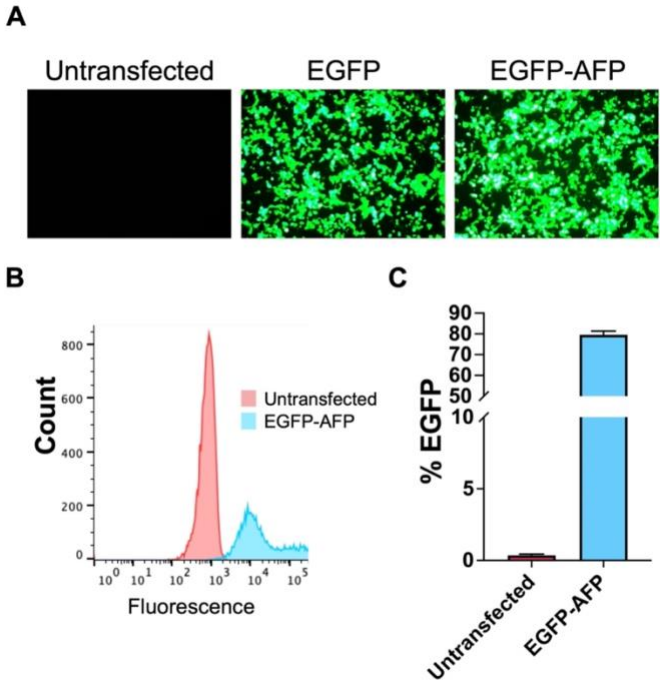

Figure 22. Transfection of HEK 293T cells. (**A**) Epifluorescent images of HEK 293T cells comparing untransfected cells and cells transfected with EGFP and EGFP-ApAFP752 (EGFP-AFP) after 48 hours photographed at 100X. (**B**) Flow cytometry analysis of AFP transfection measuring transfection efficiency of EGFP-ApAFP752 gated against untransfected cell autofluorescence. (**C**) Average transfection efficiency (% EGFP expression) for EGFP-ApAFP752 (blue) compared to untransfected cells (magenta). Mean value ± SEM. All experiments contained 3 biological repeats (*n*=3) with each containing 3 technical repeats.

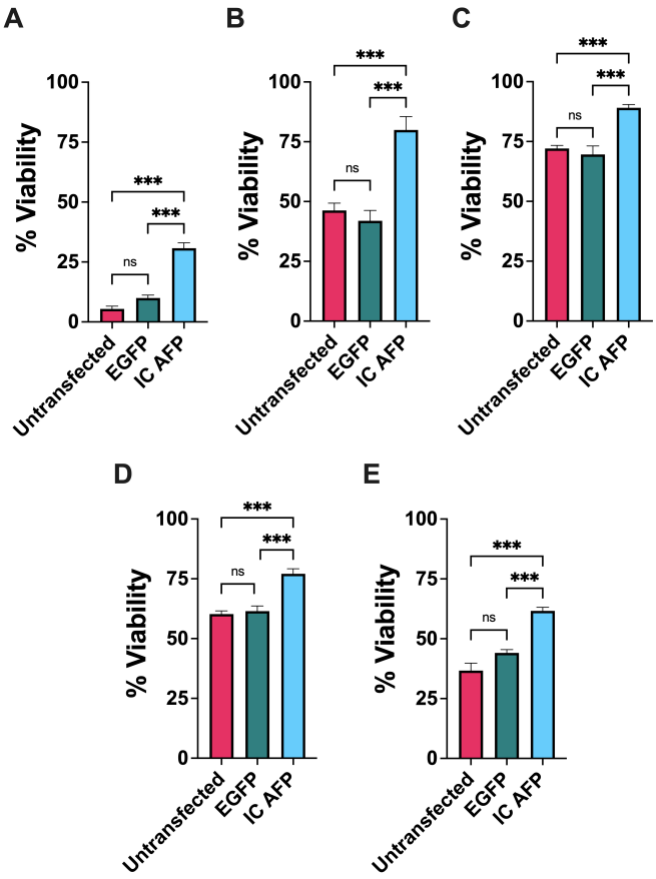

Figure 23. Analysis of cell viability by trypan blue exclusion in untransfected, EGFP transfected, and EGFP-AFP transfected (IC AFP) HEK 293T cells after cryopreservation. 5 × 10^6 cells were cryopreserved with (**A**) 0, (**B**) 5, (**C**) 10, (**D**) 15, and (**E**) 20 % (v/v) concentrations of dimethyl sulfoxide (DMSO) and stored in liquid nitrogen for ≥ 4 weeks. Data was analyzed using a one-way analysis of variance (ANOVA) and a Tukey's post hoc test was used for pairwise comparisons of experimental groups. All experiments contained 3 biological repeats (n=3) with each containing 3 technical repeats. Mean value ± SEM (n.s. $p > 0.05$, ***$p \leq 0.001$).

Untransfected vs. EGFP vs. IC AFP

EGFP and untransfected cells are the negative controls to rule out any potential cryoprotective activity from the EGFP part of the EGFP-AFP fusion protein for IC AFP. Untransfected, EGFP transfected, and EGFP-ApAFP752 transfected cells (IC AFP) were cryopreserved with 0, 5, 10, 15, and 20 % (v/v) concentrations of cell culture grade DMSO. These concentrations were chosen because 5-10% DMSO are the concentrations most

commonly used for cell cryoprotection, and we sought to compare a wide range for determining DMSO activity [164]. Cells were then stored in liquid nitrogen vapor phase (-196 °C) for ≥ 4 weeks. Cells that were frozen and thawed without cryoprotectants (0% DMSO, untransfected cells), Fig. 2A, exhibited lowest viability, ~5% on average (Table 1). 5% and 10% DMSO increased the survival of untransfected HEK 293T cells, however higher DMSO concentrations of 15% and 20% decreased cell survival, implying the toxicity of higher DMSO concentrations to cells (Figure 23 and Table 1). Post-thaw testing showed a significant increase in viability for cells transfected with AFP (IC AFP) vs. untransfected cells or cells transfected with EGFP across all treatments using the trypan blue viability assay (Figure 23). The results are summarized in Table 1. There were no significant differences between untransfected cells and cells transfected with EGFP across each DMSO concentration.

Table 1. Average % viability of HEK 293T cells across treatments as determined by trypan blue assay.

	0% DMSO	**5% DMSO**	**10% DMSO**	**15% DMSO**	**20% DMSO**
Untransfected	5	46	72	60	37
EGFP	10	42	70	62	44
IC AFP	31	80	89	77	62
IC AFP vs. Untransfected	+26 (***)	+34 (***)	+17 (***)	+17 (***)	+25 (***)
IC AFP vs. EGFP	+21 (***)	+38 (***)	+19 (***)	+15 (***)	+18 (***)

All experiments contained 3 biological repeats (n=3) with each containing 3 technical repeats. ***$p \leq 0.001$

Post-thaw cell damage was measured using an LDH assay (Figure 24). The assay showed a significant decrease in LDH release for IC AFP cells vs. untransfected cells, or cells transfected with EGFP across all treatments except 20% DMSO. The findings are summarized in Table 2. There were no significant differences between untransfected cells and cells transfected with EGFP across each DMSO concentration.

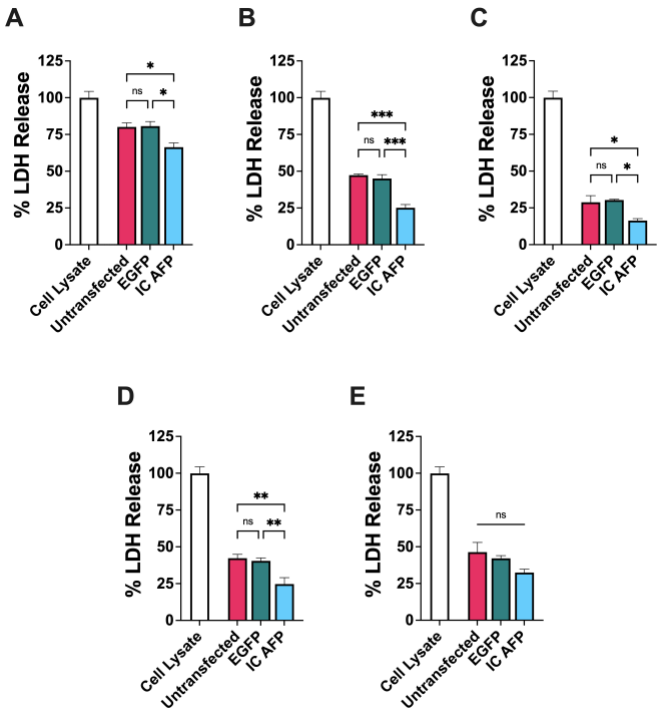

Figure 24. LDH assay of cell damage for untransfected, EGFP transfected, and EGFP-AFP transfected (IC AFP) HEK 293T cells after cryopreservation. 5 × 10^6 cells were cryopreserved with (**A**) 0, (**B**) 5, (**C**) 10, (**D**) 15, and (**E**) 20 % (v/v) concentrations of DMSO and stored in liquid nitrogen vapor phase (-196 °C) for ≥ 4 weeks. All values are media subtracted and cell damage is expressed as % total cellular LDH. Data was analyzed using a one-way analysis of variance (ANOVA) and a Tukey's post hoc test was used for pairwise comparisons of experimental groups All experiments contained 3 biological repeats (n=3) with each containing 3 technical repeats. Mean value ± SEM (n.s. $p > 0.05$, *$p \leq 0.05$, **$p \leq 0.01$, ***$p \leq 0.001$).

Table 2. Average LDH release of HEK 293T cells across treatments expressed as % total cellular LDH.

	0% DMSO	5% DMSO	10% DMSO	15% DMSO	20% DMSO
Untransfected	80	47	29	42	46
EGFP	81	45	30	40	42
IC AFP	66	25	16	25	32
IC AFP vs. Untransfected	-14 (*)	-22 (***)	-13 (*)	-17 (**)	-14 (ns)
IC AFP vs. EGFP	-15 (*)	-20 (***)	-14 (*)	-15 (**)	-10 (ns)

All experiments contained 3 biological repeats (n=3) with each containing 3 technical repeats. n.s. $p > 0.05$, *$p \leq 0.05$, **$p \leq 0.01$, ***$p \leq 0.001$

The MTS assay showed no significant differences in metabolic activity between untransfected, EGFP transfected, and AFP transfected cells for each DMSO concentration, indicating both the accuracy of the trypan blue and LDH release assays performed within 12 hours post-thaw, and no mitogenic effects of AFP for HEK 293T cells (Figure 25).

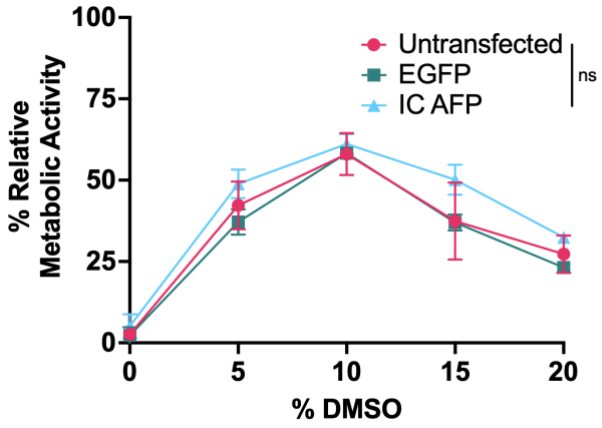

Figure 25. Relative metabolic activity assessed via MTS assay performed on untransfected, EGFP transfected, and EGFP-AFP transfected (IC AFP) HEK 293T cells after cryopreservation. 5 × 10^6 cells were cryopreserved with 0, 5, 10, 15, and 20% (v/v) concentrations of DMSO and stored in liquid nitrogen vapor phase (-196 °C) for ≥ 4 weeks. Media was changed after 24 hours and MTS assay was performed after 48 hours with % metabolic activity measured relative to fresh, non-cryopreserved HEK 293T cells. Data was analyzed using a one-way analysis of variance (ANOVA) and a Tukey's post hoc test was used for pairwise comparisons of experimental groups All experiments contained 3 biological repeats (*n*=3) with each containing 3 technical repeats. Mean value ± SEM (n.s. $p > 0.05$)

Intracellular vs. Extracellular AFP

In order to determine whether the cryoprotective activity of IC AFP is more potent than extracellular AFP (EC AFP), the two conditions were directly compared to untransfected cells. Due to no increased cryoprotective effects observed for 15 or 20% v/v DMSO over 5 and 10% v/v DMSO, and with the aim to use as little DMSO as necessary for cryopreservation, DMSO concentrations were kept at those most commonly used for cryopreservation (5 and 10% v/v) for intracellular vs. extracellular (IC vs. EC) AFP testing [164]. We tested two concentrations (5 µM and 15 µM) of EC AFP to establish its efficacy in cryopreservation, and 5 µM was chosen as the minimal concentration as we have previously shown that this was the minimal concentration at which purified TrxA-ApAFP752 exhibited potent ice-recrystallization inhibition (IRI) behavior [124]. The trypan

blue assay showed a significant increase in viability for all AFP treatments (Figure 26 A-C). Cells cryopreserved with both extracellular and intracellular (EC and IC) AFP compared to untransfected HEK 293T cells yielded the highest levels of cryoprotection. These viability increases are summarized in Table 3.

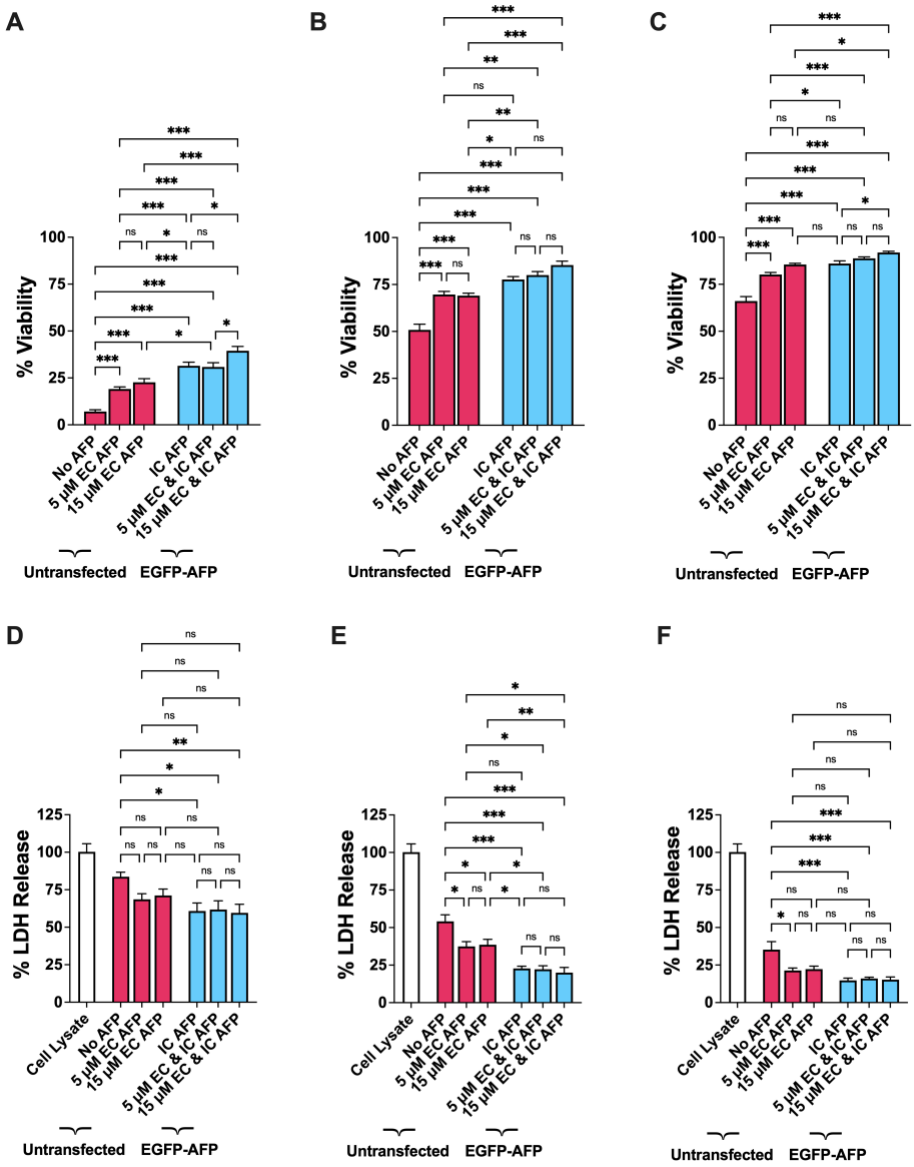

Figure 26. (**A-C**) Trypan blue exclusion assay in untransfected and AFP transfected (IC AFP) HEK 293T cells after cryopreservation. 5 × 10^6 cells were cryopreserved with (**A**) 0, (**B**) 5, and (**C**) 10 % (v/v) concentrations of DMSO and/or 5 or 15 µM (0.132 or 0.396 mg/ml) TrxA-ApAFP752 (EC AFP) and stored in liquid nitrogen vapor phase (-196 °C) for ≥ 4 weeks. (**D-F**) LDH assay measurement of cell damage for untransfected and AFP transfected (IC AFP) HEK 293T cells after cryopreservation. 5 × 10^6 cells were cryopreserved with (**D**) 0, (**E**) 5, and (**F**) 10 % (v/v) concentrations of DMSO and/or 5 or 15 µM (0.132 or 0.396 mg/ml) TrxA-ApAFP752 (EC AFP) and stored in liquid nitrogen vapor phase (-196 °C) for ≥ 4 weeks. All values are media subtracted and cell damage is expressed as % total cellular LDH. Data was analyzed using a one-way analysis of variance (ANOVA) and a Tukey's post hoc test was used for pairwise comparisons of experimental groups All experiments contained 3 biological repeats (n=3) with each containing 3 technical repeats. Mean value ± SEM (n.s. $p > 0.05$, *$p \leq 0.05$, **$p \leq 0.01$, ***$p \leq 0.001$)

Table 3. Average increased % viability of HEK 293T cells across treatments for extracellular (EC) AFP and intracellular (IC) AFP vs. cells without AFP (untransfected), as determined by trypan blue assay.

	5 µM EC AFP	**15 µM EC AFP**	**IC AFP**	**5 µM EC & IC AFP**	**15 µM EC & IC AFP**
0% DMSO	+12 (***)	+16 (***)	+24 (***)	+24 (***)	+32 (***)
5% DMSO	+19 (***)	+18 (***)	+27 (***)	+29 (***)	+34 (***)
10% DMSO	+14 (***)	+20 (***)	+20 (***)	+23 (***)	+26 (***)

All experiments contained 3 biological repeats (*n*=3) with each containing 3 technical repeats. ****p* ≤ 0.001

Post-thaw cell damage was measured using an LDH assay comparing untransfected cells to the various AFP treatments (Figure 26 D-F). For 5 µM vs. 15 µM EC AFP, significant decreases in LDH release were not found in 0% DMSO samples (Figure 26 D). There was also no significant decrease in LDH release for cells cryopreserved with 15 µM EC AFP at 10% DMSO (Figure 26 F). It should be noted that this value is very nearly statistically significant (p = 0.06), and this treatment may still be biologically significant. A significant decrease in LDH release was found in all IC AFP treatments and the results are summarized in Table 4 and Table S2.

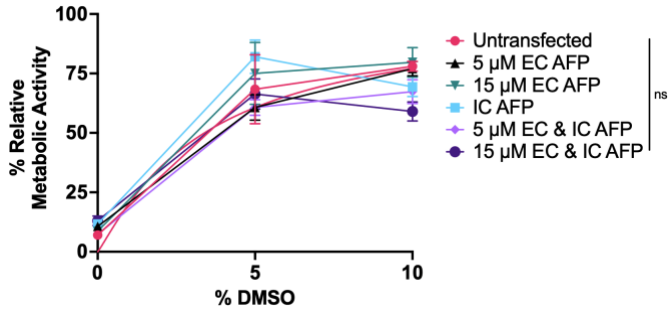

Figure 27. Relative metabolic activity assessed via MTS assay performed on untransfected and AFP transfected (IC AFP) HEK 293T cells after cryopreservation. 5 × 10^6 cells were cryopreserved with 0, 5, and 10 % (v/v) concentrations of DMSO and/or 5 or 15 µM (0.132 or 0.396 mg/ml) TrxA-ApAFP752 (EC AFP) and stored in liquid nitrogen vapor phase (-196 °C) for ≥ 4 weeks. Media was changed after 24 hours and MTS assay was performed after 48 hours with % metabolic activity measured relative to fresh, non-cryopreserved HEK 293T cells. Data was analyzed using a one-way analysis of variance (ANOVA) and a Tukey's post hoc test was used for pairwise comparisons of experimental groups All experiments contained 3 biological repeats (n=3) with each containing 3 technical repeats. Mean value ± SEM (n.s. $p > 0.05$)

Table 4. Average LDH release of HEK 293T cells expressed as % total cellular LDH across treatments for extracellular (EC) AFP and intracellular (IC) AFP vs. cells without AFP.

	5 µM EC AFP	**15 µM EC AFP**	**IC AFP**	**5 µM EC & IC AFP**	**15 µM EC & IC AFP**
0% DMSO	-15 (ns)	-13 (ns)	-23 (*)	-22 (*)	-24 (**)
5% DMSO	-17 (*)	-15 (*)	-31 (***)	-32 (***)	-34 (***)
10% DMSO	-14 (*)	-13 (ns)	-20 (***)	-19 (***)	-20 (***)

All experiments contained 3 biological repeats (n=3) with each containing 3 technical repeats. n.s. $p > 0.05$, *$p \leq 0.05$, **$p \leq 0.01$, ***$p \leq 0.001$

The MTS assay showed no significant differences in metabolic activity between post-thaw untransfected cells and EGFP-ApAFP752 transfected (IC AFP) cells for each condition for each DMSO concentration (Figure 27). This indicates the accuracy of the trypan blue and LDH assays performed within 12 hours post-thaw and no mitogenic effects of EC AFP or IC AFP for HEK 293T cells.

IV. Discussion

Effective cryopreservation and long-term storage are essential requirements for the use of cells in research and clinical applications of cell-based therapies and improving cryopreservation materials and procedures is critical for many cell types [173,224]. There are two major categories of CPAs: penetrating and non-penetrating [154,164]. As their names imply, non-penetrating CPAs are extracellular with some examples being polymers, such as polyvinyl alcohol (PVA) or polyampholytes [165,166]. Penetrating CPAs such as DMSO or glycerol are intracellular and are the most commonly used of all CPAs [152,168], and in mammalian cell culture, most cryopreservation procedures utilize DMSO as the cryoprotectant. The concentration of DMSO as well as exposure time must be optimized to a level that yields the most cryoprotective benefit with the least cytotoxic effects, and in most applications, cells are incubated in the presence of 5-10% v/v of DMSO for 10 minutes prior to freezing to allow penetration of DMSO. The cells are then cooled at a rate of -1 °C/min in a standard freezing container down to -80 °C before moving the frozen cell suspension to liquid nitrogen storage (-196 °C) [164]. A non-toxic alternative or addition to DMSO would be beneficial to increase cryopreservation efficacy and potentially reduce the amount of DMSO required, thereby reducing the toxic effects. Here, ApAFP752 demonstrated significant extra- and intracellular cryoprotective activity. By transfecting AFP into cells, the AFP is given the ability to protect cells from within, improving its cryoprotective potency compared to when it is confined to the extracellular medium. This transient transfection also allows for AFP expression and cryoprotection in a non-heritable manner.

The trypan blue assay showed a significant increase in post-thaw viability for HEK 293T cells transfected with EGFP-ApAFP752 (IC AFP) (Figure 23). Interestingly, though viability was optimized at 10 % DMSO, continued cryoprotection and potential attenuation of cytotoxic levels of DMSO was observed for IC AFP at 15 and 20% DMSO (Figure 23, Figure 24) [225]. Though extracellular TrxA-ApAFP752 (EC AFP) also provided a significant increase in post-thaw viability, IC AFP demonstrated significantly higher post-thaw viability for the 0% and 5% DMSO concentrations (Figure 26 A-B), and at 10% DMSO, 15 µM EC AFP displayed the same increased viability as IC AFP, with no significant difference between the two conditions (Figure 26 C). This could be due to the fact that the post-thaw viability with 10% DMSO alone was an average of 66% (Table S1), and there was less room for improvement. Interestingly, there was significantly improved post-thaw viability for the combined approach of 15 µM EC & IC AFP over IC AFP alone at 0 and 10% DMSO, while at 5% DMSO there was no statistically significant change in viability (Figure 26, Table S1). Overall, 15 µM EC & IC AFP yielded the most potent cryoprotective activity across every DMSO concentration tested. For example, at 10% DMSO, 15 µM EC & IC AFP HEK 293T cells demonstrated 92% viability on average after freeze/thaw (Figure 26, Table S1). It is also worth noting at 5% DMSO, IC AFP offers improved cryoprotective activity over 10% DMSO alone (Figure 23, Figure 26, Table 1, Table S1), demonstrating IC AFP can be implemented as a means of reducing DMSO. Also, 5% DMSO with 5 and 15 µM EC & IC AFP gives similar post-thaw viability as 10% DMSO with 5 and 15 µM EC AFP (Figure 26, Table S1). This further demonstrates EC and IC AFP can be used to reduce the amount DMSO required for cryoprotection.

The LDH release assay results were in agreement with the trypan blue viability results, only with the LDH release assay, cell damage is quantified. IC AFP significantly reduced the amount of LDH released by cells at 0, 5, 10, and 15% DMSO concentrations (Figure 24, Table 2, Figure 26, Table 3, Table S2). No significant decreases in LDH release were detected for the combined approach of 5 and 15 µM EC & IC AFP over IC AFP alone, indicating IC AFP is mainly responsible for the significant decrease in LDH release (Figure 26 D-F, Table 4, Table S2). For the MTS assay, no significant differences in the relative metabolic activity measurements across treatments for each DMSO concentration demonstrated the accuracy of these initial viability counts (Figure 25, Figure 27). It should be noted that cells exhibiting low metabolic activity, as at confluence, are still alive [226-228]. The consistent reduction in post-thaw metabolic activity was not surprising, as cryopreserved mammalian cells have been shown to have reduced cellular proliferation as measured by metabolic activity, and cells can take up to 96 hours to recover pre-freeze proliferation rates [181,229,230].

A major role of AFPs is the inhibition of ice recrystallization during the thawing process and in the frozen state during temperature cycling. Ice recrystallization refers to the phenomenon that larger ice crystals grow more preferentially than smaller ones in order to minimize the total surface energy. The small ice crystals fuse together, increase their size significantly, and cause physical damage to cells. Inhibition of ice recrystallization is important in the control of crystal size in cryopreservation of cells and tissues [94,231,232]. Another distinction between AFPs relating to their measured ability to create a gap between the freezing point and melting point of water, known as thermal hysteresis activity (THA), and in this regard, AFPs are considered either moderately

active or hyperactive [80,104]. Possibly more important for cryopreservation is that moderately active and hyperactive AFPs also differ in their ice crystal shaping ability. Moderately active AFPs bind to the prism and/or pyramidal planes of ice, limiting ice crystal expansion to the c-axis, resulting in a needle-like ice crystal shape [6,30,80]. Hyperactive AFPs bind to both the basal and prism planes of ice, restricting ice crystal growth along all axes, and resulting in a rounded ice crystal shape [6,81]. The fusion TrxA-ApAFP752 antifreeze activity has been previously characterized by us and others for ice-recrystallization inhibition activity and affecting ice crystal size and shape [115,123,124] and THA [123,124]. We have shown that purified Trx-ApAFP752 demonstrates functional ice-recrystallization inhibition behavior at 5 μM or higher concentrations [124], which is why we used 5 μM and 15 μM concentrations for the extracellular AFP assays. Ice-recrystallization inhibition activity, and ice shaping are likely much more important contributors to cryoprotection in cells than THA, which does not likely play much of a role when cells are stored at cryogenic temperatures.

Previous studies using hyperactive AFPs as part of the extracellular freezing solution have shown increased cryoprotective activity in mammalian cells [115,216]. The aforementioned differences between hyperactive and moderately active AFPs may explain why improved intracellular cryoprotective activity was observed here compared to previous studies using moderately active AFPs [209]. It should be noted that these previous studies used different mammalian cells, and our findings with HEK 293T cells may not apply to all mammalian cells. The methodology used here was also vastly different than any previous study. By transfecting mammalian cells and expressing AFP within them, there are minimal manipulations necessary to obtain intracellular AFP. This

ensures cells are not exposed to any additional stresses prior to freezing. This approach yielded stronger cryoprotection by ApAFP752 than our previous studies in which we either supplemented the freezing medium for human skin fibroblast cells with purified TrxA-ApAFP752 [115] or microinjected amphibian cells (frog *Xenopus laevis* eggs and embryos) with the protein [124].

GFP-AFP fusion proteins have been shown to retain or even enhance the cryoprotective activity of similar insect AFPs such as RiAFP and TmAFP [80,214]. This is thought to be due to the increased size of the fusion protein from the 27 kDa GFP combined with the 12.8 kDa (RiAFP) or 9 kDa (TmAFP) AFPs [102,125,233]. These data are further corroborated by our findings here. By transfecting AFP into cells, the otherwise non-penetrating cryoprotectant AFP is given the ability to protect the cells from within, as penetrating cryoprotectants do. This intracellular cryoprotective activity is increased for AFP in a manner similar to studies of intracellular delivery of other non-penetrating CPAs [224]. Including extracellular AFP along with intracellular AFP may provide the best cryoprotection.

One of the main goals of this study was to use well-established technologies and methods and to maintain a straightforward experimental design that builds off of current protocols. In addition, the tests performed are rapid, commercially available, and relatively low cost, making them suitable options for virtually all cell culture facilities [143]. Furthermore, these protocols follow best practices and combine several types of assays (membrane integrity, metabolic activity, etc.) necessary to achieve a comprehensive assessment of cryopreservation efficacy [151]. Because cell viability after freeze/thaw is increased with intracellular AFP, other types of cells may be studied and a unique,

cryoprotected cell line with stable and inheritable AFP expression can be developed with numerous, far-reaching practical applications. This work sheds light on potential improvements to current cryopreservation protocols by the addition of an AFP transfection step 48 hours prior to freezing, while still using widely available and well-established methods. For example, cells especially susceptible to cryoinjury, such as immune cells, could be transiently transfected with AFP prior to freezing to improve post-thaw cell viability [234,235]. Within just a few replication cycles after thawing, these cells would no longer produce AFP and could be used for other research purposes, including plasmid transfection, drug testing, etc. Further studies could also include determining localization of EGFP-AFP in mammalian cells to help elucidate any membrane localization during freezing using new methods of confocal microscopy on frozen samples [236].

V. Conclusions

This study presented insight into differences between extracellular and intracellular cryoprotective activity of AFP. This proof of concept shows a means of effective intracellular delivery of AFP yielding both biologically and statistically significant increases in cell viability following cryopreservation compared to current protocols. Reducing or ultimately eliminating DMSO is the ultimate goal for expanding and improving cellular storage, vaccine, and therapeutic methods seeking to avoid its toxic effects, but still retain effective means of cryopreservation.

Supplementary Materials: The following supporting information can be downloaded at: www.mdpi.com/xxx/s1, Figure S1: Gating strategy for flow cytometry assessment of EGFP-AFP transfection; Table S1: Average increased % viability of HEK 293T cells across treatments for extracellular (EC) AFP and intracellular (IC) AFP and comparisons

vs. cells without AFP (untransfected), as determined by trypan blue assay; Table S2: Average LDH release of HEK 293T cells expressed as % total cellular LDH across treatments for extracellular (EC) AFP and intracellular (IC) AFP and comparisons vs. cells without AFP (untransfected).

Author Contributions: Conceptualization, J.A.S., T.L.F, and K.V.; methodology, J.A.S., T.L.F, and K.V.; formal analysis, J.A.S.; investigation, J.A.S.; resources, T.L.F. and K.V.; data curation, J.A.S.; writing—original draft preparation, J.A.S.; writing—review and editing, J.A.S., T.L.F., and K.V.; visualization, J.A.S.; funding acquisition, T.L.F. and K.V. All authors have read and agreed to the published version of the manuscript.

Funding: This research was supported by an Institutional Development Award (IDeA) [CIBBR, P20GM113131] and by the award [GM135903] from the National Institute of General Medical Sciences of the National Institutes of Health. This work was also partially supported by the National Aeronautics and Space Administration EPSCoR program [80NSSC18M0034], and the by the National Science Foundation (awards CHE-1740399).

Institutional Review Board Statement: Not applicable.

Informed Consent Statement: Not applicable.

Data Availability Statement: All data reported are included and represented in the manuscript.

Acknowledgments: The authors would like to thank Sherine Elsawa and Mona Karbalivand for their scientific guidance. The authors would also like to thank Iago Hale

for his consultation on the statistical analysis. In addition, the authors would like to thank Rachel Badger for her technical assistance.

CHAPTER 5

CONCLUSIONS AND SUMMARY

Project: Cryopreservation studies of the antifreeze protein ApAFP752

Antifreeze proteins show great promise in the field of cryopreservation. We have worked to determine the cryoprotective activity of the antifreeze protein ApAFP752. To that end, we have improved our understanding of both the functional and cryopreservative aspects of the protein. In focusing on three primary aims, we have been able to answer multiple questions.

Aim 1: Characterize the antifreeze activity of the antifreeze protein ApAFP752. We hypothesized that ApAFP752 not only exhibits thermal hysteresis activity but also potent ice recrystallization inhibition. The observed thermal hysteresis activity of the TrxA-ApAFP752 (thioredoxin tagged ApAFP752) fusion protein was 0.65 °C, much lower than that of other insect antifreeze proteins. However, this was measured by differential scanning calorimetry, and other insect antifreeze proteins have been measured via nanoliter osmometry. It would be interesting to measure multiple insect antifreeze proteins with both methods to determine potential differences in observed thermal hysteresis activity. More importantly for cryopreservation, TrxA-ApAFP752 demonstrated potent ice recrystallization inhibition at concentrations as low as 5 µM. Ice recrystallization activity was still observed at 2.5 µM, though crystals began to grow in size. TrxA-ApAFP752 retained functional activity in terms of both thermal hysteresis

activity and ice recrystallization inhibition after lyophilization, indicating no functional alteration of TrxA-ApAFP752 when lyophilized.

Aim 2: Examine the extracellular cryoprotective activity of ApAFP752 for mammalian cell cryopreservation and **Aim 3: Examine the intracellular cryoprotective activity of ApAFP752 in mammalian cells** concerned the application of ApAFP752 in mammalian cell cryopreservation, and we tested these applications. We hypothesized that purified ApAFP752 added to the freezing solution would offer cryoprotection to mammalian cells during freeze/thaw. We also hypothesized that intracellular ApAFP752 would offer better cryoprotection during freeze/thaw than extracellular AFP. The data we collected shows that HEK 293T cells transfected with EGFP-ApAFP752 (intracellular or IC AFP) showed significantly improved viability after freezing to liquid nitrogen vapor phase (-196 °C) for ≥ 4 weeks then thawing. Intracellular AFP improved cell viability when combined with both 5 and 10% v/v DMSO, over cells treated with DMSO alone. IC AFP also showed significantly increased cryoprotective activity over cells treated with TrxA-ApAFP752 at 5 and 15 µM concentrations (extracellular or EC AFP) at both 0 and 5% DMSO. For cells frozen with 10% DMSO, significantly improved post-thaw viability for IC AFP was only observed compared to cells frozen with 5 µM, but not 15 µM EC AFP. Across all treatments and DMSO concentrations, IC AFP combined with EC AFP demonstrated the most potent cryoprotective activity. Additional studies involving intracellular delivery of ApAFP752 as a cryoprotective agent are underway in cells more susceptible to freeze/thaw damage such as hepatocytes or immune cells.

APPENDIX

Materials and Methods

Plasmid Constructs: The fusion protein TrxA-ApAFP752 plasmid construct was obtained as a gift from Dr. Ji Ma at XinJiang University, Urumqi, China. This fusion protein is engineered with a pET32a construct and it contains an enterokinase cleavage site between the thioredoxin A (TrxA) and the ApAFP752 with a C-terminal 6-His histidine tag located on the TrxA portion of the fusion protein.

Supplementary Information
Intracellular and Extracellular Antifreeze Protein Significantly Improves Mammalian Cell Cryopreservation

Jonathan A. Sreter [1], Thomas L. Foxall [2], and Krisztina Varga [1,*]

[1] Department of Molecular, Cellular and Biomedical Sciences, University of New Hampshire, Durham, NH, 03824, USA
[2] Department of Biological Sciences, University of New Hampshire, Durham, NH, 03824, USA
***** Correspondence: krisztina.varga@unh.edu; Tel.: (603) 862-5375

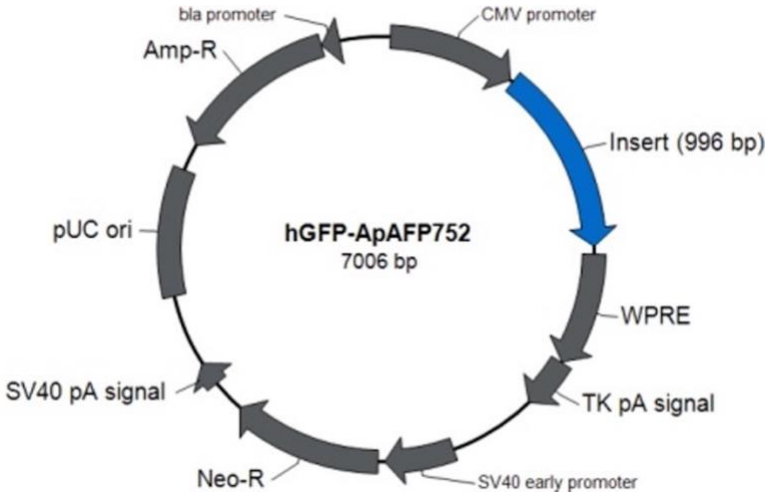

Figure S1. Plasmid map of EGFP-ApAFP752.

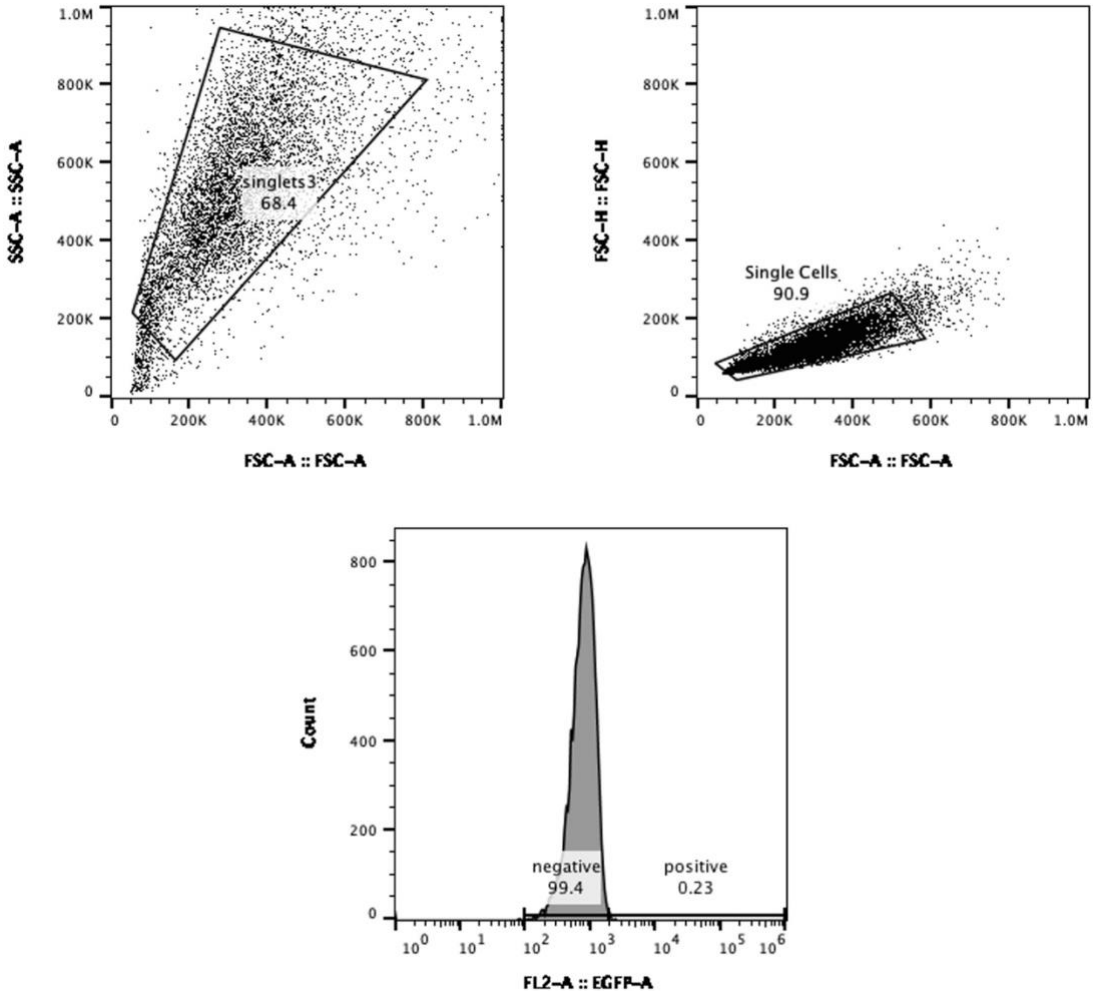

Figure S2. Gating strategy for flow cytometry assessment of EGFP-AFP transfection.

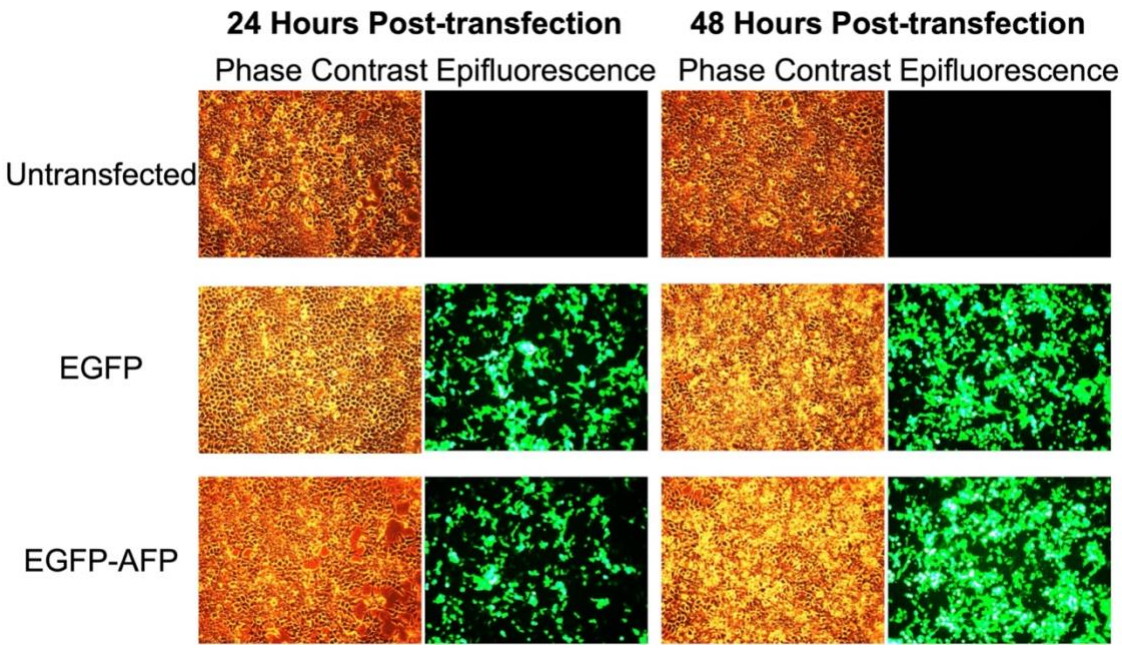

Figure S3: 24- and 48-hour post-transfection microscopy images. All images were photographed at 100X.

Table S1. Average increased % viability of HEK 293T cells across treatments for extracellular (EC) AFP and intracellular (IC) AFP and comparisons vs. cells without AFP (untransfected), as determined by trypan blue assay.

	0% DMSO	5% DMSO	10% DMSO
Untransfected	7	51	66
5 μM EC AFP	19	70	80
15 μM EC AFP	23	69	86
IC AFP	31	78	86
5 μM EC & IC AFP	31	80	89
15 μM EC & IC AFP	39	85	92
5 μM EC AFP vs. Untransfected	12 (***)	+19 (***)	+14 (***)
15 μM EC AFP vs. Untransfected	+16 (***)	+18 (***)	+20 (***)
IC AFP vs. Untransfected	+24 (***)	+27 (***)	+20 (***)
5 μM EC & IC AFP vs. Untransfected	+24 (***)	+29 (***)	+23 (***)
15 μM EC & IC AFP vs. Untransfected	+32 (***)	+34 (***)	+26 (***)

$n = 3$, ***$p \leq 0.001$

Table S2. Average LDH release of HEK 293T cells expressed as % total cellular LDH across treatments for extracellular (EC) AFP and intracellular (IC) AFP and comparisons vs. cells without AFP (untransfected).

	0% DMSO	5% DMSO	10% DMSO
Untransfected	84	54	35
5 μM EC AFP	69	37	21
15 μM EC AFP	71	39	22
IC AFP	61	23	15
5 μM EC & IC AFP	62	22	16
15 μM EC & IC AFP	60	20	15
5 μM EC AFP vs. Untransfected	-15 (ns)	-17 (*)	-14 (*)
15 μM EC AFP vs. Untransfected	-13 (ns)	-15 (*)	-13 (ns)
IC AFP vs. Untransfected	-23 (*)	-31 (***)	-20 (***)
5 μM EC & IC AFP vs. Untransfected	-22 (*)	-32 (***)	-19 (***)
15 μM EC & IC AFP vs. Untransfected	-24 (**)	-34 (***)	-20 (***)

$n = 3$, n.s. $p > 0.05$, *$p \leq 0.05$, **$p \leq 0.01$, ***$p \leq 0.001$

References

1 Duman, J. G. Animal ice-binding (antifreeze) proteins and glycolipids: an overview with emphasis on physiological function. *J. Exp. Biol.* **218**, 1846-1855, doi:10.1242/jeb.116905 (2015).

2 Eickhoff, L. *et al.* Contrasting Behavior of Antifreeze Proteins: Ice Growth Inhibitors and Ice Nucleation Promoters. *J. Phys. Chem. Lett.* **10**, 966-972, doi:10.1021/acs.jpclett.8b03719 (2019).

3 DeVries, A. L. & Wohlschlag, D. E. Freezing resistance in some Antarctic fish. *Science* **163**, 1073-1075 (1969).

4 Bar Dolev, M., Braslavsky, I. & Davies, P. L. in *Annual Review of Biochemistry, Vol 85* Vol. 85 *Annual Review of Biochemistry* (ed R. D. Kornberg) 515-542 (Annual Reviews, 2016).

5 Voets, I. K. From ice-binding proteins to bio-inspired antifreeze materials. *Soft Matter* **13**, 4808-4823, doi:10.1039/c6sm02867e (2017).

6 Kim, H. J. *et al.* Marine Antifreeze Proteins: Structure, Function, and Application to Cryopreservation as a Potential Cryoprotectant. *Marine Drugs* **15**, 27, doi:10.3390/md15020027 (2017).

7 Griffith, M. & Yaish, M. W. F. Antifreeze proteins in overwintering plants: a tale of two activities. *Trends in Plant Science* **9**, 399-405, doi:10.1016/j.tplants.2004.06.007 (2004).

8 Devries, A. L. Antifreeze glycopeptides and peptides - Interactions with ice and water. *Methods in Enzymology* **127**, 293-303 (1986).

9 Bar-Dolev, M., Celik, Y., Wettlaufer, J. S., Davies, P. L. & Braslavsky, I. New insights into ice growth and melting modifications by antifreeze proteins. *J. R. Soc. Interface* **9**, 3249-3259, doi:10.1098/rsif.2012.0388 (2012).

10 DeVries, A. L. The role of antifreeze glycopeptides and peptides in the freezing avoidance of antarctic fishes. *Comparative Biochemistry and Physiology Part B: Comparative Biochemistry* **90**, 611-621, doi:https://doi.org/10.1016/0305-0491(88)90302-1 (1988).

11 Cheng, C.-H. C. Evolution of the diverse antifreeze proteins. *Current Opinion in Genetics & Development* **8**, 715-720, doi:https://doi.org/10.1016/S0959-437X(98)80042-7 (1998).

12 Bale, J. S. & Hayward, S. A. L. Insect overwintering in a changing climate. *J. Exp. Biol.* **213**, 980-994, doi:10.1242/jeb.037911 (2010).

13 Clark, M. S. & Worland, M. R. How insects survive the cold: molecular mechanisms-a review. *Journal of Comparative Physiology B-Biochemical Systemic and Environmental Physiology* **178**, 917-933, doi:10.1007/s00360-008-0286-4 (2008).

14 Doucet, D., Walker, V. K. & Qin, W. The bugs that came in from the cold: molecular adaptations to low temperatures in insects. *Cellular and Molecular Life Sciences* **66**, 1404-1418, doi:10.1007/s00018-009-8320-6 (2009).

15 Davies, P. L. & Graham, L. A. Protein evolution revisited. *Systems Biology in Reproductive Medicine* **64**, 403-416, doi:10.1080/19396368.2018.1511764 (2018).

16 Amir, G. Preservation of myocyte structure and mitochondrial integrity in subzero cryopreservation of mammalian hearts for transplantation using antifreeze proteins—an electron microscopy study. *European Journal of Cardio-Thoracic Surgery* **24**, 292-297, doi:10.1016/s1010-7940(03)00306-3 (2003).
17 Amir, G. *et al.* Prolonged 24-hour subzero preservation of heterotopically transplanted rat hearts using antifreeze proteins derived from arctic fish. *The Annals of thoracic surgery* **77**, 1648-1655, doi:10.1016/j.athoracsur.2003.04.004 (2004).
18 Griffith, M. & Yaish, M. W. Antifreeze proteins in overwintering plants: a tale of two activities. *Trends in plant science* **9**, 399-405, doi:10.1016/j.tplants.2004.06.007 (2004).
19 Brockbank, K. G., Campbell, L. H., Greene, E. D., Brockbank, M. C. & Duman, J. G. Lessons from nature for preservation of mammalian cells, tissues, and organs. *In vitro cellular & developmental biology. Animal* **47**, 210-217, doi:10.1007/s11626-010-9383-2 (2011).
20 Tomczak, M. M. *et al.* A Mechanism for Stabilization of Membranes at Low Temperatures by an Antifreeze protein. *Biophysical journal* **82**, 874-881, doi:10.1016/S0006-3495(02)75449-0 (2002).
21 Haymet, A. D., Ward, L. G., Harding, M. M. & Knight, C. A. Valine substituted winter flounder 'antifreeze': preservation of ice growth hysteresis. *FEBS letters* **430**, 301-306 (1998).
22 Howard, E. I. *et al.* Neutron structure of type-III antifreeze protein allows the reconstruction of AFP-ice interface. *Journal of Molecular Recognition* **24**, 724-732, doi:10.1002/jmr.1130 (2011).
23 Devries, A. L. Glycoproteins as Biological Antifreeze Agents in Antarctic Fishes. *Science* **172**, 1152-1155 (1971).
24 Venketesh, S. & Dayananda, C. Properties, potentials, and prospects of antifreeze proteins. *Critical reviews in biotechnology* **28**, 57-82 (2008).
25 Komatsu, S. K., DeVries, A. L. & Feeney, R. E. Studies of the structure of freezing point depressing glycoproteins from an Antarctic fish. *Journal of Biological Chemistry* **245**, 2909-2913 (1970).
26 Harding, M. M., Anderberg, P. I. & Haymet, A. D. J. 'Antifreeze' glycoproteins from polar fish. *European Journal of Biochemistry* **270**, 1381-1392, doi:https://doi.org/10.1046/j.1432-1033.2003.03488.x (2003).
27 Lin, Y., Duman, J. G. & DeVries, A. L. Studies on the structure and activity of low molecular weight glycoproteins from an antarctic fish. *Biochem. Biophys. Res. Commun.* **46**, 87-92, doi:https://doi.org/10.1016/0006-291X(72)90633-X (1972).
28 Graether, S. P. in *Biochemistry and Function of Antifreeze Proteins* (ed Vladimir N. Uversky) 221 (Nova Science Publishers, Inc., New York, 2010).
29 Zhang, W. Structure-function relationships in a type I antifreeze polypeptide: the role of threonine methyl and hydroxyl groups in antifreeze activity. *Journal of Biological Chemistry* **273**, 34806-34812, doi:10.1074/jbc.273.52.34806 (1998).
30 Knight, C. A., Cheng, C. C. & Devries, A. L. ADSORPTION OF ALPHA-HELICAL ANTIFREEZE PEPTIDES ON SPECIFIC ICE CRYSTAL-SURFACE PLANES. *Biophysical Journal* **59**, 409-418, doi:10.1016/s0006-3495(91)82234-2 (1991).

31 Sicheri, F. & Yang, D. S. C. Ice-binding structure and mechanism of an antifreeze protein from winter flounder. *Nature* **375**, 427-431, doi:10.1038/375427a0 (1995).
32 Kajava, A. V. Tandem repeats in proteins: from sequence to structure. *Journal of structural biology* **179**, 279-288, doi:10.1016/j.jsb.2011.08.009 (2012).
33 Sun, T. J., Lin, F. H., Campbell, R. L., Allingham, J. S. & Davies, P. L. An Antifreeze Protein Folds with an Interior Network of More Than 400 Semi-Clathrate Waters. *Science* **343**, 795-798, doi:10.1126/science.1247407 (2014).
34 Gronwald, W. *et al.* The solution structure of type II antifreeze protein reveals a new member of the lectin family. *Biochemistry* **37**, 4712-4721 (1998).
35 Liu, Y. *et al.* Structure and Evolutionary Origin of Ca2+-Dependent Herring Type II Antifreeze Protein. *PLoS One* **2**, e548, doi:10.1371/journal.pone.0000548 (2007).
36 Nishimiya, Y. *et al.* Crystal Structure and Mutational Analysis of Ca2+-Independent Type II Antifreeze Protein from Longsnout Poacher, Brachyopsis rostratus. *Journal of Molecular Biology* **382**, 734-746, doi:https://doi.org/10.1016/j.jmb.2008.07.042 (2008).
37 Gronwald, W. *et al.* The Solution Structure of Type II Antifreeze Protein Reveals a New Member of the Lectin Family. *Biochemistry* **37**, 4712-4721, doi:10.1021/bi972788c (1998).
38 Yamashita, Y. *et al.* Type II antifreeze protein from a mid-latitude freshwater fish, Japanese smelt (Hypomesus nipponensis). *Biosci Biotechnol Biochem* **67**, 461-466, doi:10.1271/bbb.67.461 (2003).
39 Ewart, K. V., Lin, Q. & Hew, C. L. Structure, function and evolution of antifreeze proteins. *Cellular and Molecular Life Sciences CMLS* **55**, 271-283, doi:10.1007/s000180050289 (1999).
40 Antson, A. A. *et al.* Understanding the mechanism of ice binding by type III antifreeze proteins. *Journal of Molecular Biology* **305**, 875-889, doi:10.1006/jmbi.2000.4336 (2001).
41 Yeh, Y. & Feeney, R. E. Antifreeze proteins: Structures and mechanisms of function. *Chem. Rev.* **96**, 601-617, doi:10.1021/cr950260c (1996).
42 Desjardins, M., Le François, N. R., Fletcher, G. L. & Blier, P. U. High antifreeze protein levels in wolffish (Anarhichas lupus) make them an ideal candidate for culture in cold, potentially ice laden waters. *Aquaculture* **272**, 667-674, doi:https://doi.org/10.1016/j.aquaculture.2007.08.016 (2007).
43 Chao, H., Sönnichsen, F. D., DeLuca, C. I., Sykes, B. D. & Davies, P. L. Structure-function relationship in the globular type III antifreeze protein: identification of a cluster of surface residues required for binding to ice. *Protein science : a publication of the Protein Society* **3**, 1760-1769, doi:10.1002/pro.5560031016 (1994).
44 Leiter, A. *et al.* Influence of heating temperature, pressure and pH on recrystallization inhibition activity of antifreeze protein type III. *J. Food Eng.* **187**, 53-61, doi:10.1016/j.jfoodeng.2016.04.019 (2016).
45 Garnham, C. P. *et al.* Compound Ice-Binding Site of an Antifreeze Protein Revealed by Mutagenesis and Fluorescent Tagging. *Biochemistry* **49**, 9063-9071, doi:10.1021/bi100516e (2010).

46 Deng, G. J., Andrews, D. W. & Laursen, R. A. Amino acid sequence of a new type of antifreeze protein: From the longhorn sculpin Myoxocephalus octodecimspinosis. *Febs Letters* **402**, 17-20, doi:10.1016/s0014-5793(96)01466-4 (1997).
47 Deng, G. & Laursen, R. A. Isolation and characterization of an antifreeze protein from the longhorn sculpin, Myoxocephalus octodecimspinosis. *Biochimica et Biophysica Acta (BBA) - Protein Structure and Molecular Enzymology* **1388**, 305-314, doi:https://doi.org/10.1016/S0167-4838(98)00180-0 (1998).
48 Gauthier, S. Y. *et al.* A re-evaluation of the role of type IV antifreeze protein. *Cryobiology* **57**, 292-296, doi:https://doi.org/10.1016/j.cryobiol.2008.10.122 (2008).
49 Lee, J. K. & Kim, H. J. Cloning, expression, and activity of type IV antifreeze protein from cultured subtropical olive flounder (Paralichthys olivaceus). *Fisheries and Aquatic Sciences* **19**, 33, doi:10.1186/s41240-016-0033-9 (2016).
50 Lee, J. K. *et al.* Molecular and comparative analyses of type IV antifreeze proteins (AFPIVs) from two Antarctic fishes, Pleuragramma antarcticum and Notothenia coriiceps. *Comparative Biochemistry and Physiology Part B: Biochemistry and Molecular Biology* **159**, 197-205, doi:https://doi.org/10.1016/j.cbpb.2011.04.006 (2011).
51 Zhang, D. Q., Liu, B., Feng, D. R., He, Y. M. & Wang, J. F. Expression, purification, and antifreeze activity of carrot antifreeze protein and its mutants. *Protein expression and purification* **35**, 257-263, doi:10.1016/j.pep.2004.01.019 (2004).
52 Gupta, R. & Deswal, R. Antifreeze proteins enable plants to survive in freezing conditions. *J. Biosci.* **39**, 931-944 (2014).
53 Kuiper, M. J., Davies, P. L. & Walker, V. K. A Theoretical Model of a Plant Antifreeze Protein from Lolium perenne. *Biophysical Journal* **81**, 3560-3565, doi:https://doi.org/10.1016/S0006-3495(01)75986-3 (2001).
54 Middleton, A. J. *et al.* Antifreeze Protein from Freeze-Tolerant Grass Has a Beta-Roll Fold with an Irregularly Structured Ice-Binding Site. *Journal of Molecular Biology* **416**, 713-724, doi:10.1016/j.jmb.2012.01.032 (2012).
55 Middleton, A. J., Brown, A. M., Davies, P. L. & Walker, V. K. Identification of the ice-binding face of a plant antifreeze protein. *FEBS Letters* **583**, 815-819, doi:https://doi.org/10.1016/j.febslet.2009.01.035 (2009).
56 Di Matteo, A. *et al.* The crystal structure of polygalacturonase-inhibiting protein (PGIP), a leucine-rich repeat protein involved in plant defense. *Proceedings of the National Academy of Sciences* **100**, 10124, doi:10.1073/pnas.1733690100 (2003).
57 Maddah, M., Shahabi, M. & Peyvandi, K. How Does DcAFP, a Plant Antifreeze Protein, Control Ice Inhibition through the Kelvin Effect? *Industrial & Engineering Chemistry Research* **60**, 18230-18242, doi:10.1021/acs.iecr.1c02559 (2021).
58 Zhang, D. Q., Liu, B., Feng, D. R., He, Y. M. & Wang, J. F. Expression, purification, and antifreeze activity of carrot antifreeze protein and its mutants. *Protein Expression and Purification* **35**, 257-263, doi:10.1016/j.pep.2004.01.019 (2004).

59 Naing, A. H. & Kim, C. K. A brief review of applications of antifreeze proteins in cryopreservation and metabolic genetic engineering. *3 Biotech* **9**, 329-329, doi:10.1007/s13205-019-1861-y (2019).
60 Graham, L. A., Liou, Y. C., Walker, V. K. & Davies, P. L. Hyperactive antifreeze protein from beetles. *Nature* **388**, 727-728, doi:10.1038/41908 (1997).
61 Kristiansen, E. *et al.* Hyperactive antifreeze proteins from longhorn beetles: Some structural insights. *Journal of Insect Physiology* **58**, 1502-1510, doi:10.1016/j.jinsphys.2012.09.004 (2012).
62 Kondo, H. *et al.* Ice-binding site of snow mold fungus antifreeze protein deviates from structural regularity and high conservation. *Proceedings of the National Academy of Sciences of the United States of America* **109**, 9360-9365, doi:10.1073/pnas.1121607109 (2012).
63 Kim, M., Gwak, Y., Jung, W. & Jin, E. Identification and Characterization of an Isoform Antifreeze Protein from the Antarctic Marine Diatom, Chaetoceros neogracile and Suggestion of the Core Region. *Marine drugs* **15**, 318, doi:10.3390/md15100318 (2017).
64 Garnham, Christopher P. *et al.* A Ca2+-dependent bacterial antifreeze protein domain has a novel β-helical ice-binding fold. *Biochemical Journal* **411**, 171-180, doi:10.1042/BJ20071372 (2008).
65 Duman, J. G. Antifreeze and Ice Nucleator Proteins in Terrestrial Arthropods. *Annual Review of Physiology* **63**, 327-357, doi:10.1146/annurev.physiol.63.1.327 (2001).
66 Rahman, A. T. *et al.* Ice recrystallization is strongly inhibited when antifreeze proteins bind to multiple ice planes. *Sci Rep* **9**, 9, doi:10.1038/s41598-018-36546-2 (2019).
67 Scotter, A. J. *et al.* The basis for hyperactivity of antifreeze proteins. *Cryobiology* **53**, 229-239, doi:10.1016/j.cryobiol.2006.06.006 (2006).
68 Marshall, C. B., Fletcher, G. L. & Davies, P. L. Hyperactive antifreeze protein in a fish. *Nature* **429**, 153-153, doi:10.1038/429153a (2004).
69 Graham, L. A., Marshall, C. B., Lin, F.-H., Campbell, R. L. & Davies, P. L. Hyperactive Antifreeze Protein from Fish Contains Multiple Ice-Binding Sites. *Biochemistry* **47**, 2051-2063, doi:10.1021/bi7020316 (2008).
70 Li, J. Q., Ma, W. J. & Ma, J. HEAT INDUCIBLE EXPRESSION OF ANTIFREEZE PROTEIN GENES FROM THE BEETLES Tenebrio molitor AND Microdera punctipennis. *CryoLetters* **37**, 10-18 (2016).
71 Liou, Y. C. *et al.* Folding and structural characterization of highly disulfide-bonded beetle antifreeze protein produced in bacteria. *Protein expression and purification* **19**, 148-157, doi:10.1006/prep.2000.1219 (2000).
72 Midya, U. S. & Bandyopadhyay, S. Hydration Behavior at the Ice-Binding Surface of the Tenebrio molitor Antifreeze Protein. *J. Phys. Chem. B* **118**, 4743-4752, doi:10.1021/jp412528b (2014).
73 Garnham, C. P., Campbell, R. L. & Davies, P. L. Anchored clathrate waters bind antifreeze proteins to ice. *Proceedings of the National Academy of Sciences of the United States of America* **108**, 7363-7367 (2011).

74 Davies, P. L., Baardsnes, J., Kuiper, M. J. & Walker, V. K. Structure and function of antifreeze proteins. *Philosophical transactions of the Royal Society of London. Series B, Biological sciences* **357**, 927-935, doi:10.1098/rstb.2002.1081 (2002).
75 Liou, Y.-C., Tocilj, A., Davies, P. L. & Jia, Z. Mimicry of ice structure by surface hydroxyls and water of a [beta]-helix antifreeze protein. *Nature* **406**, 322-324 (2000).
76 Hanada, Y., Nishimiya, Y., Miura, A., Tsuda, S. & Kondo, H. Hyperactive antifreeze protein from an Antarctic sea ice bacterium Colwellia sp. has a compound ice-binding site without repetitive sequences. *The FEBS Journal* **281**, 3576-3590, doi:https://doi.org/10.1111/febs.12878 (2014).
77 Graether, S. P. *et al.* Beta-helix structure and ice-binding properties of a hyperactive antifreeze protein from an insect. *Nature* **406**, 325-328 (2000).
78 Davies, P. L., Baardsnes, J., Kuiper, M. J. & Walker, V. K. Structure and function of antifreeze proteins. *Philosophical Transactions of the Royal Society B: Biological Sciences* **357**, 927-935 (2002).
79 Kristiansen, E. *et al.* Structural characteristics of a novel antifreeze protein from the longhorn beetle Rhagium inquisitor. *Insect biochemistry and molecular biology* **41**, 109-117 (2011).
80 Drori, R., Celik, Y., Davies, P. L. & Braslavsky, I. Ice-binding proteins that accumulate on different ice crystal planes produce distinct thermal hysteresis dynamics. *J. R. Soc. Interface* **11**, 10, doi:10.1098/rsif.2014.0526 (2014).
81 Braslavsky, I. & Drori, R. LabVIEW-operated Novel Nanoliter Osmometer for Ice Binding Protein Investigations. *J. Vis. Exp.*, 6, doi:10.3791/4189 (2013).
82 Basu, K. *et al.* Determining the ice-binding planes of antifreeze proteins by fluorescence-based ice plane affinity. *Journal of visualized experiments : JoVE*, e51185-e51185, doi:10.3791/51185 (2014).
83 Elliott, K. W. *Biophysical Properties of an Antifreeze Protein and the Effects of Ionic Liquids on the Model Protein GB1* PhD thesis, University of New Hampshire, (2018).
84 Hobbs, P. V. *Ice Physics*. (Oxford University Press, 1974).
85 Knight, C. A., De Vries, A. L. & Oolman, L. D. Fish antifreeze protein and the freezing and recrystallization of ice. *Nature* **308**, 295-296, doi:10.1038/308295a0 (1984).
86 Knight, C. A., Wen, D. & Laursen, R. A. Nonequilibrium antifreeze peptides and the recrystallization of ice. *Cryobiology* **32**, 23-34 (1995).
87 Marchand, P. J. *Life in the Cold: An Introduction to Winter Ecology*. 3rd edn, (University Press of New England, 1996).
88 Capicciotti, C. J., Doshi, M. & Ben, R. N. *Ice Recrystallization Inhibitors: From Biological Antifreezes to Small Molecules*. (2013).
89 Rubinsky, B. Principles of low temperature cell preservation. *Heart Fail. Rev.* **8**, 277-284, doi:10.1023/a:1024734003814 (2003).
90 Davies, P. L. Ice-binding proteins: a remarkable diversity of structures for stopping and starting ice growth. *Trends in Biochemical Sciences* **39**, 548-555, doi:10.1016/j.tibs.2014.09.005 (2014).

91 Knight, C. A., Hallett, J. & DeVries, A. L. Solute effects on ice recrystallization: An assessment technique. *Cryobiology* **25**, 55-60, doi:https://doi.org/10.1016/0011-2240(88)90020-X (1988).
92 Baures, P. & Moore, B. *A Reduced-Cost Apparatus for Observing Ice Recrystallization Inhibition*. (2019).
93 Congdon, T., Notman, R. & Gibson, M. I. Antifreeze (Glyco)protein Mimetic Behavior of Poly(vinyl alcohol): Detailed Structure Ice Recrystallization Inhibition Activity Study. *Biomacromolecules* **14**, 1578-1586, doi:10.1021/bm400217j (2013).
94 Knight, C. A. & Duman, J. G. Inhibition of recrystallization of ice by insect thermal hysteresis proteins: A possible cryoprotective role. *Cryobiology* **23**, 256-262, doi:http://dx.doi.org/10.1016/0011-2240(86)90051-9 (1986).
95 Sidebottom, C. *et al.* Heat-stable antifreeze protein from grass. *Nature* **406**, 256-256, doi:10.1038/35018639 (2000).
96 Eskandari, A., Leow, T. C., Rahman, M. B. A. & Oslan, S. N. Antifreeze Proteins and Their Practical Utilization in Industry, Medicine, and Agriculture. *Biomolecules* **10**, 1649 (2020).
97 Kristiansen, E. & Zachariassen, K. E. The mechanism by which fish antifreeze proteins cause thermal hysteresis. *Cryobiology* **51**, 262-280, doi:10.1016/j.cryobiol.2005.07.007 (2005).
98 Cziko, P. A., DeVries, A. L., Evans, C. W. & Cheng, C.-H. C. Antifreeze protein-induced superheating of ice inside Antarctic notothenioid fishes inhibits melting during summer warming. *Proceedings of the National Academy of Sciences* **111**, 14583-14588, doi:10.1073/pnas.1410256111 (2014).
99 Raymond, J. A. & Devries, A. L. Adsorption inhibition as a mechanism of freezing resistance in polar fishes. *Proceedings of the National Academy of Sciences of the United States of America* **74**, 2589-2593, doi:10.1073/pnas.74.6.2589 (1977).
100 Fuller, B. J. Cryoprotectants: the essential antifreezes to protect life in the frozen state. *CryoLetters* **25**, 375-388 (2004).
101 Devries, A. L. & Lin, Y. Structure of a peptide antifreeze and mechanism of adsorption to ice. *Biochimica et Biophysica Acta* **495**, 388-392, doi:10.1016/0005-2795(77)90395-6 (1977).
102 Drori, R., Davies, P. L. & Braslavsky, I. Experimental correlation between thermal hysteresis activity and the distance between antifreeze proteins on an ice surface. *RSC Adv.* **5**, 7848-7853, doi:10.1039/C4RA12638F (2015).
103 Gerhäuser, J. & Gaukel, V. Detailed Analysis of the Ice Surface after Binding of an Insect Antifreeze Protein and Correlation with the Gibbs–Thomson Equation. *Langmuir* **37**, 11716-11725, doi:10.1021/acs.langmuir.1c01620 (2021).
104 Jia, Z. C. & Davies, P. L. Antifreeze proteins: an unusual receptor-ligand interaction. *Trends in Biochemical Sciences* **27**, 101-106, doi:10.1016/s0968-0004(01)02028-x (2002).
105 Mao, X., Liu, Z., Ma, J., Pang, H. & Zhang, F. Characterization of a novel β-helix antifreeze protein from the desert beetle *Anatolica polita*. *Cryobiology* **62**, 91-99 (2011).

106 Fairley, K. *et al.* Type I shorthorn sculpin antifreeze protein - Recombinant synthesis, solution conformation, and ice growth inhibition studies. *Journal of Biological Chemistry* **277**, 24073-24080, doi:10.1074/jbc.M200307200 (2002).
107 Haymet, A. D. J., Ward, L. G. & Harding, M. M. Winter flounder "antifreeze" proteins: Synthesis and ice growth inhibition of analogues that probe the relative importance of hydrophobic and hydrogen-bonding interactions. *J. Am. Chem. Soc.* **121**, 941-948, doi:10.1021/ja9801341 (1999).
108 Meister, K. *et al.* Observation of ice-like water layers at an aqueous protein surface. *Proceedings of the National Academy of Sciences of the United States of America* **111**, 17732-17736, doi:10.1073/pnas.1414188111 (2014).
109 Zepeda, S., Yokoyama, E., Uda, Y., Katagiri, C. & Furukawa, Y. In situ observation of antifreeze glycoprotein kinetics at the ice interface reveals a two-step reversible adsorption mechanism. *Crystal Growth & Design* **8**, 3666-3672, doi:10.1021/cg800269w (2008).
110 Ba, Y., Wongskhaluang, J. & Li, J. B. Reversible binding of the HPLC6 isoform of type I antifreeze proteins to ice surfaces and the antifreeze mechanism studied by multiple quantum filtering-spin exchange NMR experiment. *J. Am. Chem. Soc.* **125**, 330-331, doi:10.1021/ja027557u (2003).
111 Celik, Y. *et al.* Microfluidic experiments reveal that antifreeze proteins bound to ice crystals suffice to prevent their growth. *Proceedings of the National Academy of Sciences of the United States of America* **110**, 1309-1314, doi:10.1073/pnas.1213603110 (2013).
112 Drori, R., Davies, P. L. & Braslavsky, I. When Are Antifreeze Proteins in Solution Essential for Ice Growth Inhibition? *Langmuir* **31**, 5805-5811, doi:10.1021/acs.langmuir.5b00345 (2015).
113 Ma, J., Wang, J., Mao, X. F. & Wang, Y. Differential expression of two antifreeze proteins in the desert beetle Anatolica polita (Coleoptera: Tenebriondae): seasonal variation and environmental effects. *CryoLetters* **33**, 337-348 (2012).
114 Mao, X., Liu, Z., Li, H., Ma, J. & Zhang, F. Calorimetric studies on an insect antifreeze protein ApAFP752 from Anatolica polita. *Journal of Thermal Analysis and Calorimetry* **104**, 343-349, doi:10.1007/s10973-010-1067-3 (2010).
115 Kratochvilova, I. *et al.* Theoretical and experimental study of the antifreeze protein AFP752, trehalose and dimethyl sulfoxide cryoprotection mechanism: correlation with cryopreserved cell viability. *RSC Adv.* **7**, 352-360, doi:10.1039/c6ra25095e (2017).
116 Liu, Z. Y., Li, H. L., Pang, H., Ma, J. & Mao, X. F. Enhancement effect of solutes of low molecular mass on the insect antifreeze protein ApAFP752 from Anatolica polita. *Journal of Thermal Analysis and Calorimetry* **120**, 307-315, doi:10.1007/s10973-014-4171-y (2015).
117 Shen, Y., Vernon, R., Baker, D. & Bax, A. De novo protein structure generation from incomplete chemical shift assignments. *Journal of Biomolecular NMR* **43**, 63-78, doi:10.1007/s10858-008-9288-5 (2009).
118 Shen, Y. *et al.* Consistent blind protein structure generation from NMR chemical shift data. *Proceedings of the National Academy of Sciences of the United States of America* **105**, 4685-4690, doi:10.1073/pnas.0800256105 (2008).

119 Amornwittawat, N. *et al.* Effects of polyhydroxy compounds on beetle antifreeze protein activity. *Biochimica Et Biophysica Acta-Proteins and Proteomics* **1794**, 341-346, doi:10.1016/j.bbapap.2008.10.011 (2009).
120 Daley, M. E., Spyracopoulos, L., Jia, Z., Davies, P. L. & Sykes, B. D. Structure and dynamics of a beta-helical antifreeze protein. *Biochemistry* **41**, 5515-5525 (2002).
121 Falk, M. *et al.* Chromatin architecture changes and DNA replication fork collapse are critical features in cryopreserved cells that are differentially controlled by cryoprotectants. *Sci Rep* **8**, 14694, doi:10.1038/s41598-018-32939-5 (2018).
122 Kratochvílová, I. *et al.* Changes in Cryopreserved Cell Nuclei Serve as Indicators of Processes during Freezing and Thawing. *Langmuir*, doi:10.1021/acs.langmuir.8b02742 (2018).
123 Mao, X. F., Liu, Z. Y., Li, H. L., Ma, J. & Zhang, F. C. Calorimetric studies on an insect antifreeze protein ApAFP752 from Anatolica polita. *Journal of Thermal Analysis and Calorimetry* **104**, 343-349, doi:10.1007/s10973-010-1067-3 (2011).
124 Jevtić, P. *et al.* An insect antifreeze protein from Anatolica polita enhances the cryoprotection of Xenopus laevis eggs and embryos. *J. Exp. Biol.*, jeb.243662, doi:10.1242/jeb.243662 (2022).
125 Pertaya, N. *et al.* Fluorescence Microscopy Evidence for Quasi-Permanent Attachment of Antifreeze Proteins to Ice Surfaces. *Biophysical Journal* **92**, 3663-3673, doi:https://doi.org/10.1529/biophysj.106.096297 (2007).
126 Drori, R., Celik, Y., Davies, P. L. & Braslavsky, I. Ice-binding proteins that accumulate on different ice crystal planes produce distinct thermal hysteresis dynamics. *J. R. Soc. Interface* **11**, 20140526, doi:doi:10.1098/rsif.2014.0526 (2014).
127 Sieme, H., Oldenhof, H. & Wolkers, W. F. Mode of action of cryoprotectants for sperm preservation. *Anim. Reprod. Sci.* **169**, 2-5, doi:10.1016/j.anireprosci.2016.02.004 (2016).
128 Walters, C., Wheeler, L. & Stanwood, P. C. Longevity of cryogenically stored seeds. *Cryobiology* **48**, 229-244, doi:https://doi.org/10.1016/j.cryobiol.2004.01.007 (2004).
129 Reed, B. M. Plant cryopreservation: a continuing requirement for food and ecosystem security. *In Vitro Cellular & Developmental Biology - Plant* **53**, 285-288, doi:10.1007/s11627-017-9851-4 (2017).
130 Choudhery, M. S., Badowski, M., Muise, A., Pierce, J. & Harris, D. T. Cryopreservation of whole adipose tissue for future use in regenerative medicine. *Journal of Surgical Research* **187**, 24-35, doi:10.1016/j.jss.2013.09.027 (2014).
131 Hunt, C. J. Technical Considerations in the Freezing, Low-Temperature Storage and Thawing of Stem Cells for Cellular Therapies. *Transfusion Medicine and Hemotherapy* **46**, 134-150, doi:10.1159/000497289 (2019).
132 Moore, S. G. & Hasler, J. F. A 100-Year Review: Reproductive technologies in dairy science. *Journal of Dairy Science* **100**, 10314-10331, doi:https://doi.org/10.3168/jds.2017-13138 (2017).
133 Streczynski, R. *et al.* Current issues in plant cryopreservation and importance for ex situ conservation of threatened Australian native species. *Australian Journal of Botany* **67**, 1-15 (2019).

134 Wurm, F. M. Production of recombinant protein therapeutics in cultivated mammalian cells. *Nat. Biotechnol.* **22**, 1393-1398, doi:10.1038/nbt1026 (2004).
135 Tai, W. *et al.* A novel receptor-binding domain (RBD)-based mRNA vaccine against SARS-CoV-2. *Cell Research* **30**, 932-935, doi:10.1038/s41422-020-0387-5 (2020).
136 de Vries, R. J. *et al.* Supercooling extends preservation time of human livers. *Nat. Biotechnol.* **37**, 1131-1136, doi:10.1038/s41587-019-0223-y (2019).
137 Chen, S., Du, K. & Zou, C. Current progress in stem cell therapy for type 1 diabetes mellitus. *Stem Cell Research & Therapy* **11**, 275, doi:10.1186/s13287-020-01793-6 (2020).
138 Stuckey, D. W. & Shah, K. Stem cell-based therapies for cancer treatment: separating hope from hype. *Nature Reviews Cancer* **14**, 683-691, doi:10.1038/nrc3798 (2014).
139 Scolding, N. J., Pasquini, M., Reingold, S. C., Cohen, J. A. & Sclerosis:, I. C. o. C.-B. T. f. M. Cell-based therapeutic strategies for multiple sclerosis. *Brain* **140**, 2776-2796, doi:10.1093/brain/awx154 (2017).
140 Kean, L. S. Defining success with cellular therapeutics: the current landscape for clinical end point and toxicity analysis. *Blood* **131**, 2630-2639, doi:10.1182/blood-2018-02-785881 (2018).
141 Bender, E. Cell-based therapy: Cells on trial. *Nature* **540**, S106-S108, doi:10.1038/540S106a (2016).
142 Müller, P., Lemcke, H. & David, R. Stem Cell Therapy in Heart Diseases – Cell Types, Mechanisms and Improvement Strategies. *Cellular Physiology and Biochemistry* **48**, 2607-2655, doi:10.1159/000492704 (2018).
143 Meneghel, J., Kilbride, P. & Morris, G. J. Cryopreservation as a Key Element in the Successful Delivery of Cell-Based Therapies—A Review. *Frontiers in Medicine* **7**, doi:10.3389/fmed.2020.592242 (2020).
144 *Cellular & Gene Therapy Products*, <https://www.fda.gov/vaccines-blood-biologics/cellular-gene-therapy-products> (2021).
145 Cardoso, L. M. d. F., Pinto, M. A., Henriques Pons, A. & Alves, L. A. Cryopreservation of rat hepatocytes with disaccharides for cell therapy. *Cryobiology* **78**, 15-21, doi:https://doi.org/10.1016/j.cryobiol.2017.07.010 (2017).
146 Mendicino, M., Bailey, Alexander M., Wonnacott, K., Puri, Raj K. & Bauer, Steven R. MSC-Based Product Characterization for Clinical Trials: An FDA Perspective. *Cell Stem Cell* **14**, 141-145, doi:https://doi.org/10.1016/j.stem.2014.01.013 (2014).
147 Poulsen, K. P., Lindelov, F. in *Water activity: Influences on food quality* 651-678 (Academic Press, 1981).
148 Caurie, M. Bound water: its definition, estimation and characteristics. *International Journal of Food Science & Technology* **46**, 930-934, doi:https://doi.org/10.1111/j.1365-2621.2011.02581.x (2011).
149 Kerch, G. Distribution of tightly and loosely bound water in biological macromolecules and age-related diseases. *International Journal of Biological Macromolecules* **118**, 1310-1318, doi:https://doi.org/10.1016/j.ijbiomac.2018.06.187 (2018).

150 Hyclone Labs., I. Freezing and thawing serum and other biological materials: Optimal procedures minimize damage and maximize shelf-life. *Art to Science in Tissue Culture* (1992).
151 Baust, J. M., Campbell, L. H. & Harbell, J. W. Best practices for cryopreserving, thawing, recovering, and assessing cells. *In Vitro Cellular & Developmental Biology - Animal* **53**, 855-871, doi:10.1007/s11626-017-0201-y (2017).
152 Raju, R., Bryant, S. J., Wilkinson, B. L. & Bryant, G. The need for novel cryoprotectants and cryopreservation protocols: Insights into the importance of biophysical investigation and cell permeability. *Biochimica et Biophysica Acta (BBA) - General Subjects* **1865**, 129749, doi:https://doi.org/10.1016/j.bbagen.2020.129749 (2021).
153 Bryant, G. DSC Measurement of Cell Suspensions during Successive Freezing Runs: Implications for the Mechanisms of Intracellular Ice Formation. *Cryobiology* **32**, 114-128, doi:https://doi.org/10.1006/cryo.1995.1011 (1995).
154 Karow, A. Cryoprotectants–a new class of drugs. *J Pharm Pharmacol* **21**, 209-223 (1969).
155 Oughton, J., Xu, S. & Battino, R. The Purification of Water by Freeze-Thaw or Zone Melting. *J. Chem. Educ.* **78**, 1373, doi:10.1021/ed078p1373 (2001).
156 Lovelock, J. E. Het mechanism of the protective action of glycerol against haemolysis by freezing and thawing. *Biochimica et Biophysica Acta* **11**, 28-36, doi:https://doi.org/10.1016/0006-3002(53)90005-5 (1953).
157 Wolfe, J. & Bryant, G. Cellular cryobiology: thermodynamic and mechanical effects. *International Journal of Refrigeration* **24**, 438-450, doi:https://doi.org/10.1016/S0140-7007(00)00027-X (2001).
158 Baust, J. M., Corwin, W. L., Snyder, K. K., Baust, J. G. & Van Buskirk, R. G. Development and Assessment of a Novel Device for the Controlled, Dry Thawing of Cryopreserved Cell Products. *BioProcessing* **15**, 1538-8786 (2016).
159 Baust, J. M., Corwin, W. L., VanBuskirk, R. & Baust, J. G. Biobanking: The Future of Cell Preservation Strategies. *Adv Exp Med Biol* **864**, 37-53, doi:10.1007/978-3-319-20579-3_4 (2015).
160 Mazur, P., Leibo, S. P. & Chu, E. H. Y. A two-factor hypothesis of freezing injury: Evidence from Chinese hamster tissue-culture cells. *Experimental Cell Research* **71**, 345-355, doi:https://doi.org/10.1016/0014-4827(72)90303-5 (1972).
161 Mazur, P. KINETICS OF WATER LOSS FROM CELLS AT SUBZERO TEMPERATURES AND THE LIKELIHOOD OF INTRACELLULAR FREEZING. *J Gen Physiol* **47**, 347-369, doi:10.1085/jgp.47.2.347 (1963).
162 Mazur, P. The role of intracellular freezing in the death of cells cooled at supraoptimal rates. *Cryobiology* **14**, 251-272, doi:https://doi.org/10.1016/0011-2240(77)90175-4 (1977).
163 Baust, J. M., Van Buskirk, R. & Baust, J. G. Cell viability improves following inhibition of cryopreservation-induced apoptosis. *In Vitro Cellular & Developmental Biology - Animal* **36**, 262-270, doi:10.1290/1071-2690(2000)036<0262:CVIFIO>2.0.CO;2 (2000).
164 Elliott, G. D., Wang, S. & Fuller, B. J. Cryoprotectants: A review of the actions and applications of cryoprotective solutes that modulate cell recovery from ultra-

low temperatures. *Cryobiology* **76**, 74-91, doi:https://doi.org/10.1016/j.cryobiol.2017.04.004 (2017).
165 Matsumura, K., Hayashi, F., Nagashima, T., Rajan, R. & Hyon, S.-H. Molecular mechanisms of cell cryopreservation with polyampholytes studied by solid-state NMR. *Communications Materials* **2**, 15, doi:10.1038/s43246-021-00118-1 (2021).
166 Bachtiger, F., Congdon, T. R., Stubbs, C., Gibson, M. I. & Sosso, G. C. The atomistic details of the ice recrystallisation inhibition activity of PVA. *Nature Communications* **12**, 1323, doi:10.1038/s41467-021-21717-z (2021).
167 Uchida, T., Furukawa, M., Kikawada, T., Yamazaki, K. & Gohara, K. Trehalose uptake and dehydration effects on the cryoprotection of CHO–K1 cells expressing TRET1. *Cryobiology* **90**, 30-40, doi:https://doi.org/10.1016/j.cryobiol.2019.09.002 (2019).
168 Poisson, J. S., Acker, J. P., Briard, J. G., Meyer, J. E. & Ben, R. N. Modulating Intracellular Ice Growth with Cell-Permeating Small-Molecule Ice Recrystallization Inhibitors. *Langmuir* **35**, 7452-7458, doi:10.1021/acs.langmuir.8b02126 (2019).
169 Meryman, H. T. Cryoprotective agents. *Cryobiology* **8**, 173-183, doi:https://doi.org/10.1016/0011-2240(71)90024-1 (1971).
170 Gao, D. & Critser, J. K. Mechanisms of Cryoinjury in Living Cells. *ILAR Journal* **41**, 187-196, doi:10.1093/ilar.41.4.187 (2000).
171 Hubálek, Z. Protectants used in the cryopreservation of microorganisms. *Cryobiology* **46**, 205-229, doi:https://doi.org/10.1016/S0011-2240(03)00046-4 (2003).
172 Mazur, P. in *Life in the Fozen State* (ed Lane N Fuller BJ, Benson EE) Ch. 1, 3-65 (CRC Press, 2004).
173 Best, B. P. Cryoprotectant Toxicity: Facts, Issues, and Questions. *Rejuvenation Res* **18**, 422-436, doi:10.1089/rej.2014.1656 (2015).
174 Taylor, R., Adams, G. D. J., Boardman, C. F. B. & Wallis, R. G. Cryoprotection—Permeant vs nonpermeant additives. *Cryobiology* **11**, 430-438, doi:https://doi.org/10.1016/0011-2240(74)90110-2 (1974).
175 Wolfe, J. & Bryant, G. Freezing, Drying, and/or Vitrification of Membrane–Solute–Water Systems. *Cryobiology* **39**, 103-129, doi:https://doi.org/10.1006/cryo.1999.2195 (1999).
176 Crowe, J. H., Carpenter, J. F., Crowe, L. M. & Anchordoguy, T. J. Are freezing and dehydration similar stress vectors? A comparison of modes of interaction of stabilizing solutes with biomolecules. *Cryobiology* **27**, 219-231, doi:https://doi.org/10.1016/0011-2240(90)90023-W (1990).
177 Stroncek, D. F. *et al.* Adverse reactions in patients transfused with cryopreserved marrow. *Transfusion* **31**, 521-526, doi:https://doi.org/10.1046/j.1537-2995.1991.31691306250.x (1991).
178 Mukherjee, I. N., Song, Y. C. & Sambanis, A. Cryoprotectant delivery and removal from murine insulinomas at vitrification-relevant concentrations. *Cryobiology* **55**, 10-18, doi:https://doi.org/10.1016/j.cryobiol.2007.04.002 (2007).
179 Robb, K. P., Fitzgerald, J. C., Barry, F. & Viswanathan, S. Mesenchymal stromal cell therapy: progress in manufacturing and assessments of potency. *Cytotherapy* **21**, 289-306, doi:10.1016/j.jcyt.2018.10.014 (2019).

180 Miyazaki, T. & Suemori, H. Slow Cooling Cryopreservation Optimized to Human Pluripotent Stem Cells. *Adv Exp Med Biol* **951**, 57-65, doi:10.1007/978-3-319-45457-3_5 (2016).
181 Baboo, J. *et al.* The Impact of Varying Cooling and Thawing Rates on the Quality of Cryopreserved Human Peripheral Blood T Cells. *Sci Rep* **9**, 3417, doi:10.1038/s41598-019-39957-x (2019).
182 Morris, T. J. *et al.* The effect of Me2SO overexposure during cryopreservation on HOS TE85 and hMSC viability, growth and quality. *Cryobiology* **73**, 367-375, doi:https://doi.org/10.1016/j.cryobiol.2016.09.004 (2016).
183 Yang, B. *et al.* Cryopreservation of Bone Marrow Mononuclear Cells Alters Their Viability and Subpopulation Composition but Not Their Treatment Effects in a Rodent Stroke Model. *Stem Cells Int.* **2016**, 5876836-5876836, doi:10.1155/2016/5876836 (2016).
184 Yuan, Y. *et al.* Efficient long-term cryopreservation of pluripotent stem cells at −80 °C. *Sci Rep* **6**, 34476, doi:10.1038/srep34476 (2016).
185 Baust, J. M., Vogel, M. J., Van Buskirk, R. & Baust, J. G. A Molecular Basis of Cryopreservation Failure and its Modulation to Improve Cell Survival. *Cell Transplantation* **10**, 561-571, doi:10.3727/000000001783986413 (2001).
186 Lekshmi, A. *et al.* A quantitative real-time approach for discriminating apoptosis and necrosis. *Cell Death Discovery* **3**, 16101, doi:10.1038/cddiscovery.2016.101 (2017).
187 Chan, F. K.-M., Moriwaki, K. & De Rosa, M. J. in *Immune Homeostasis: Methods and Protocols* (eds Andrew L. Snow & Michael J. Lenardo) 65-70 (Humana Press, 2013).
188 Gerlier, D. & Thomasset, N. Use of MTT colorimetric assay to measure cell activation. *Journal of Immunological Methods* **94**, 57-63, doi:https://doi.org/10.1016/0022-1759(86)90215-2 (1986).
189 Back, S. A., Khan, R., Gan, X., Rosenberg, P. A. & Volpe, J. J. A new Alamar Blue viability assay to rapidly quantify oligodendrocyte death. *Journal of Neuroscience Methods* **91**, 47-54, doi:https://doi.org/10.1016/S0165-0270(99)00062-X (1999).
190 Sosef, M. N. *et al.* Cryopreservation of isolated primary rat hepatocytes: enhanced survival and long-term hepatospecific function. *Ann Surg* **241**, 125-133, doi:10.1097/01.sla.0000149303.48692.0f (2005).
191 Sugimachi, K. *et al.* Long-Term Function of Cryopreserved Rat Hepatocytes in a Coculture System. *Cell Transplantation* **13**, 187-195, doi:10.3727/000000004773301799 (2004).
192 Hayflick, L. The Cell Biology of Human Aging. *New England Journal of Medicine* **295**, 1302-1308, doi:10.1056/NEJM197612022952308 (1976).
193 Hayflick, L. The Cell Biology of Aging. *Journal of Investigative Dermatology* **73**, 8-14, doi:https://doi.org/10.1111/1523-1747.ep12532752 (1979).
194 Chao, H., Hodges, R. S., Kay, C. M., Gauthier, S. Y. & Davies, P. L. A natural variant of type I antifreeze protein with four ice-binding repeats is a particularly potent antifreeze. *Protein Science* **5**, 1150-1156 (1996).
195 *Biochemisty and Function of Antifreeze Proteins*. (Nova Science Publishers, Inc., 2010).

196 Haridas, V. & Naik, S. Natural macromolecular antifreeze agents to synthetic antifreeze agents. *Rsc Advances* **3**, 14199-14218, doi:10.1039/c3ra00081h (2013).
197 Scotter, A. J. *et al.* The basis for hyperactivity of antifreeze proteins. *Cryobiology* **53**, 229-239, doi:10.1016/j.cryobiol.2006.06.006 (2006).
198 Doucet, D., Walker, V. & Qin, W. The bugs that came in from the cold: molecular adaptations to low temperatures in insects. *Cellular and Molecular Life Sciences* **66**, 1404-1418 (2009).
199 Mao, X., Liu, Z., Li, H., Ma, J. & Zhang, F. Calorimetric studies on an insect antifreeze protein ApAFP752 from Anatolica polita. *Journal of Thermal Analysis and Calorimetry* **104**, 343-349, doi:10.1007/s10973-010-1067-3 (2011).
200 Amornwittawat, N., Wang, S., Duman, J. G. & Wen, X. Polycarboxylates enhance beetle antifreeze protein activity. *Biochimica et Biophysica Acta (BBA) - Proteins and Proteomics* **1784**, 1942-1948, doi:http://dx.doi.org/10.1016/j.bbapap.2008.06.003 (2008).
201 Liou, Y. C., Tocilj, A., Davies, P. L. & Jia, Z. Mimicry of ice structure by surface hydroxyls and water of a β-helix antifreeze protein. *Nature* **406**, 322-324 (2000).
202 Tomczak, M. M., Marshall, C. B., Gilbert, J. A. & Davies, P. L. A facile method for determining ice recrystallization inhibition by antifreeze proteins. *Biochem. Biophys. Res. Commun.* **311**, 1041-1046 (2003).
203 Sreter, J. A., Foxall, T. L. & Varga, K. Intracellular and Extracellular Antifreeze Protein Significantly Improves Mammalian Cell Cryopreservation. *Biomolecules* **12**, doi:10.3390/biom12050669 (2022).
204 Post, M. J. Cultured meat from stem cells: Challenges and prospects. *Meat Science* **92**, 297-301, doi:https://doi.org/10.1016/j.meatsci.2012.04.008 (2012).
205 Stout, A. J., Mirliani, A. B., Soule-Albridge, E. L., Cohen, J. M. & Kaplan, D. L. Engineering carotenoid production in mammalian cells for nutritionally enhanced cell-cultured foods. *Metabolic Engineering* **62**, 126-137, doi:https://doi.org/10.1016/j.ymben.2020.07.011 (2020).
206 Stacey, G. N. *et al.* Preservation and stability of cell therapy products: recommendations from an expert workshop. *Regenerative Medicine* **12**, 553-564, doi:10.2217/rme-2017-0073 (2017).
207 Lovelock, J. E. & Bishop, M. W. H. Prevention of Freezing Damage to Living Cells by Dimethyl Sulphoxide. *Nature* **183**, 1394-1395, doi:10.1038/1831394a0 (1959).
208 Kratochvílová, I. *et al.* Changes in Cryopreserved Cell Nuclei Serve as Indicators of Processes during Freezing and Thawing. *Langmuir* **35**, 7496-7508, doi:10.1021/acs.langmuir.8b02742 (2019).
209 Tomas, R. M. F., Bailey, T. L., Hasan, M. & Gibson, M. I. Extracellular Antifreeze Protein Significantly Enhances the Cryopreservation of Cell Monolayers. *Biomacromolecules* **20**, 3864-3872, doi:10.1021/acs.biomac.9b00951 (2019).
210 Briard, J. G. *et al.* Small molecule ice recrystallization inhibitors mitigate red blood cell lysis during freezing, transient warming and thawing. *Sci Rep* **6**, 10, doi:10.1038/srep23619 (2016).

211 Hirano, Y. *et al.* Hypothermic preservation effect on mammalian cells of type III antifreeze proteins from notched-fin eelpout. *Cryobiology* **57**, 46-51, doi:https://doi.org/10.1016/j.cryobiol.2008.05.006 (2008).
212 Ideta, A. *et al.* Prolonging hypothermic storage (4 C) of bovine embryos with fish antifreeze protein. *J Reprod Dev* **61**, 1-6, doi:10.1262/jrd.2014-073 (2015).
213 Fletcher, G. L., Hew, C. L. & Davies, P. L. Antifreeze Proteins of Teleost Fishes. *Annual Review of Physiology* **63**, 359-390, doi:10.1146/annurev.physiol.63.1.359 (2001).
214 Hakim, A. *et al.* Crystal structure of an insect antifreeze protein and its implications for ice binding. *Journal of Biological Chemistry* **288**, 12295-12304, doi:10.1074/jbc.M113.450973 (2013).
215 Halwani, D. O., Brockbank, K. G. M., Duman, J. G. & Campbell, L. H. Recombinant Dendroides canadensis antifreeze proteins as potential ingredients in cryopreservation solutions. *Cryobiology* **68**, 411-418, doi:https://doi.org/10.1016/j.cryobiol.2014.03.006 (2014).
216 Kim, H. J., Shim, H. E., Lee, J. H., Kang, Y. C. & Hur, Y. B. Ice-Binding Protein Derived from Glaciozyma Can Improve the Viability of Cryopreserved Mammalian Cells. *J. Microbiol. Biotechnol.* **25**, 1989-1996, doi:10.4014/jmb.1507.07041 (2015).
217 Hunt, M. A., Currie, M. J., Robinson, B. A. & Dachs, G. U. Optimizing transfection of primary human umbilical vein endothelial cells using commercially available chemical transfection reagents. *J Biomol Tech* **21**, 66-72 (2010).
218 Baust, J. M., Vogel, M. J., Snyder, K. K., Van Buskirk, R. G. & Baust, J. G. Activation of Mitochondrial-Associated Apoptosis Contributes to Cryopreservation Failure. *Cell Preservation Technology* **5**, 155-164, doi:10.1089/cpt.2007.9990 (2007).
219 Strober, W. Trypan Blue Exclusion Test of Cell Viability. *Curr Protoc Immunol* **111**, A3.B.1-A3.B.3, doi:10.1002/0471142735.ima03bs111 (2015).
220 Kim, J. S. *et al.* Comparison of the automated fluorescence microscopic viability test with the conventional and flow cytometry methods. *J Clin Lab Anal* **25**, 90-94, doi:10.1002/jcla.20438 (2011).
221 Vembadi, A., Menachery, A. & Qasaimeh, M. A. Cell Cytometry: Review and Perspective on Biotechnological Advances. *Front Bioeng Biotechnol* **7**, 147-147, doi:10.3389/fbioe.2019.00147 (2019).
222 Kumar, P., Nagarajan, A. & Uchil, P. D. Analysis of Cell Viability by the Lactate Dehydrogenase Assay. *Cold Spring Harb Protoc* **2018**, doi:10.1101/pdb.prot095497 (2018).
223 Buttke, T. M., McCubrey, J. A. & Owen, T. C. Use of an aqueous soluble tetrazolium/formazan assay to measure viability and proliferation of lymphokine-dependent cell lines. *Journal of Immunological Methods* **157**, 233-240, doi:https://doi.org/10.1016/0022-1759(93)90092-L (1993).
224 Eroglu, A. *et al.* Intracellular trehalose improves the survival of cryopreserved mammalian cells. *Nat Biotechnol* **18**, 163-167, doi:10.1038/72608 (2000).
225 Da Violante, G. *et al.* Evaluation of the Cytotoxicity Effect of Dimethyl Sulfoxide (DMSO) on Caco2/TC7 Colon Tumor Cell Cultures. *Biological and Pharmaceutical Bulletin* **25**, 1600-1603, doi:10.1248/bpb.25.1600 (2002).

226 Castor, L. N. Control of division by cell contact and serum concentration in cultures of 3T3 cells. *Experimental Cell Research* **68**, 17-24, doi:https://doi.org/10.1016/0014-4827(71)90581-7 (1971).
227 Dulbecco, R. Topoinhibition and Serum Requirement of Transformed and Untransformed Cells. *Nature* **227**, 802-806, doi:10.1038/227802a0 (1970).
228 Bereiter-Hahn, J., Münnich, A. & Woiteneck, P. Dependence of energy metabolism on the density of cells in culture. *Cell Struct Funct* **23**, 85-93, doi:10.1247/csf.23.85 (1998).
229 Nitsch, S., Chatterjee, A., Hofmann, N. & Glasmacher, B. Impact of cryopreservation on histone modifications of mesenchymal stem cells. *Biomedizinische Technik* **59**, S294-297 (2014).
230 Lauterboeck, L., Saha, D., Chatterjee, A., Hofmann, N. & Glasmacher, B. Xeno-Free Cryopreservation of Bone Marrow-Derived Multipotent Stromal Cells from Callithrix jacchus. *Biopreserv. Biobank.* **14**, 530-538, doi:10.1089/bio.2016.0038 (2016).
231 Lee, H. H. *et al.* Effects of antifreeze proteins on the vitrification of mouse oocytes: comparison of three different antifreeze proteins. *Hum. Reprod.* **30**, 2110-2119, doi:10.1093/humrep/dev170 (2015).
232 Carpenter, J. F. & Hansen, T. N. Antifreeze protein modulates cell survival during cryopreservation: mediation through influence on ice crystal growth. *Proceedings of the National Academy of Sciences of the United States of America* **89**, 8953-8957, doi:10.1073/pnas.89.19.8953 (1992).
233 DeLuca, C. I., Comley, R. & Davies, P. L. Antifreeze proteins bind independently to ice. *Biophysical Journal* **74**, 1502-1508 (1998).
234 Matissek, S. J. *et al.* Epigenetic targeting of Waldenström macroglobulinemia cells with BET inhibitors synergizes with BCL2 or histone deacetylase inhibition. *Epigenomics* **13**, 129-144, doi:10.2217/epi-2020-0189 (2021).
235 Karbalivand, M., Almada, L. L., Ansell, S. M., Fernandez-Zapico, M. E. & Elsawa, S. F. MLL1 inhibition reduces IgM levels in Waldenström macroglobulinemia. *Leukemia Research* **116**, 106841, doi:https://doi.org/10.1016/j.leukres.2022.106841 (2022).
236 Scandella, V., Paolicelli, R. C. & Knobloch, M. A novel protocol to detect green fluorescent protein in unfixed, snap-frozen tissue. *Sci Rep* **10**, 14642, doi:10.1038/s41598-020-71493-x (2020).